RAPID DETECTION AND CHARACTERIZATION OF MYCOBACTERIA USING MICROCHANNEL ELECTRICAL IMPEDANCE SPECTROSCOPY

A Dissertation

presented to

the Faculty of the Graduate School

at the University of Missouri - Columbia

In Partial Fulfillment

of the requirements for the Degree

Doctor of Philosophy

---

by

ROLI KARGUPTA

Dr. Shramik Sengupta, Dissertation Supervisor

May 2017

The undersigned, appointed by the dean of the Graduate School, have examined the Dissertation entitled

RAPID DETECTION AND CHARACTERIZATION OF MYCOBACTERIA USING MICROCHANNEL ELECTRICAL IMPEDANCE SPECTROSCOPY

presented by Roli Kargupta,

A candidate for the degree of Doctor of Philosophy,

and hereby certify that, in their opinion, it is worthy of acceptance.

Dr. Shramik Sengupta, Department of Bioengineering

Dr. Azlin Mustapha, Department of Food Science

Dr. Shubhra Gangopadhyay, Department of Bioengineering

Dr. Raghuraman Kannan, Department of Bioengineering

Dr. Caixia Wan, Department of Bioengineering

I dedicate this work to my family and friends who have been there alongside me. Special thanks to my parents, husband, brother, and my in-laws for all the guidance and support they have offered me through all these years.

ACKNOWLEDGEMENTS

I would like to express my heartfelt gratitude and appreciation to all the people who have helped me both professionally and personally to achieve my goals. My parents have been my pillar of strength. Without their inspiration and support, I would not have been able to reach my aim. I would like to thank my husband Dr. Sagnik Basuray for his constant support and guidance. My brother has always been my inspiration and played a crucial role in shaping my life. I would also like to thank my in-laws for their endless enthusiasm and encouragement. Also, I would like to thank my lab members and friends who have always been there for me.

A special thanks to my advisor, Dr. Shramik Sengupta, for guiding and encouraging me. He has been an excellent mentor both on professional and personal fronts. He has been extremely patient and been a constant support during my doctoral studies. I would also like to thank all my committee members for agreeing to serve on my committee and providing me advice and guidance regarding my research work. The constructive discussions I had with my committee members helped me to complete my research studies. I will always be thankful to the University of Missouri for providing me the opportunity to conduct my research and would like to express my gratitude to all the professors, mentors and administrative staffs who have helped me through my journey of doctoral studies.

TABLE OF CONTENTS

ACKNOWLEDGEMENTS..... ii

LIST OF ILLUSTRATIONS..... vii

LIST OF TABLES..... xiv

LIST OF ABBREVIATIONS.....xv

ABSTRACT..... xvii

Chapter

1 INTRODUCTION.....1

1.1 MOTIVATION..... 1

1.2 HEALTHCARE-ASSOCIATED INFECTIONS (HAIS)..... 2

1.3 EMERGING INFECTIOUS DISEASES..... 5

1.4 CURRENT GOLD STANDARD FOR MICROORGANISM DETECTION..... 8

2 COATINGS AND SURFACE MODIFICATIONS IMPARTING ANTIMICROBIAL ACTIVITY TO THE ORTHOPEDIC IMPLANTS.....10

2.1 INTRODUCTION..... 11

2.2 BIOLOGY OF ORTHOPEDIC INFECTIONS..... 13

2.3 APPROACHES TO PREVENT AND MANAGE ORTHOPEDIC INFECTIONS..... 15

2.4 ANTIMICROBIAL COATINGS..... 21

2.4.1 Coatings that prevent bacterial adhesion..... 22

2.4.1.1 Sacrificial coatings..... 22

2.4.1.2 Adhesion-resistant coatings 23
2.4.2 Coatings that kill adherent bacteria 26
2.4.2.1 Photoactive coatings 28
2.4.2.2 Metal-impregnated surface coatings 28
2.4.2.3 Surface-anchored antimicrobial peptides 31
2.4.2.4 Surface quaternary ammonium salts 32
2.4.2.5 Nitric Oxide 32
2.4.3 Coatings that release antimicrobial agents 33
2.4.3.1 Antibiotic-loaded bone cement 33
2.4.3.2 Polyhydroxyalkanoates 35
2.4.3.3 Mesoporous materials 36
2.4.3.4 Hydrogels 36
2.4.3.5 Drug-eluting degradable coatings 37
2.4.4 Coatings that accelerate osteocyte adhesion 43
2.4.4.1 Incorporation of growth factors 43
2.4.4.2 Bioglass 44
2.4.4.3 Silicon carbide ceramics 44
2.4.4.4 Coating with extracellular bone matrix (ECM) 45
2.4.5 Coatings with multiple modes of action 45
2.5 CONCLUSIONS 50
3 FOAMING BETADINE SPRAY AS A POTENTIAL AGENT FOR NON-LABOR-INTENSIVE PREOPERATIVE SURGICAL SITE PREPARATION 52
3.1 BACKGROUND 53

3.2 MATERIALS AND METHODS 55
3.2.1 Overview *55*
3.2.2 Bacterial cell culture *57*
3.2.3 Selection of substrates *57*
3.2.4 Selection of antimicrobial agents for testing *57*
3.2.5 Evaluation of bactericidal activity *58*
3.2.6 Statistical analysis *61*
3.3 RESULTS 61
3.4 DISCUSSION 65
3.5 CONCLUSION 65
4 MICROCHANNEL ELECTRICAL IMPEDANCE SPECTROSCOPY 67
5 MYCOBACTERIA 76
5.1 BACKGROUND 76
5.2 TRANSMISSION 77
5.3 STAINING 78
5.4 STRUCTURE 80
5.5 DIGESTION AND DECONTAMINATION 80
6 RAPID CULTURE-BASED DETECTION OF LIVING MYCOBACTERIA USING MICROCHANNEL ELECTRICAL IMPEDANCE SPECTROSCOPY (M-EIS) 82
6.1 INTRODUCTION 83
6.2 METHOD 91
6.2.1 Background and Overview *91*

6.2.2 Mycobacterial cell culture *93*

6.2.3 microchannel Electrical Impedance Spectroscopy (m-EIS) *94*

6.2.4 Statistical analysis *95*

6.3 RESULTS 96

6.4 DISCUSSION 98

7 DETECTION BY DEATH: A RAPID WAY TO DETECT VIABLE SLOW-GROWING MICROORGANISMS ACHIEVED USING MICROCHANNEL ELECTRICAL IMPEDANCE SPECTROSCOPY (M-EIS) 103

7.1 INTRODUCTION 104

7.2 METHODS 108

7.2.1 Rationale and Overview *108*

7.2.2 Bacterial cell cultures *111*

7.2.3 Rationale for choice of antibiotics *112*

7.2.4 Digestion and decontamination *114*

7.2.5 microchannel Electrical Impedance Spectroscopy (m-EIS) *115*

7.2.6 Statistical analysis *118*

7.3 RESULTS 119

7.4 DISCUSSION 123

8 CONCLUSION AND FUTURE WORK 126

REFERENCE 130

VITA 165

LIST OF ILLUSTRATIONS

2-1 A pictographic representation of the steps in bacterial biofilm formation using a Pseudomonas aeruginosa case study (44). (a) Bacteria adhere loosely and reversibly to the surface by non-specific binding, (b) Bacteria attach irreversibly to the surface and begin forming cell clusters, (c) Accumulation – Multiple layers of bacteria form and EPS layer provides protection to bacterial community, (d) Maturation - Biofilm reaches maximum thickness, and cells communicate via quorum sensing, and (e) Dispersion – Clusters detach and infection spreads to new areas. (Reprinted with permission from Ref [44]. Copyright 2003 Nature Publishing Group)..... 14

2-2 A schematic illustrating the various modes of action of different coatings and surface modifications. (a) Prevention of bacterial adhesion is possible due to physical actions like presence of polymer brush, (b) Prevention of bacterial adhesion owing to the presence of a sacrificial layer which do not allow the bacteria to adhere to the surface, (c) Killing of bacteria due to the release of antimicrobial agents to the surrounding regions, (d) Killing of adherent bacteria owing to the presence of antimicrobial agents present on the surface and (c) Promotion and acceleration of desired cells which competes with the bacteria to promote osseointegration and prevent colonization. 21

2-3 Schematic representation of multilayer biodegradable films produced by a layer-by-layer deposition method. Multiple layers of (heparin/chitosan)-(polyvinylpyrrolidone/poly(acrylic acid))x [(HEP/CHI)x−(PVP/PAA)x], where ‘x’ denotes the number of layers, are constructed based on electrostatic

interaction for HEP/CHI and hydrogen bond interaction for PVP/PAA, followed by thermal treatment at 110 °C for 16 h for crosslinking to form anhydride groups. In simulated physiological condition (e.g. PBS buffer at 37 °C), $(PVP/PAA)_{10}$ layers were degradable in 24 hours, leading to almost no bacterial adhesion. After degradation of (PVP/PAA) layers, the underlying $(HEP/CHI)_x$ layers displayed contact killing of bacteria (79). (Reprinted with permission from Ref [79]. Copyright 2013 American Chemical Society) 25

2-4 A) A substrate modified by grafting to approach in which the initially adsorbed polymer impedes further deposition, resulting in a low density of brushes. B) Modification of a substrate by the grafting of the approach in which an initiator-bearing substrate is exposed to the monomer to afford thick, dense polymer brushes (86). C) Schematic of grafting poly(SPMA) on the 3D printed structures (91): to initiate atom transfer radical polymerization (ATRP), the Br-containing vinyl-terminated initiator [2-(2-bromoisobutyryloxy)ethyl methacrylate (BrMA)] was pre-mixed with the resin consisting of acrylate-based pre-polymers, crosslinking agents, and a phosphine oxide-based photoinitiator. The acrylate-terminated polymers were utilized to incorporate with the initiator to achieve covalent bonding, and BrMA was used without affecting the photopolymerization during 3D printing processes. (A, B): Reprinted with permission from Ref [86]. Copyright 2009 American Vacuum Society, C: Reprinted with permission from Ref [91]. Copyright 2013 Royal Society of Chemistry) 27

2-5 Schematic illustrating bactericidal process for E. coli cells on Cu/TiO_2 thin film

under weak UV light irradiation (96). (a) E. coli cell membranes are shown, (b) reactive species generated by the TiO_2 photocatalyst attack and open the outer membrane, and (c) Cu ions effectively penetrate into the cell cytoplasmic membrane, resulting in cell lysis. (Reprinted with permission from Ref [96]. Copyright 2003 American Chemical Society) 29

2-6 (a) Schematic showing the antimicrobial effect of a porous sol-gel coating incorporating a silver ion (Ag+)-generating "ionosol" on E. coli cells, (b) Cross-sectional SEM images of the antimicrobial coatings revealing porous structure throughout the coating (102). (Reprinted with permission from Ref [102]. Copyright 2012 American Chemical Society) 30

3-1 Schematic of the method of testing the bactericidal efficacy. This schematic details the methodology of screening the bactericidal efficacy using Povidone-iodine aerosol foam, sponge based applicator, and flood coverage with liquid Betadine. 56

3-2 Steps involved in evaluating bactericidal activity on nutrient agar plates. Steps involved in treating the agar plates with flood coverage of Betadine aerosolized foam and sponge based applicator and evaluating its bactericidal activity. 59

3-3 Steps involved in assessing bactericidal activity on porcine skin. Steps involved in treating the porcine skin with flood coverage of Betadine aerosolized foam and sponge based applicator and evaluating its bactericidal activity 60

3-4 Viable bacterial count for different bacteria tested on agar plates. Number of live bacteria (CFU/100µL) observed on agar plate after 24 hours and 48 hours for negative control (no treatment done), application of aerosolized foam,

application of sponge based applicator and positive control (application of 5% Betadine) for S. aureus (top left)[n=4], P. aeruginosa (top right)[n=5] and S. epidermis (bottom left) [n=5]. 62

3-5 Viable bacterial count for different bacteria tested on porcine skin. Number of live bacteria (CFU/100µL) observed on porcine skin after 24 hours and 48 hours for negative control (no treatment done), application of aerosolized foam, application of sponge based applicator and positive control (application of 5% Betadine) for S. aureus (top left)[n=4], P. aeruginosa (top right)[n=5] and S. epidermis ((bottom left)[n=5] 63

4-1 (a) Microfluidic channel with gold electrodes inserted at 1cm interval used for EIS analysis of bacterial solution. (b) Electrical circuit model to represent the presence of bacteria between two electrodes when a voltage is applied across them (205). 69

4-2 Z-view® software used for EIS data fitting. Inset (Equivalent circuit model) 74

5-1 (a) Kinyoun acid fast staining of M. bovis BCG (b) SEM image of M. bovis BCG, (c) Kinyoun acid fast staining of M. smegmatis (b) SEM image of M. smegmatis. 79

6-1 Electrical model and cassettes used for impedance measurement. (a) Electrical model representing two electrodes submerged in a microorganism suspension enclosed in a thin capillary channel (b) 3D printed long and narrow microfluidic channels with two gold electrode inserted for impedance measurement (inset) and schematic showing electrical lines of forces between two electrodes in the channel [205] (c) Modified electrical model which uses CPE instead of ideal

capacitors to detect the presence of microorganisms in a suspension. 90

6-2 Experimental set-up for determining TTD of mycobacteria. 2 sets of similar samples are prepared by inoculating with mycobacteria and incubated at 37C. One set is sent to the Hospital microbiology lab for detection using MGIT 960 automated culture-based system while the other set of sample is tested using our technique. For our technique, at regular intervals of time, small aliquots of sample are drawn and its impedance is tested using impedance analyzer. The data is fitted to an equivalent circuit to generate a Nyquist plot [259] and thereby estimates the values of the desired circuit parameters. We show on the graph three sets of data: those obtained at 2 hr, 8hr, and 12hrs for a culture of M. smegmatis (large, medium, and small semi-circles). The inset shows the software output for circuit parameters obtained by fitting the data at 12 hrs to the circuit. 92

6-3 TTD of M. bovis BCG samples. The plot of bulk capacitance obtained over time for samples with (a) low initial loads (~$1x10^3$ CFU/ml) and (b) high initial loads (~$1x10^5$ CFU/ml) for M. bovis BCG. The error bars indicate the standard deviation of the readings (n=5) taken at each time interval. Statistical analysis is used to compare the baseline reading with the various time interval readings ($U_{critical}$=2). [Note: NSH = Not significantly higher, SH = Significantly higher] 100

6-4 TTD of M. smegmatis samples. The plot of bulk capacitance obtained over time for samples with (a) low initial loads (~$1x10^3$ CFU/ml) and (b) high initial loads (~$1x10^5$ CFU/ml) for M. smegmatis. The error bars indicate the standard deviation of the readings (n=4) taken at each time interval. Statistical analysis

is used to compare the baseline reading with the various time interval readings ($U_{critical}$=0). [Note: NSH = Not significantly higher, SH = Significantly higher] 101

7-1 Experimental set-up to demonstrate the ability of the "detection by death" approach to detect the presence/absence of mycobacteria in a sputum sample (a) Artificial sputum sample, containing both pathogen of interest (mycobacteria) and commensal bacteria (gram positive and gram negative), is prepared (b) Standard protocol (treatment with NaOH-NALC) is used to liquefy the (artificial) sputum and decontaminate it (kill all non-mycobacterial microorganisms). The addition of PBS and centrifugation to obtain cells is also part of the protocol (c) Collected cells are resuspended in two broths: one containing Carbenicillin in 7H9 media, and the other containing both Carbenicillin and Ampicillin in 7H9 media, (d) at regular intervals of time (every hour), 50ul aliquots are extracted and scanned electrically 110

7-2 Expected plots of bulk capacitance versus time that we expect to obtain for the two conditions tested (with carbenicillin and amaikacin, and with carbenicillin alone) for the control (no-bacteria) and two possible cases likely to be encountered (mycobacteria present along with commensal bacteria and only commensal bacteria present) 113

7-3 (a) Electrical equivalent circuit model that represents our microfluidic cassette which is used for measuring the impedance of the bacteria. (b) Microfluidic cassettes with two gold electrodes inserted at a distance of 1 cm (inset) and schematic of electric lines of forces present between the two electrodes when an AC voltage is applied to the system. [205] (c) Agilent Impedance Analyzer

is used to do the electrical scans at multiple frequencies and commercially available Z view® software is used to analyze the data to obtain the values for the various electrical parameters, and (d) The bulk capacitance values obtained from data analysis is plotted against time. The decrease in the bulk capacitance values (black line) is due to cell death while the rise is due to bulk capacitance (red line) values is due to the cell growth. 116

7-4 Average bulk capacitance versus time graph for the 6 cases using M. smegmatis. S = significant difference, NS= not significant difference 120

7-5 Average bulk capacitance versus time graph for the 6 cases using M. bovis BCG. S = significant difference, NS= not significant difference 121

7-6 Partial decontamination of simulated sputum samples containing non-mycobacterial cultures are exposed to two conditions namely, Condition A : cocktail of two antibiotics, Amikacin and Carbenicillin and Condition B: only Carbenicillin. Average bulk capacitance estimated from the m-EIS scans is plotted against time done. 124

LIST OF TABLES

Table		Page
2.1	The different categories of orthopedic infections based on time of infection with respect to the operation……	16
2.2	A summary of the various coatings and surface modifications imparting antimicrobial activity to orthopedic implants and their duration of efficacy……	47
3.1	p-values calculated using null hypothesis for all applications. List of p-values, as calculated for the null hypothesis that the two disinfection protocols (aerosolized foam and sponge based applicator) are equally effective. (n = 4 for *S. aureus*; n=5 for *S. epidermis* and *P. aeruginosa*)……	64
6.1	Comparison of TTD values obtained by our technique to BD BACTEC MGIT 960 system. Compares the TTD values obtained for the various concentrations of *M. bovis BCG* and *M. smegmatis* by our technique and that obtained by the commercially available automated system BD BACTEC MGIT 960……	97

LIST OF ABBREVIATIONS

WHO – World Health Organizations

HAI – Healthcare-associated infections

SSI - surgical site infections

CDC – Centers for Disease Control and Prevention

TB – Tuberculosis

EIS – Electrical Impedance Spectroscopy

mEIS – Microchannel Electrical Impedance Spectroscopy

MGIT – Mycobacteria Growth Indicator Tubes

S. aureus – Staphylococcus aureus

P. aeruginosa – Pseudomonas aeruginosa

AC – Alternating current

TSA – Tryptic Soy Agar

CFU – Colony Forming Unit

ANOVA – Analysis of Variance

PBS – Phosphate Buffered Saline

CPE – Constant Phase Element

C_b – Bulk capacitance

M. tuberculosis – *Mycobacterium tuberculosis*

M. smegmatis – *Mycobacterium smegmatis*

M. bovis BCG – *Mycobacterium bovis Bacillus Calmette-Guérin*

NaOH – Sodium Hydroxide

NALC – N-acetyl-L-cysteine

TTD – Time to detection

MHz – Megahertz

OD – Optical density

TSB – Tryptic Soy Broth

ABSTRACT

The presence of virulent, pathogenic bacteria in our body, food, water and other consumables is harmful and causes enormous economic and personal losses. Here we will be looking at developing a platform technology that can rapidly detect pathogenic bacteria. The platform will be based on an electrical spectroscopic method called microchannel Electrical Impedance Spectroscopy (m-EIS). Initially, we will look at the growth of bacteria as our primary method to detect the presence of bacteria and find the time-to-detection. Following this, we will study the death of bacteria in a suspension using our technique of m-EIS to reduce the time-to-detection further. We want to detect the pathogenic *Mycobacteria Tuberculosis* (that causes Tuberculosis in humans), which according to WHO, is the second leading cause of death due to infectious diseases. As proof of concept, surrogates like *Mycobacterium bovis BCG* and *Mycobacterium smegmatis* will be taken up for detection using our technique of m-EIS. However, our first focus is to prevent surgical site infections.

Transmission of contagious infections like tuberculosis or infections occurring post-surgery like surgical site infections can be reduced and prevented, to some extent by proper treatment and correct use of antibiotics. For example, surgical site infection, occurring after insertion of implants can be reduced by use of coatings and other surface modifications. Many of these amendments ensure prevention of bacterial adhesion and kill surrounding bacteria near the implant. Further, in some cases, they promote the growth of desired cells that warrants proper integration of the implants with the bone. Surgical site infections occurring post-surgery can be reduced by following proper preoperative skin preparations. Several techniques are applied in the hospitals like 2-step scrubbing and painting, 2-step scrubbing and drying, and 1-step painting with

a drying time. However, most of these techniques are time-consuming and labor-intensive. Here, we have demonstrated that the antimicrobial efficacy of a spray-on formulation containing Betadine is comparable to the existing techniques. The spray-on Betadine formulation is significantly less time-consuming and is not labor-intensive.

Though prevention is necessary, often time, the pathogens have to be detected and identified as early as possible. In recent times, several molecular, serological and proteomic-based methods have been developed. However, these methods have several disadvantages such as they are expensive, labor-intensive, bulky, among others. The culture-based techniques are considered the gold standard. Though sensitive, they too suffer from inherent disadvantages of long time-to-detection. Hence, there is an urgent need for the development of rapid and cost-effective techniques for detection and identification of bacterial pathogens.

Here, we present an approach that can detect the presence of viable microorganisms in suspensions, much faster than culture-based technique. The existing automated culture-based systems detect the metabolic changes in the growth media and the environment of the bottles containing the media (parameters monitored like pH, Oxygen, Carbon Dioxide among others) that change as the bacteria proliferates. As this changes in pH, Oxygen and others can be minuscule, a large number of bacteria is needed before the changes can be detected. This increases the time-to-detection significantly for culture-based techniques. Our technique, microchannel Electrical Impedance Spectroscopy (m-EIS), relies on the fact that on the application of an AC electric field to a bacterial suspension, the viable bacterial cells become polarized and store charges due to the presence of intact cell membranes. As a result, they behave as electrical capacitors. Any change in the number of bacterial cells in the suspension (like growth or death of cells) is reflected by a concomitant shift in the storage of bacterial charges and capacitance of the bulk. Due to the unique

geometry of the measuring device (microfluidic cassettes) used by us, we can distinguish between the capacitance arising due to the bacterial cells and that of the parasitic double layer capacitance.

A practical application of this technique has been found to be useful for detection of clinically significant slow-growing mycobacterial cultures. Most of the automated culture-based systems available in the market are based on the measurement of the growth dynamics of the microorganisms. However, as the generation time of the slow growing bacteria is long, these systems take a long time (6-8 weeks) to generate results. With the use of our m-EIS measurement technique, we can reduce the times-to-detection by ~50%.

Further, we observed that the time-to-detection is further reduced by monitoring cell death in real time using our technique. As only living entities can be killed, our technique can detect the presence of viable cells in a suspension by monitoring their death. It has been observed that using our technique following the death dynamics is much faster than growth dynamics. The death of microorganisms that have long generation times like mycobacteria can be achieved by use of antibiotics (depending on which antibiotics and its concentration) at a much faster rate than their growth in a nutrient media. Real-time monitoring of death shows a decrease in the bulk capacitance values which provides us the time-to-detection much more rapidly.

CHAPTER 1

1 INTRODUCTION

1.1 Motivation

Bacteria is ubiquitous. Though most bacteria are harmless, some are virulent and can cause diseases. These harmful, pathogenic bacteria may be present in our body, food, water and other consumables and can cause huge damage and losses. For examples, pathogens in the human body like *Escherichia coli, Salmonella*, *Staphylococcus aureus, Psedumonas aeruginosa, Mycobacterium tuberculosis,* result in infections and contagious diseases like food poisoning, wound infections, toxic shock syndrome, meningitis, tuberculosis, and eventually, may lead to morbidity and mortality (1). Among the top ten leading causes of death in 2011, World Health Organizations (WHO) identifies infectious and parasitic diseases, lower respiratory tract infections and tuberculosis as the second, third and seventh leading causes of mortality (2). These infections also result in significant production losses.

Recent developments in the manufacture of food products and other consumables involve techniques like pasteurization, canning, which have led to the reduction of harmful bacteria. However, some hardy bacteria like *Listeria monocytogenes, Clostridium botulinum* etc. survive these techniques and cause spoilage of food products. These bacteria often lead to an outbreak of illness and epidemic diseases amongst people consuming the contaminated products. Recent estimates show that these can result in loss of about 1 billion dollars each year (3). Mead et. al found that contaminated food products result in 76 million foodborne illness and about 5000 deaths in the United States alone (4).

Thus, there is an urgent need for proper detection, characterization, identification and treatment of diseases caused by bacterial pathogens. Proper detection and identification of pathogens become significantly complicated as in many cases they do not have definitive clinical manifestation. This also makes early screening difficult (1). Moreover, most times it is difficult to differentiate between closely related species.

Current gold standard for detection of bacteria is culturing techniques. The culturing technique involves growing bacteria in liquid or solid media, and either measure the colonies formed or the various growth indicators like metabolic products produced, pH changes, etc. over the extended incubation period. Recent molecular methods based on genomics and proteomics have significant advantages over conventional culture-based techniques; that is, they do not involve lengthy incubation period and thereby reduce the time for analysis (5, 6). However, these methods are expensive and in many cases often cannot distinguish between viable and non-viable bacteria.

Rapid identification and detection of bacteria are essential for public health and clinical diagnosis. In some cases, bacterial identification can influence the course of treatment and decrease the propagation of antibiotic resistant bacteria and hence, the spread of infection. In case of foodborne illness, the detection techniques need to be rapid so that the contaminated products is removed from public to prevent an epidemic. There is also a need for rapid detection of biological warfare agents in case of bioterrorism (2). Hence, recent focus has shifted to rapid detection and identification of pathogenic bacteria and their control/elimination in public health, clinical and environmental settings and food safety monitoring (5).

1.2 Healthcare-associated infections (HAIs)

During treatment, infections may occur in hospitalized patients being treated for other illnesses (7). This transmission of infection in hospitalized patients may be due to various reasons like their weak immune systems or the invasive procedures being performed on them or the poor infection control procedures in the hospitals and are known as Healthcare-associated infections. HAIs not only increase patient mortality and morbidity but also prove to be an enormous economic burden to the patients. It often leads to patient inconvenience and loss of productivity. HAIs include central line-associated bloodstream infections (CLABI), catheter-associated urinary tract infections (CAUTI), ventilator-associated pneumonia (VAP), surgical site infections (SSI) and Clostridium difficile-associated disease (CDI) (8). Centers for Disease Control and Prevention (CDC) tracks the HAIs occurring in the healthcare system and provides guidelines to prevent/ reduce the number of incidences occurring (9). Scott et. al has estimated the overall cost of treating HAIs as approximately 4.5 HAIs for every 100 hospital admissions to about $6.65 billion dollars in 2007 (post correction of inflation) (8).

It has been estimated that about 50% of HAIs is preventable (10). So, it can be seen that there is significant scope for improvement and reduction in the number of HAIs and to save lives. Although it is not possible to emphasize on all area of HAIs, we have attempted here to reduce the number of infections occurring due to SSIs. In chapter 2, the SSIs occurring due to orthopedic implants is studied. Though these SSIs are less common, they are more difficult to treat as they need long and stringent antibiotic treatments and may need surgical procedures (11).

Over the years, there has been a tremendous increase in the usage of orthopedic implants for short term or long term to assist in the normal function of the human body.

The usage of implants has been found to be increasing with increasing life expectancy and also, due to the increase in the number of accidents and injuries resulting from our modern and dynamic lifestyle. Other factors involved include an increase in public awareness and availability of improved/ better medical procedures. After being introduced in the body, these implants encounter various body fluids like blood, proteinaceous matter, and cells present in the body. Often these interactions lead to the development of biofilms at the site of implants and result in infections. Also, it can result in improper osseointegration. Both of these conditions might delay patient recovery, lead to extreme morbidity and sometimes in mortality.

To treat SSI resulting from implants, clinicians either rely on the usage of antibiotics or debridement techniques or in some cases, use a combination of both. Therefore, researchers are looking for techniques, which will slow the onset of infections while improving osseointegration. An ideal preventive method should be able to prevent biofilm formation and kill the infection-causing bacteria surrounding the implant while help in the healing process. In Chapter 2 the current implant surface modification and coating techniques that are available which prevent infection are examined in depth. The contents chapter 2 have been published as a manuscript entitled "Coatings and surface modifications imparting antimicrobial activity to orthopedic implants" in the journal Nanomedicine and Nanobiotechnology.

The occurrence of SSIs after any surgery is of concern, be it orthopedic or any other surgery. Among all nosocomial infections, SSI accounts for about 20% of infections, and the estimated cost of treating SSIs is about 10 billion dollars (8, 12-14). Bacteria can enter a patient's body through the operation site (15). Healthcare providers try and prevent SSIs

through a combination of techniques. Common techniques that are used before any surgery involves sterilization of operating rooms, proper cleaning, and de-hairing of the surgical site and cleaning of surgical sites using antibiotics. Some of the commonly used antibiotics involve Iodine, Betadine, alcohol, among others (16).

Chapter 3, compares an in-house antibiotic spray-on protocol to the 5-minute antibiotic scrub protocol which is commonly used for surgical site preparation (17). The results from the *in-vitro* testing of the spray-on surgical site preparation method on both agar plates and porcine skin are compared to the scrub protocol. The contents of chapter 3 have been published as a manuscript entitled " Foaming Betadine Spray as a potential agent for non-labor-intensive preoperative surgical site preparation" in Annals of Clinical Microbiology and antimicrobials.

1.3 Emerging Infectious Diseases

Pathogenic microorganisms (bacteria, fungi, viruses, parasites) are responsible for causing various infectious diseases in humans (18). These diseases are contagious and can be transmitted by direct (coming in contact with an infected person) or indirect means (spread by a vector). Researchers have used the term emerging infectious diseases to define infections that are newly appearing in humans or are rapidly spreading amongst humans or are widespread in any geographic areas (19, 20). Some of the examples of infectious disease involve multidrug-resistant tuberculosis, pandemic influenza, HIV/AIDS, severe acute respiratory syndrome (SARS) (21). If undetected, these diseases lead to economic losses, social stigma, widespread fear, morbidity, and mortality. According to the Report on Infectious Diseases published by WHO in 1999, out of the 54 million deaths happening due to various causes, about 13 million deaths were solely due to infectious diseases (18).

The bulk of the deaths resulted from pneumonia, diarrheal diseases, and tuberculosis (7.2 million deaths) (22).

According to the 2012 Global Report for Research on Infectious Diseases of Poverty, 1 billion people are affected by one or more infectious diseases. The economic impact of these diseases is felt even by those who are not struck by the disease. The economic impact is widespread as can be seen from reports which estimate losses due to SARS to be 50-140 billion dollars while that due to N1H1 to be about 2.7-4.5 billion dollars (23).

However, the emergence of infectious disease can be avoided or controlled and cured by proper treatment using antibiotics (24). Misdiagnosis and overuse of antibiotics have often resulted in antibiotic resistance in the causative organisms. Hence, there is an urgent need for rapid and timely detection as well as proper and effective treatment of infectious diseases.

Tuberculosis is considered to be the second deadliest infectious disease after HIV. In 2012, about 1.2 million people died due to tuberculosis (25). Tuberculosis can be prevented and cured by timely diagnosis and proper treatment. Between 1995 and 2011, about 51 million lives had been saved by effective treatment strategy adopted by WHO (25). However, the microbiological detection and drug susceptibility of tuberculosis are critical and take a long time when culture-based methods are adopted. Currently, automated culture-based techniques are mainly used to detect the presence of viable bacteria and considered to be the gold standard. However they have long time-to-detections. The use of electrical impedance spectroscopy (EIS), where AC voltage is applied to bacterial suspension enables us to significantly reduce the time taken to detect mycobacteria. The

basics of EIS are given in Chapter 4.

Mycobacteria is very different from other bacteria as is described in detail in Chapter 5. Mycobacteria have mycolic acid present in their cell walls, and as a result, they are resistant to decolorization by acids and gram staining cannot be done for them (26). Usually, the acid-fast stain is performed to estimate the presence of mycobacteria in a sample where they are stained red and appear as long rod-shaped species under a microscope. In addition, due to long doubling times of mycobacteria the time to detection is very long on culture-based techniques.

Chapter 6, compares the times-to-detection for estimating the presence of mycobacteria in an *in-vitro* commercially available fully automated MGIT 960 system against our technology, based on electrical impedance spectroscopy (EIS). Commercial culture-based systems study and record the bacterial growth based on their metabolic products produced or by detecting a change in the system due to the metabolic products. Our system studies the change in the bulk capacitance of the system over time, which is an indication of the bacterial dynamics in the system. In this chapter, we demonstrate that our system has lower times to detection that is considerably lower than that obtained by the automated culture based systems. The contents of chapter 6 have been submitted as a manuscript entitled "Rapid culture-based detection of living Mycobacteria using microchannel Electrical Impedance Spectroscopy" to Biological Research Journal.

Chapter 7 is based on the fact that since only living entities can be killed, an approach that can detect the death of microorganisms should confirm the presence of viable organism. Most of the commercially available techniques detect the presence of mycobacteria based on the growth of the bacterial colonies or their metabolism/ growth

signature. However, we have seen that impedance spectroscopy can detect both growth and death of bacteria over time. By following the real time death of organism using EIS, the time-to-detection becomes dependent not on the growth dynamics but on how fast the organisms can be killed.

1.4 Current gold standard for microorganism detection

For health care personnel to treat his/her patients, they need medical knowledge to be supported by patient history, clinical microbiology laboratory facts and pharmacokinetics of antibiotics (27). Blood cultures are the current gold standard available for clinicians for detection of viable microorganisms (27, 28). Efforts have been made to implement automated culture-based diagnostic platforms which have high sensitivity and need minimum human intervention.

There are several automated systems currently available in the market like BacT/Alert™ from BioMeriux, Bactec™ from BD, ESP™ from Difco for blood culture tests while MGIT 960 system from BD, VersaTrek Mycobacteria detection system from VersaTrek for mycobacterial detection. When a sample containing viable bacteria is loaded into these instruments, the bacteria in the presence of nourishment (growth media) tend to grow, metabolize and increase in numbers. These automated devices monitor the metabolites generated, or they measure the changes in the system due to the generated metabolites to infer the presence of viable bacteria. Hence, the time to detection for these instruments is directly related to the doubling time of the microorganism. Longer the doubling time, the longer will be the time to detection, resulting in a delay in initiation of treatment.

The only disadvantage associated blood culture techniques is a long period taken

to detect viable organisms. However, with recent advances, several novel, non-culture-based techniques like PCR, molecular probes, have been developed. These techniques though much faster, are expensive and need specialization. Moreover, unlike the culture-based diagnostic techniques, these non-culture based techniques can perform limited drug susceptibility testing. To reduce and prevent infections, rapid detection, and timely treatment is of paramount importance.

In addition to blood, several other samples of sputum, stool, can be tested. For example, to detect tuberculosis, the sputum obtained from the patient is decontaminated to kill all other bacteria and then the decontaminated sputum is cultured to estimate the presence of viable bacteria. As the causative organism, *Mycobacterium tuberculosis*, is a very slow growing mycobacteria, with a growth time of ~24 hours, the culture techniques may take weeks to become positive. The cultures are held on for 6-8 weeks before being deemed negative. Hence, culture-based diagnosis can take anywhere from 3 days for blood culture works to ~6- 8 weeks for mycobacterial detection. As identification of organism is delayed, proper treatment is delayed. During this period the patient is typically administered broad spectrum antibiotics which result in antibiotic resistant organisms. This also results in an increase in patient morbidity and mortality.

Therefore, there is an urgent need to develop a culture-based technique that is highly sensitive and can rapidly determine the presence of viable microorganisms while reducing the time necessary to do so. Thereby, we can initiate faster and proper treatment of the patients.

CHAPTER 2

2 COATINGS AND SURFACE MODIFICATIONS IMPARTING ANTIMICROBIAL ACTIVITY TO THE ORTHOPEDIC IMPLANTS

The material presented in this chapter was reviewed and published as "**Coatings and surface modifications imparting antimicrobial activity to orthopedic implants**"

Roli Kargupta, Sangho Bok, Charles M. Darr, Brett D. Crist, Keshab Gangopadhyay, Shubhra Gangopadhyay and Shramik Sengupta

Wiley Interdiscip Rev Nanomed Nanobiotechnol, 2014. 6(5): p. 475-95.

Bacterial colonization and biofilm formation on an orthopedic implant surface is one of the worst possible outcomes of orthopedic intervention in terms of both patient prognosis and healthcare costs. Making the problem even more vexing is the fact that infections are often caused by events beyond the control of the operating surgeon and may manifest weeks to months after the initial surgery. Herein, we review the costs and consequences of implant infection as well as methods of prevention and management. In particular, we focus on coatings and other forms of implant surface modification in a manner that imparts some antimicrobial benefit to the implant device. Such coatings can be classified generally based on their mode of action: surface adhesion prevention, bactericidal, antimicrobial-eluting, osseointegration promotion, and combinations of the above. Despite several advances in the efficacy of these antimicrobial methods, a remaining major challenge is ensuring retention of the antimicrobial activity over a period of months to years post-operation, an issue that has so far been inadequately addressed. Finally, we provide an overview of additional figures of merit that will determine whether

a given antimicrobial surface modification warrants adoption for clinical use.

2.1 Introduction

Orthopedic implants are widely used devices in orthopedic surgery to provide rigid support for fractured bones and joint augmentation or replacement for pain relief and improved function. A plethora of orthopedic implants has been developed including fracture fixation devices (e.g. intramedullary nails, pins, plates, screws) and prosthetic joints (e.g. partial and full knee, hip, and shoulder). Once inserted, orthopedic implants may be required to function for decades (i.e. arthroplasty). During this time, implant materials not only come into intimate contact with various bodily fluids, proteinaceous matter, and host cells but also are expected to integrate and bond with the surrounding osseous tissue. Failed or Incomplete osseointegration is often associated with the presence of bacteria, which form an impenetrable biofilm that initiates host immune responses. If left unchecked, infection ultimately leads to tissue morbidity at the bone-implant interface and implant failure (29). *Staphylococcus* species account for nearly 30% of all implant infections, which not only threaten the implant and affected bone, but can result in systemic infection and loss of life and limb if not judiciously identified and managed (30-33). Compounding this issue is the drastic rise in usage rates in the last 20 years as a result of increasing trends in life expectancy, higher quality-of-life expectations, patient confidence in implant procedures, and improved surgical techniques. The 2010 National Health Discharge Survey by the Centers for Disease Control and Prevention (CDC) reported over 719,000 total knee arthroplasty (TKR), 332,000 total hip arthroplasty (THR), and 438,000 fracture surgeries with internal fixation increased from 129,000 TKR, 119,000 THR, and 305,000 fracture reduction surgeries in 1990 (34, 35). This staggering number represented

a 2010 global annual market for orthopedic implant devices of more than $30 billion with a compounded annual growth rate (CAGR) of 8.2% (36), providing an expected market of more than $50 billion by 2018. Despite modern advances in aseptic technique, surgical site infections (SSIs) remain a major challenge in the world of orthopedics (30). According to the National Healthcare Safety Network (NHSN), SSIs occurred after 1.12% of orthopedic procedures between January 2006 and December 2009 (37). However, certain classes of implants are more prone to infection than others; fracture fixation devices report ~5% infection rate (11). SSIs increase the need for costly and potentially life-threatening revision surgeries with revision THR increasing by 3.7 procedures per 100,000 persons per decade and revision TKR by 5.4 procedures per 100,000 persons per decade (38).

Diagnosis and treatment of orthopedic infections can be quite challenging as the symptoms vary widely from patient to patient and may be mistaken for other conditions since they include some general indications: pain, tenderness, local warmth, fever, foul odor, and fluid discharge (32). Routine blood work may reveal systemic inflammation through elevated C-reactive proteins (CRP) or white blood cell count but does not elucidate the cause. These may still be elevated in the early postoperative course. More accurate tests such as joint aspiration or blood cultures can identify specific microorganisms but may take 2-5 days depending on the species and required tests. Furthermore, there is a potential for the aspirate to have been a false-negative (39). Radiological imaging techniques (e.g. X-ray, computer tomography (CT), magnetic resonance imaging (MRI), ultrasound) may be helpful, but may not show changes until the infection is extensive and imaging studies are expensive (33). More recently, polymerase chain reaction (PCR) DNA amplification and sequencing techniques have been used, but have limited sensitivity and specificity and

have long incubation and detection times (40). In the meantime, the patient is given potentially unnecessary, contraindicated, or counterproductive medications, resulting in increased healthcare costs and bacterial antibiotic resistance. Typical primary treatment on identification involves surgical revision including debridement of the infected tissue coupled with the use of both local and systemic antibiotics. However, infection recurs in at least ~36% of cases (41). Repeated and prolonged infection indicates complete surgical implant removal and replacement, which again increases both patient suffering and healthcare costs (32). Given the severity of these undesired outcomes, perhaps the most appropriate way to confront bacterial infection is through proactive measures that simultaneously prevent bacterial colonization and promote osseointegration. This review will provide an overview of the current state-of-art information addressing these critical needs through implant device surface modification and surface coatings as well as their role in preventing implant-related infections.

2.2 Biology of Orthopedic Infections

Significant study has been devoted to the interaction of biofilm-forming bacteria with host cells and implanted devices, though some questions remain unanswered (42, 43). It should first be noted that successful orthopedic device implantation is an inherently difficult process even in the absence of bacteria since the host immune system immediately recognizes the implant surface as “foreign” and induces the formation of a proteinaceous layer to promote wound healing. However, if bacteria happen to be present as a result of previous or *de novo* infection, this proteinaceous matter acts as a conditioning layer that enhances bacterial adhesion. An experimental investigation has suggested that biofilm formation is a five-step process (Figure 2-1) (44). Initial bacterial attachment to the implant

surface is mediated through either non-specific (e.g. hydrophobic or van der Waals interactions) interactions with the proteinaceous layer or specific interactions such as those involving the *Staphylococcus aureus* (*S. aureus*) surface protein autolysin (Figure 2-1a) (45, 46). Once securely anchored to the surface through irreversible attachment, bacteria proliferate at a rate governed by the availability of nutrients and oxygen as well as their

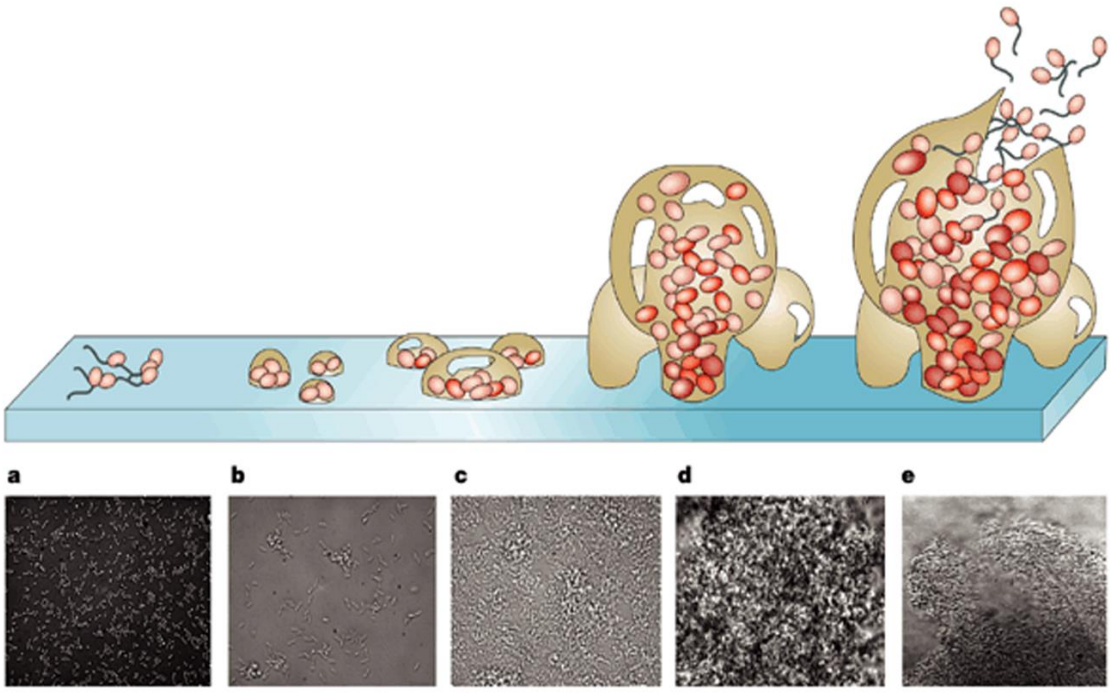

Figure 2-1 A pictographic representation of the steps in bacterial biofilm formation using a Pseudomonas aeruginosa case study (44). (a) Bacteria adhere loosely and reversibly to the surface by non-specific binding, (b) Bacteria attach irreversibly to the surface and begin forming cell clusters, (c) Accumulation – Multiple layers of bacteria form and EPS layer provides protection to bacterial community, (d) Maturation - Biofilm reaches maximum thickness, and cells communicate via quorum sensing, and (e) Dispersion – Clusters detach and infection spreads to new areas. (Reprinted with permission from **Ref [44].** Copyright 2003 Nature Publishing

intrinsic metabolism (Figure 2-1b). After a region of the implant surface reaches a certain numerical cell density, physiological changes are induced in the bacteria that lead to the formation of a "biofilm," a protective matrix composed of extracellular polymeric substance (EPS) (Figure 2-1c) (42, 47). Depending on the bacterial strain and local environmental conditions, the EPS may consist of exopolysaccharides, proteins, glycoproteins, glycolipids, teichoic acids, and extracellular DNA (42, 47). The micro-ecosystem formed within the hydrated biofilm matrix is resistant to antibiotics, detergents, phagocytosis and other human immune system responses and further enables the interiorized cells to communicate through quorum sensing (Figure 2-1d) (44, 48). During the final step, the previously protected bacteria detach from the biofilm, migrate to a new area, and colonize the surrounding surfaces, resulting in spread of infection (Figure 2-1e). Pathogen dispersal from the biofilm can be truly devastating to patient health, leading to life-threatening downstream diseases ranging from endocarditis to sepsis (49).

2.3 Approaches to Prevent and Manage Orthopedic Infections

Pathogenic bacteria most often enter the host body at three critical periods: traumatic lacerations at the time of the incident, at the date of procedure, or during postoperative healing (50). Preoperative infections occurring in other parts of the body should also be identified and under control to prevent the possibility of hematogenous infections (51). The probability of implant infection can be reduced significantly by eliminating preoperative sources of bacterial contamination. Common preoperative strategies to reduce infection during implantation include hand cleaning by surgeons with alcohol-based antimicrobial agents, and preoperative antimicrobial skin preparations, commonly but not always, followed by patient hair removal at the incision site (52, 53). Other factors that need to be

taken into consideration include instrument sterilization, operating room air quality, use of laminar airflow systems, controlling the entry and exit of personnel from the operating room, and sterile gowns and uniforms (51, 54). Preoperative administration of antibiotic prophylaxis has also been found to be effective in reducing infections (51, 54). A recent study by Rao et al. showed that found that *S. aureus* positive THR/TKR patients receiving intranasal mupirocin and chlorhexidine experienced no SSIs within a two-year follow-up period (54). However, patient non-compliance with drug administration results in about 10% of hospital admissions related to implant site infection, reducing the overall effectiveness of this technique significantly (55).

Table 2.1: The different categories of orthopedic infections based on time of infection with respect to the operation.

Category of infection	**Time period**	**Causative agent**	**Symptoms**	**Treatment**
Early (33, 56-58)	<3 months	Virulent bacteria (e.g. *S. aureus*)	Pain, fever, swelling, tender wounds	Antibiotics; no surgery required
Delayed (33, 56)	Three months to 2 years	Small number of low-virulence bacteria (e.g. coagulase-negative *Staphylococci*)	Acute inflammation, infection, implant loosening observed	Antibiotics ineffective even with surgical intervention (e.g. debridement)

Late (49, 50)	>2 years	Hematogeneous infections caused by bacterial colonies present in dental, urinary, or respiratory systems	Severe pain	Surgical intervention

Orthopedic infections can be organized into three distinct categories based on the time of infection on the operation: early, delayed, and late (Table 2.1) (56). The risk of bacterial infection is typically highest immediately following implant placement, especially when tissues are exposed to trauma. Early infections manifest within three months of implantation and result from virulent bacteria such as *S. aureus* (57). Symptoms associated with early infections include pain, fever, swelling, surgical site tenderness and drainage. These can be potentially treated with antibiotics and sometimes implant retention is possible. For arthroplasty, the polyethylene components are typically exchanged. However, early infections may still result in chronic and systemic infection if left untreated (33, 58). Meanwhile, delayed infections manifest between 3 to 12 months post-operation with some authors extending this period to 24 months (33, 56). These are associated with acute inflammation and severe pain but may include implant loosening and sepsis. Delayed infection can result from either a very low number of initial infecting bacteria, unfavorable growth conditions, or low-virulence bacteria (e.g. coagulase-negative *Staphylococci*) (56, 57). These infections normally do not respond well to antibiotics even after surgical debridement of the affected tissue. Implant removal, surgical debridement, and local antibiotic delivery systems (antibiotic cement) is standard for arthroplasties. As long as a

fracture is still healing and the fracture implants are still stable, the implant retention is attempted. Late infections manifest at least two-years post-operation. These are typically latent hematogenous infections resulting from bacterial colonies already present in the dental, urinary, or respiratory systems.

Infection classification by postoperative period is important in developing a treatment strategy, but cannot be the sole basis for the decision. Other factors impacting the course of treatment include patient medical conditions and preference, surgical procedure and implant type, type and location of tissue infected, species of infecting organisms, infection severity at the time of detection, and inherent patient resistance to infection (11, 32, 57). The procedure suggested depends on the patient ability to endure treatment, including the increased cost, discomfort or disability, and hospital stay. Antimicrobial therapy is essential to combat infection (59, 60). In fact, doctors may prefer a more conservative antibiotic treatment to surgery in cases when the patient's medical conditions preclude the ability to tolerate multiple surgeries. The most common antibiotics prescribed are cephalosporins, oxacillin, and vancomycin. However, local antibiotic resistance patterns vary and may require input from local infectious disease specialists.

Some of the surgical approaches adopted include implant retention with debridement, implant removal with staged replantation, and arthrodesis/amputation. Debridement comprises the removal of damaged or infected tissue surrounding a well-fixed implant. In this case, the implant is retained, and antibiotics are provided to prevent the spread of further infection (33), but there is no consensus as to the type or duration of antibiotic therapy (61). This treatment is suitable for patients with early postoperative infections with intact implants and confirmed pathogenic species. A higher failure rate has

been demonstrated in cases of debridement and retention where symptoms of infection persisted for more than one week before treatment or if a sinus tract was present (62). Moreover, the probability of infection recurrence is ~54% in prosthetic joint infections due to *S. aureus*, likely a result of the virulence of this strain (63). Implant revision is a one- or two-stage surgical procedure to remove and replace an infected implant. In the one-stage procedure, the infected implant is removed, infected tissue is debrided, and a new implant is inserted immediately. The one-step procedure is indicated only for those patients who cannot withstand the physical demands of the two-step procedure. The two-stage version is more common than others. In this version, the implant is removed and local antibiotics, such as antibiotic-impregnated cement, are placed in addition to systemic antibiotics. Typically, the second stage of replantation occurs after a six-week course of antibiotics is completed and normalization of the inflammatory markers occurs. However, this is dependent upon the pathogenic organism and may be delayed for a year for gram-negative organisms. The delay between debridement and implant insertion has been demonstrated to be a crucial factor in the success of the revision implantation, but the duration of the delay varies (32, 64). Delays ranging from 4 weeks to 3 months have been reported (65). Antibiotic-impregnated spacers have proven effective in reducing hospital stay duration and increasing patient mobility after THR (65). Vergidis et al. further observed the lower incidence of infection in cases of revision hip arthroplasty in which antibiotics were administered both systematically and in a bone cement (60). Typically, arthrodesis or amputation are reserved for patients with severe or recurrent infections and are more common in patients with severe medical problems (66). These are typically seen as last resort.

Antibiotic administration and surgical intervention are only necessary if the infection is present. A more desirable option would be proactive prevention of bacterial colonization to circumvent infection altogether. Engineering the implant surface to provide some antimicrobial or osseointegration benefit is one line of development that has been taken up in recent years. Essential characteristics of well-designed implants include porosity to enable strong bony ingrowth (i.e. osseointegration) (67) in long-term implants but prevent bony ingrowth in short-term implants, appropriate mechanical strength and elasticity to match the host tissue, low surface friction, corrosion resistance, ability to reduce inflammation, improved tribology, and reduced bacterial adhesion to the surface. In many ways, reducing bacterial adhesion and improving osseointegration are inherently coupled since there is surface binding competition between bacteria and host bone cells. Forming a strong bone-implant bond requires the formation of an apatite layer at the bone-implant interface (29). Proper osseointegration not only allows for swift patient recovery but also prevents implant migration and failure.

A variety of approaches has been attempted to improve osseointegration while simultaneously reducing infection and include: modifying implant surface energy, surface charge, composition, surface morphology and roughness, as well as the addition of functional surface coatings (68). In the following sections, we will report on the critical advancements being made in antimicrobial implant surface coatings and their effectiveness at preventing or mitigating the severity of bacterial infections and reducing patient recovery time. A particular emphasis will be placed on coating longevity or use life. While this information is not always readily available, we believe this property will have a significant impact on which technologies will gain wider acceptance shortly.

2.4 Antimicrobial Coatings

A wide variety of functional antimicrobial coatings is already available on the market today. Some examples of FDA-approved implant coatings include INFUSE^{TM} bone graft from Medtronic (69), CarriGen porous bone substitute material from ETEX (70), Cerasorb from Curasam (71), and Spineplex P Bone Cement from Stryker (72, 73). Many others are at various stages of development and testing for regulatory approval. In this review, we classify antimicrobial coatings into five general categories based on their method of intervention in the infection and biofilm formation process: (1) Coatings that physically

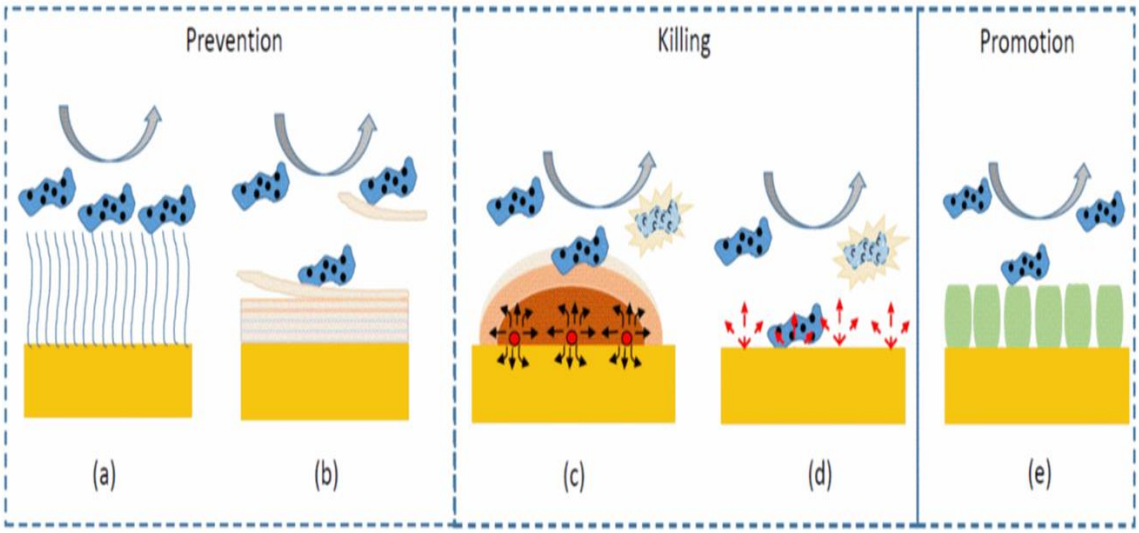

Figure 2-2 A schematic illustrating the various modes of action of different coatings and surface modifications. (a) Prevention of bacterial adhesion is possible due to physical actions like presence of polymer brush, (b) Prevention of bacterial adhesion owing to the presence of a sacrificial layer which do not allow the bacteria to adhere to the surface, (c) Killing of bacteria due to the release of antimicrobial agents to the surrounding regions, (d) Killing of adherent bacteria owing to the presence of antimicrobial agents present on the surface and (c) Promotion and acceleration of desired cells which competes with the bacteria to promote osseointegration and prevent colonization.

prevent bacterial adhesion, (2) Coatings that kill adherent bacteria, (3) Coatings that release antimicrobial agents to the surrounding region, (4) Coatings that accelerate adherence of desired cells (osteocytes), and (5) Coatings presenting more than one mode of action. A schematic illustrating the general principles of different coatings is shown in Figure 2-2. A summary of the various coatings and surface modifications imparting antimicrobial activity to orthopedic implants and their duration of efficacy can be found in Table 2.2.

2.4.1 Coatings that prevent bacterial adhesion

The first approach to preventing infection is to prepare a surface that microbes find difficult to colonize in the first place. This can be achieved through some ways including biodegradable surfaces to slough off adhered bacteria, and adhesion-resistant coatings as will be detailed below.

2.4.1.1 Sacrificial coatings

Modifying the implant surface with a sacrificial layer that dissolves away after a short time can be used to draw out any bacteria that had adhered to the original surface (74). Some biodegradable polymers have been used to this effect including polylactide (75, 76), glycolides (77), and lactones (78). Most resorbable polymers are designed to degrade within 9–10 weeks followed by controlled drug release for a subsequent 2–3 weeks (74). More recently, Wang et al. reported a degradable multilayer anti-adhesive coating using polyvinylpyrrolidone/poly(acrylic acid) (PVP/PAA) on top of a pre-existing multilayer antimicrobial coating of heparin/chitosan (HEP/CHI) (79). Thermal crosslinking the multilayer PVP/PAA films for specific periods are used to modulate the degradation rate (Figure 2-3). Complete degradation of the top PVP/PAA multilayer film occurred within 24 hours, after which the underlying multilayer antibacterial HEP/CHI film remained and

continued to supply benefit to the implant. This layer-by-layer technique showed significant promise toward multi-functional time-release coatings but requires more work before the extensive clinical application will be feasible.

2.4.1.2 Adhesion-resistant coatings

One of the approaches to prevent an infection from developing is to prepare a surface to which microbes find it hard to become strongly attached via chemical bonds. They include polyethylene glycol (PEG), diamond-like carbon (DLC), and polymer brushes as explained below.

1. Unstructured polymer coatings

Polyethylene glycol (PEG, $[CH_2CH_2O]n$) was first used for inhibition of microbial adhesion by introducing to modified polyurethane surfaces (80). Bacterial resistance by PEG-modified or "PEGylated" surfaces results from some material properties such as PEG chain density, length, and conformation. Proper selection of these properties allows the polymer to retain interfacial water, which does not favor microbial adhesion. Furthermore, PEG is resistant to compressive forces due to its tendency to remain in extended coil conformation and dynamic chain movement (80-82). PEGylated surfaces effectively inhibit microbial adhesion by up to a 3 log unit reduction in attached microbes, and is also effective in reducing adherent proteins and mammalian cells (82). Other hydrophilic polymers such as poly(2-hydroxyethyl methacrylate) (83) and phosphoryl choline-based polymers (84) also resist protein adsorption. The creation of PEGylated surfaces requires multi-step synthesis. PEG-based surface treatment has developed as a self-assembled monolayer (SAM), polymer brush, and hydrogel (81).

2. Polymer brush coatings

Polymer brushes exhibit some useful properties for anti-adhesive coatings such as excellent long-term stability, chemical robustness, biocompatibility, and controllable thickness (85, 86). Polymer brushes are assemblies of one or more polymers with one side tethered to the implant surface using either the "graft-to" or "graft-from" approach (Figure 2-4). The "grafting-to" approach employs a preformed polymer with a reactive end group while the "grafting from" approach involves building up the polymer *in situ*. Grafting-to typically produces low polymer densities due to steric hindrance. On the other hand, grafting-from typically results in high-density self-assembled monolayers (SAMs). Furthermore, polymer brushes can differ from linear to branched, like star-shaped, and from homopolymers to block-copolymers. Details about the grafting can be found in other literature (85-88).

Polymer brushes have been used in some medical applications including diagnostics, cell culture, scaffolds for tissue engineering, and orthopedic implants, the latter of which titanium (Ti) and its alloys are typically employed (86). Ren et al. demonstrated the use of polymer brushes on Ti surfaces (89). Ti was first coated with a SAM of the initiator (ω-mercaptoundecyl Bromo isobutyrate) and then the polymer Polyoligo-(ethylene glycol) methacrylate-r-2-hydroxyethyl methacrylate [Poly(OEGMA-r-HEMA)]. The modified surface was resistant to cell adhesion, but further immobilization of recombinant human bone morphogenetic protein-2 induced adhesion of MC3T3 cells. Similarly, Anagnostou et al. demonstrated that functionalized poly(methyl methacrylate) (PMMA)-based terpolymers inhibited more than 90% of *S. aureus* adhesion compared to untreated surfaces (90). Guo et al. (91) recently demonstrated an interesting emerging technique of three-

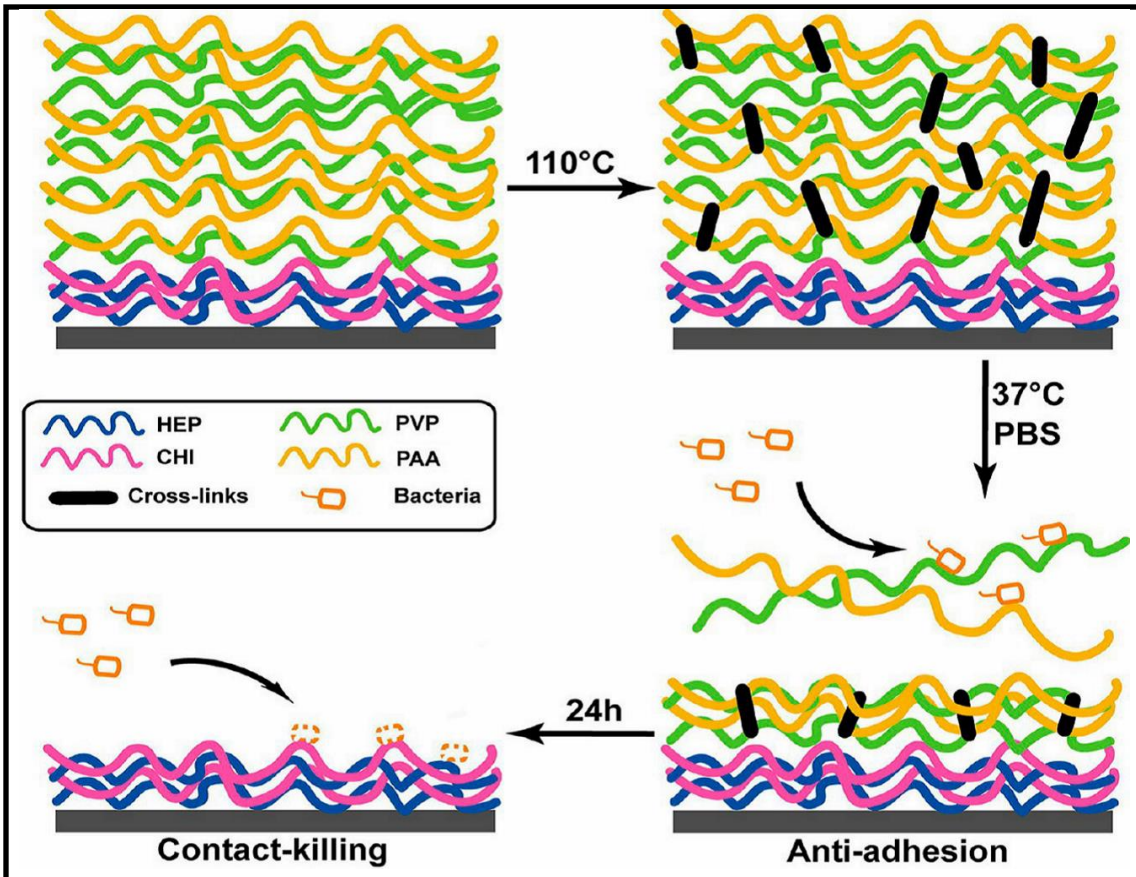

Figure 2-3 Schematic representation of multilayer biodegradable films produced by a layer-by-layer deposition method. Multiple layers of (heparin/chitosan)-(polyvinylpyrrolidone/poly(acrylic acid))x [(HEP/CHI)x−(PVP/PAA)x], where 'x' denotes the number of layers, are constructed based on electrostatic interaction for HEP/CHI and hydrogen bond interaction for PVP/PAA, followed by thermal treatment at 110 °C for 16 h for crosslinking to form anhydride groups. In simulated physiological condition (e.g. PBS buffer at 37 °C), $(PVP/PAA)_{10}$ layers were degradable in 24 hours, leading to almost no bacterial adhesion. After degradation of (PVP/PAA) layers, the underlying $(HEP/CHI)_x$ layers displayed contact killing of bacteria (79). (Reprinted with permission from **Ref [79].** Copyright 2013 American Chemical Society)

dimensional (3D) printing polymer brushes. Due to the heavy use of polymeric materials in most 3D printing, the 3D printed devices may not be feasible for biomedical purposes if these polymers are prone to bacterial colonization. However, Guo prepared a 3D printing resin by integrating with a vinyl-terminated initiator, which allows the 3D printed device to be grafted with desired polymer brushes (3-sulfopropyl methacrylate (SPMA)) by surface-initiated atom transfer radical polymerization (SI-ATRP). Gram-negative (*Escherichia coli*, ATCC 29425) and Gram-positive (*Bacillus subtilis*, ATCC 6633) bacteria were used and no visible colonization in 24 hours incubation was reported.

3. Diamond-like carbon coatings

Diamond-like carbon (DLC) is an amorphous carbon thin film initially developed and used as a protective coating in hard drive disks and recently adapted for biological applications including biocompatible surface coatings for implant devices (92). DLC benefits from a low friction, high wear resistance, chemical inertness, and optical transparency while also cheap and facile to produce. It has been reported that DLC coatings showed anti-adhesive characteristics when used as a coating on stainless steel. A comparison of bacterial adhesion to DLC-coated and uncoated stainless steel showed approximately 6×10^6 CFU/cm^2 reduction in *Pseudomonas aeruginosa* adhesion (93). DLC coatings may also be doped with material species such as silver or copper particles, yielding antimicrobial properties in addition to the anti-adhesive properties (94).

2.4.2 Coatings that kill adherent bacteria

It is unlikely a coating can ensure that not even a single bacterium will adhere to it. A different approach is to devise coatings that will kill any bacterium that does adhere.

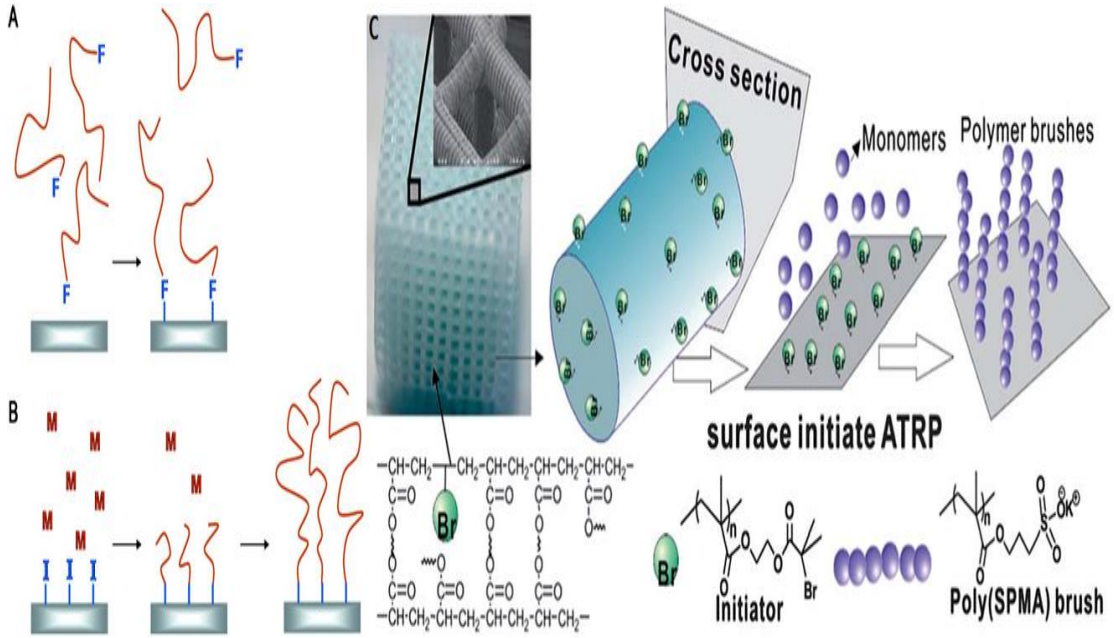

Figure 2-4 A) A substrate modified by grafting to approach in which the initially adsorbed polymer impedes further deposition, resulting in a low density of brushes. B) Modification of a substrate by the grafting of the approach in which an initiator-bearing substrate is exposed to the monomer to afford thick, dense polymer brushes (86). C) Schematic of grafting poly(SPMA) on the 3D printed structures (91): to initiate atom transfer radical polymerization (ATRP), the Br-containing vinyl-terminated initiator [2-(2-bromoisobutyryloxy)ethyl methacrylate (BrMA)] was pre-mixed with the resin consisting of acrylate-based pre-polymers, crosslinking agents, and a phosphine oxide-based photoinitiator. The acrylate-terminated polymers were utilized to incorporate with the initiator to achieve covalent bonding, and BrMA was used without affecting the photopolymerization during 3D printing processes. (A, B): Reprinted with permission from **Ref [86].** Copyright 2009 American Vacuum Society, C: Reprinted with permission from **Ref [91**]. Copyright 2013 Royal Society of Chemistry)

Some different types of coatings try to employ this method and will be discussed below.

2.4.2.1 Photoactive coatings

Titanium and its alloys are commonly used in orthopedic implants due to their excellent mechanical properties, corrosion resistivity, and biocompatibility. As such, titanium dioxide that forms on exposed titanium surfaces has been studied extensively for beneficial properties photocatalytic activity that can potentially kill adherent microbes. This effect was first demonstrated by Matsunaga et al., which showed 100% effectiveness against 10^3 CFU/ml *Saccharomyces cerevisiae* and 10^3 CFU/ml *E. coli* after 2 hours UV illumination (95). Evonik Industries (formerly Degussa) P25 manufactures the TiO_2 most widely used in antimicrobials research, consisting of an 80:20 anatase: rutile TiO_2 crystal structure, specific surface area of 50 ± 15 m^2/g, which was employed in the first demonstration of antimicrobial activity of TiO_2 by Matsunaga et al (95). In addition, many researchers prepare the TiO_2 materials by chemical vapor deposition (CVD) or sol-gel to improve the antimicrobial efficacy. Other approaches involve including metal additives such as copper and silver (96, 97). Sunada et al. (97) demonstrated the antimicrobial effect of Cu/TiO_2 materials under indoor UV irradiation (a few hundred nW/cm^2), which is about three orders of magnitude weaker than outside UV sources. The reactive species generated by the TiO_2 under weak UV radiation opened the outer membrane (Figure 2-5b) so that the Cu ions penetrated into the cytoplasmic membrane (Figure 2-5c). The TiO_2 photocatalytic reaction assists the intrusion of the Cu ions into the cell, which is why the Cu/TiO_2 film was effective against *E. coli* even under feeble UV light (97). These results, however, were reported under continuous UV radiation for several hours, which is infeasible for implants.

2.4.2.2 Metal-impregnated surface coatings

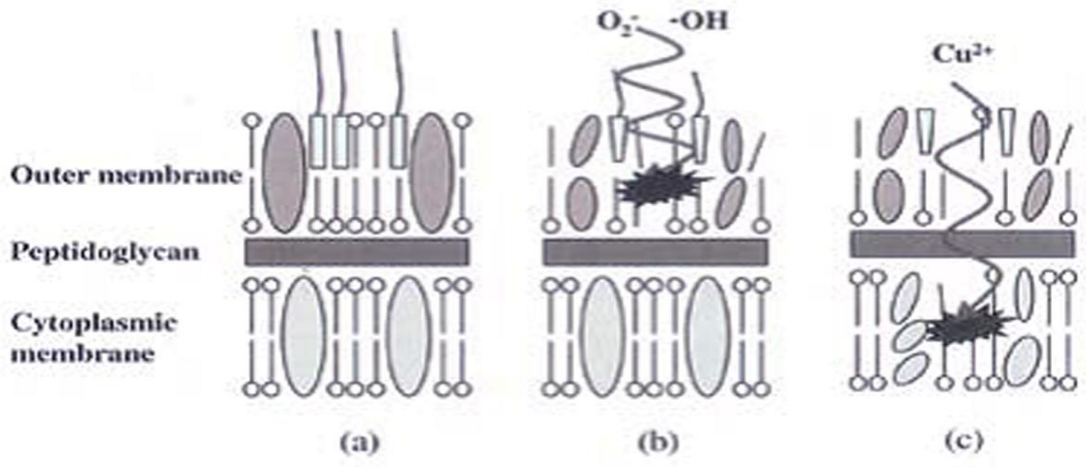

Figure 2-5 Schematic illustrating bactericidal process for *E. coli* cells on Cu/TiO_2 thin film under weak UV light irradiation (96). (a) E. coli cell membranes are shown, (b) reactive species generated by the TiO_2 photocatalyst attack and open the outer membrane, and (c) Cu ions effectively penetrate into the cell cytoplasmic membrane, resulting in cell lysis. (Reprinted with permission from **Ref [96].** Copyright 2003 American Chemical Society)

Various metal-impregnated coatings, including silver and copper, have been assessed in both *in-vitro* and *in-vivo* studies for the potential to decrease implant colonization. Metals identified as having antimicrobial activity include silver (Ag), copper oxide (Cu_2O, CuO), zinc oxide (ZnO), titanium dioxide (TiO_2), and tungsten oxide (WO_3). Ag is the most common in the literature resulting from the good antimicrobial activity, low toxicity, and established commercial use in *ex vivo* applications. The primary Ag bactericidal mechanism is through disruption of the bacterial cell membrane and metabolic protein function by binding to DNA and thiolated proteins. Ag-impregnated polymers have been successfully shown to protect the inner and outer surfaces of devices as antimicrobial coatings (98). Giglio et al. (99) demonstrated the antibacterial activity of electro-

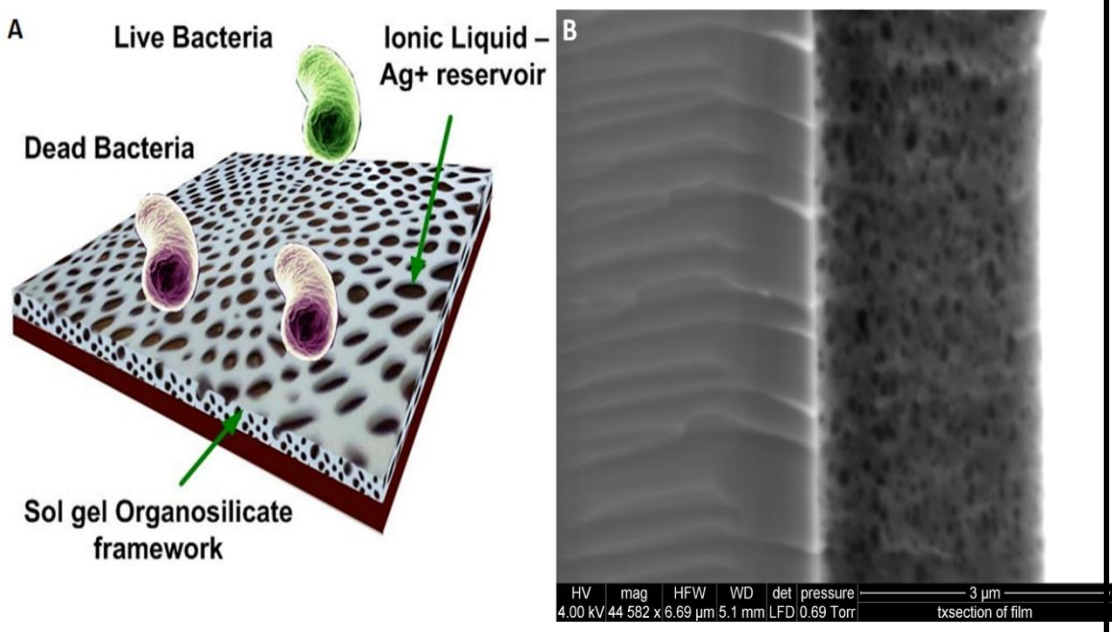

Figure 2-6 (a) Schematic showing the antimicrobial effect of a porous sol-gel coating incorporating a silver ion (Ag+)-generating "ionosol" on *E. coli* cells, (b) Cross-sectional SEM images of the antimicrobial coatings revealing porous structure throughout the coating (102). (Reprinted with permission from **Ref [102]**. Copyright 2012 American Chemical Society)

synthesized Ag nanoparticle (AgNP)-modified poly(ethylene glycol diacrylate)–co–acrylic acid (PEGDA-AA) hydrogel coatings on a Ti substrate, including both Gram-positive (*S. aureus*) and Gram-negative (*P. aeruginosa*) species. Further, AgNP-modified coatings showed no cytotoxicity toward human MG63 osteoblast-like cells after one week. Recently, Orlicki et al. (100) developed a AgNP-modified self-segregating hyperbranched polymer (HBP) polyurethane coating in which the AgNP migrate to the surface with time. The diffusion-limited spontaneous AgNP migration was enhanced by more than sevenfold using HBPs functionalized with thiol-terminated additives with associated 6-log reduction in *P. aeruginosa*, *S. aureus*, and the yeast *Candida albicans*. Colon et al. (101) showed a

simultaneous decrease in *Staphylococcus epidermis* adhesion and increase in osteoblast adhesion on nanostructured ZnO and TiO_2 when compared with micro-structured surfaces. Ionic liquids have also been used to enhance AgNP-impregnated coatings with a choice of an ionic liquid having a profound impact on antibacterial activity. Hamm et al. (102) developed an organosilica sol-gel coating with a high load Ag^0/Ag^+ NP ionosol in selected ionic liquids methyltrioctylammonium bis(trifluoromethylsulfonyl)imide ([N8881][Tf2N]) or 1-ethyl-3-methylimidazolium bis(trifluoromethyl sulfonyl)imide ([emim][Tf2N]) and tested their activity against *P. aeruginosa*. They observed significant antibacterial activity from ionosol-loaded coatings using [N8881][Tf2N] while [emim][Tf2N] had no effect. They propose that the octyl chains of the $[N8881]^+$ cation diffused through the cell wall and damaged the cytoplasmic membrane, allowing Ag^+ ions to penetrate the compromised cell and inactivate proteins by reaction with disulfide linkages, disrupting the DNA machinery and causing cell death (as shown in figure 2-6). [N8881][Tf2N]-based coatings on glass substrates showed 6-log inhibition of bacterial growth for 24 hours.

2.4.2.3 Surface-anchored antimicrobial peptides

Implant surfaces modified with natural or synthetic antimicrobial peptides (AMPs) have also shown promise for infection prevention (66, 103-105). Natural AMPs consist of relatively short, amphiphilic amino acid chains (12 to 50 amino acids with >50% hydrophobic content) and typically show broad bactericidal activity against both Gram-negative and Gram-positive bacteria (106). The complexity of their antimicrobial mechanisms makes it tough for bacteria to develop AMP resistance, overcoming one of the biggest challenges in traditional antibiotics research (105). In one recent report, an AMP

called defensin was integrated into a multi-layer alternating cationic/anionic polyelectrolyte film (103). These defensin-functionalized films inhibited 98% of *E. coli* D22 growth when positively charged poly(L-lysine) was the outer layer of the film as opposed to the negatively charged poly(L-glutamic acid) due to the different adhesive interaction behavior of the bacteria. Covalently tethering AMPs to the implant surface is particularly interesting since they contain functional groups that may be leveraged for long-term antimicrobial use (66). Similarly, Sun et al. demonstrated covalent peptide bonding to polydopamine (pDA) coated nano-hydroxyapatite (nano-HA) enhanced bioactivity and osteogenic differentiation compared with the pristine nano-HA (104). However, AMPs have lacked clinical applications due to the continued issues with tissue and cell interactions and potential cytotoxicity associated with high concentrations of AMPs (106).

2.4.2.4 Surface quaternary ammonium salts

Another possible approach to prevent biomaterial-centered infections is to render the biomaterial surface antimicrobial properties by functionalization with quaternary ammonium salts (QAS), which are widely known disinfectants (107). Chen et al. (108) decorated TiO_2 nanotubes with the QAS 3-trimethoxysily-propyldimethyloctadecyl-ammonium chloride, a positively charged QAS that attracted the relatively negatively charged bacteria and provided a 30-day ~93% antibacterial rate against *E. coli*. Further mixing AgNPs in with the QAS-loaded TiO_2 nanotubes improved the 30-day antibacterial rate to 99.9%. However, QAS surface coatings are cytotoxic to mammalian cells, which significantly limit their clinical usefulness.

2.4.2.5 Nitric Oxide

The naturally occurring small molecule nitric oxide (NO) is a known strong

oxidizer and so has been studied for antibacterial properties. NO was shown to damage the bacterial cell membrane followed by diffusion into the cells, resulting in further oxidative damage to vital cell components (109). Holt et al. (110) reported reduced bacterial colony counts for up to 48 hours in a rat model using NO-doped xerogel coatings on titanium external skeletal fixation pins. They observed that about 50% of the NO was released in the first four hours and the entire NO was released within 1-week time. Further studies need to performed to investigate the *in vivo* concentration kinetics of these coatings.

2.4.3 Coatings that release antimicrobial agents

An even more "proactive" approach than preventing bacterial adhesion is to kill bacterial cells before they come into contact with the implant surface. Controlled, time-delayed release of drugs from an implant coating allows for administering high drug concentrations at and around the implant site and further eliminates reliance on patient compliance. Moreover, the overall antibiotic load in the body can remain low, reducing effects on healthy tissues and beneficial flora, thereby increasing patient comfort and reducing follow-up care costs (55). Mechanisms of controlled release include (1) passive transport (i.e. diffusion or convection), (2) solvent-mediated activation and transport, and (3) chemical reaction, degradation, or erosion. When discussing individual materials, we identify and discuss the mechanisms governing that particular case.

2.4.3.1 Antibiotic-loaded bone cement

Antimicrobial cement has been used to prevent periprosthetic infections and enhance prosthesis fixation for more than 40 years (111-114). Before arthroplasties that promoted osseointegration, polymethylmethacrylate (PMMA) was primarily used to fix the arthroplasty to the bone. For preventing or treating infections, most cement consist of

PMMA beads (5 to 80 μm diameter) or PMMA-derived matrix, an antibiotic, and a radio-pacifier, which can be pre-mixed or mixed manually just before coating (48). Their function includes dispensing antibiotic, reducing the dead space between the implant and bone, and promoting good bone-implant interface adhesion (115). A review of bone cement release mechanisms concluded that initial antibiotic release in the first few hours after exposure to fluids was governed by surface phenomena. Presumably, desorption, while sustained release over several days was by passive bulk diffusion (48). Some factors play a role in determining the actual release rates including the antibiotic type and load, cement type, open porosity, and implant surface area available for the cement coating (116).

Elucidating the antimicrobial release kinetics and local spatial distribution is critical to understanding the efficacy of such coatings in real clinical applications. *In vitro* release kinetics of commercially available and manually blended cement were compared by Mionla et al (117). They found that the commercially-loaded cement released a higher amount of gentamicin than the hand-mixed ones, but no statistically significant difference was found in antimicrobial activity. Mass transport and distribution characteristics have been studied *in vivo* in female rabbit models (118). In this study, the MRI contrast agent gadopentetic acid (Gd-DTPA) was used as an indicator and surrogate for gentamicin and vancomycin due to its similarity in size and solubility. After 5.5 hours, they observed that spatial particle distribution was highly anisotropic and not strictly explained by diffusion. In another study performed by Webb et al., *in vivo* release of gentamicin from PMMA cement (Palacos® R-40 gentamicin, Zimmer, Inc., Warsaw, IN) was studied using fluorescence polarization immunoassay (FPIA) of urine samples from 35 human patients

undergoing THR (119). They observed a bimodal antibiotic release pattern with high initial release followed by sustained low-level release. The average release period ranged from 6 to 14 weeks. However, other studies have shown that antibiotic-loaded cement in TKR had no significant effect in reducing the two-year revision surgery rate (120).

Although antibiotic-loaded cement is efficient, cost-effective means for local antimicrobial delivery, there are disadvantages associated with their use. One of the major drawbacks is their passive, inefficient release mechanism, which might lead to induction of resistant mutant species (121). If used to treat an infection, a second surgery may be required to remove the cement after full antibiotic release. Furthermore, the cement is made by an exothermic polymerization process that may adversely affect the thermal stability of the antibiotics and also limits the choice of drugs that can be used which, in turn, limits the organisms that can be treated(121).

2.4.3.2 Polyhydroxyalkanoates

Polyhydroxyalkanoates (PHAs) are linear polyesters typically containing a β-hydroxyalkanoic acid that are produced by bacterial fermentation of sugar and lipids. They can be processed into rod or microcapsule forms to serve as drug carriers (122). An *in vivo* rabbit study by Gürsel et al. showed that drug-loaded PHA rods released drugs for at least one week following implantation(123). Turesin and coworkers further showed that adding undoped PHA layer atop the antibiotic-loaded PHA rods reduced the release rate and demonstrated diffusion-controlled kinetics. Uncoated rods released their antibiotic contents in 3 days while the coated rods released 70% of the drug over a period of 2 weeks(122). Detailed reviews on PHA coatings can be found elsewhere (124).

2.4.3.3 Mesoporous materials

The high surface area and an open porosity of mesoporous materials make them suitable vehicles for drug delivery. Mesoporous silica has been found to facilitate drug release by diffusion (125). Xia et. al. investigated the drug release properties of several gentamicin-loaded mesoporous bioactive glasses (MBG) prepared by two-step acid-catalyzed self-assembly process. They confirmed that the gentamicin release rate increased with increasing pore volume. *In vitro* comparison of MBG with other bioactive glasses showed that gentamicin release from MBG was slower than sol-gel-based bioactive glasses and release continued for more than 20 days.

One major drawback to using MBG is its poor mechanical strength. Combining MBG with more rigid polymers can be used to overcome the poor mechanical strength of MBG. Mabrouk et al. integrated MBG with poly(vinyl acetate) (PVA), which has excellent mechanical strength and biocompatibility, and loaded the composite with ciprofloxacin (59). The degradation rate of the MBG-PVA composite was significantly slower than PVA alone, but an increase in the release rate of ciprofloxacin was observed. The authors hypothesized the increase might be a result of bonding affinity between ciprofloxacin and the PVA. Interesting reviews on mesoporous materials can be found elsewhere (126).

2.4.3.4 Hydrogels

Hydrogels are a class of cross-linked polymers that swell, without dissolving, in the presence of water. The swelling characteristic of hydrogels makes them an ideal system for controlled drug release from medical implants. Hydrogels can be used with a broad spectrum of biomolecules including antibiotics, growth factors, and peptides. One study compared the release dynamics of gentamicin between beta tri-calcium phosphate (β-TCP)

and gelatin-reinforced β-TCP scaffolds *in vitro* (127). When immersed in an aqueous solution, the gelatin-reinforced β-TCP coating demonstrated zero-order sustained antibiotic release profile for 28 days while the unmodified β-TCP coating showed an initial bolus release of gentamicin within 10 hours followed by complete release within one day. The sustained release observed from gelatin reinforced β-TCP was found to be due to gradual hydrogel degradation. An *in-vitro* antibacterial assay performed on 3- and 7-day cultures of *S. aureus* further demonstrated higher antibacterial properties for gelatin-coated β-TCP compared to unmodified β-TCP coatings. Similar results were observed when the coatings were analyzed for three weeks *in vivo* in rodents suffering from osteomyelitis. In another study, the authors explored the preparation of polyacrylate-based hydrogel by electrochemical polymerization of titanium implants and loaded them with ciprofloxacin (128). Subsequent ciprofloxacin release was studied using high-performance liquid chromatography (HPLC), and antibacterial efficacy was demonstrated *in vitro* using methicillin-resistant *S. aureus* (MRSA). Mariner et. al. prepared synthetic hydrogel scaffolds that can be used to deliver rhBMP2 to critical-sized bone defect models in rats (129). Their hydrogel scaffolds compared favorably to absorbable collagen sponges, showing significantly more bone growth over a 6-week observation period.

2.4.3.5 Drug-eluting degradable coatings

Biodegradable implant coatings were first introduced by Kulkarni et al. when they presented the concept of using poly-lactic acid (PLA) fibers and films for surgical implants (130). Since then, biodegradable materials have evolved with accompanied considerably greater usage in medical devices. Biodegradable coatings reduce the risks involved with the usage of permanent implants and the need for second surgery for implant removal.

They are radiolucent and have demonstrated effective controlled drug release (131). Another advantage of using biodegradable coatings involves reduced foreign body reactions (132). The drug release kinetics can be controlled by altering the polymer degradation rate. Some of the conventional biodegradable coatings developed are biodegradable polymer coatings, calcium phosphate, chitosan, collagen, and bone grafts.

1. Polymer coatings

The first biodegradable polymer coating for implant surface prepared was poly(lactic-co-glycolic acid) copolymer (PLGA) coatings loaded with gentamicin for fracture fixation plates (133). The antimicrobial effects of the coated implants were tested by *in vitro* bacterial inhibition of *S. aureus* and were found to be effective for 24 days. Gilchrist et al. used a fusidic acid (FA)- and rifampicin (RIF)-loaded PGLA coating for biphasic delivery of drugs (134). They used the electrospinning technique to overcome the incompatibility of FA and RIF with PLGA. FA/RIF-doped PGLA-coated titanium discs were tested *in vitro* and *in vivo* against MRSA in a rodent model over a period of 7 days. Both *in-vitro* and *in vivo* models demonstrated effective inhibition of bacterial growth.

In addition to PLGA, PLA, hyaluronic acid, poly-D, L-lactide (PDLLA), poly-L-lactide (PLLA), and polyethylene glycol (PEG) have also been used in the fabrication of biodegradable coatings (135). Neut et al. (136) used gentamicin-loaded poly(trimethylene carbonate) (PTMC), which inhibits biofilm formation. PTMC is attractive as it can be degraded enzymatically without forming acidic degradation products. A gentamicin-loaded PTMC disc was found to be effective for at least 14 days *in vitro* (136). Gitelis et al. have used antibiotic-impregnated calcium sulfate implants to provide direct local

antibiotic delivery. It has been found to be effective for six weeks in animal models (137). The anti-adhesive biodegradable multi-layer PVP/PAA and HEP-CHI mentioned above also demonstrated antimicrobial activity, with HEP/CHI layers effectively killing *S. aureus* on contact for 2 to 3 weeks (79).

Although these coatings were efficient at inhibiting bacterial growth there are some inherent disadvantages involved in using such systems including low strength and being brittle, which are critical material properties for an implant device designed to take repeated mechanical loading. An et al. has reviewed in detail pre-clinical *in vivo* testing of bioabsorbable devices (138). Some of the other common biodegradable coatings developed are calcium phosphate, chitosan, collagen, and bone grafts.

2. Calcium phosphate

Calcium phosphate (CaP) has also been used as a biodegradable carrier for drug release. CaP can be utilized as a cement composition, granules, blocks, ceramics, powders, and coatings. CaP cement is favorable over acrylic (PMMA) bone cement because of their inherent porosity and endothermic process, which allows for improved thermal stability of heat-sensitive components (139). They can be injected at the site and, therefore, can fit the infection site perfectly. As this cement settle *in vivo* and have chemical and structural similarity to natural hydroxyapatites, they have greater reactivity with the host bone. Detailed discussion on other useful properties of CaPs can be found in other reviews (139, 140). Therapeutic application of CaP has been dealt in great detail by Verron et al (141).

Various synthetic CaP compositions are currently being used such as hydroxyapatite (HA), $Ca_3(PO)_4$, β-TCP, and mixtures of HA/β-TCP. HA has been used as

a component for implant coatings because of their composition and crystallographic structure similarity to the bone. Synthetic HA has excellent biocompatibility and shown to improve osseointegration since natural bone is at least 50% carbonated HA by weight (142-144). Various researchers have used antibiotic- or metal nanoparticle-doped carbonated HA coatings to improve antimicrobial efficacy and osseointegration properties(145-148). Motoc et. al. deposited active antimicrobial protein and biceramic calcium HA using pulse laser deposition on a Ti surface, which demonstrated excellent biocompatibility, human cell adhesion, and local antimicrobial efficacy (149). Nanoscale patterned materials have also been found to improve specific proteins interactions.

Zhang et al. made a biomimetic coating combining nanocrystalline HA and helical rosette nanotubes, which are very similar to nanostructured collagen (150). They observed enhanced osteoblast adhesion when smaller grain sized nanocrystalline HA was used. Huang et. al. produced a nano-HA/polyamide66 scaffold coated with berberine-doped chitosan that had both excellent antimicrobial properties as well as bone regeneration capacity (151). It has been found that nano-HA enhance osteoclast functions and osteoblast formation, which is critical since the extent of HA reabsorption by bone followed by osteoblast formation decides the fate of the implants (152). Biological evaluation of nano-HA coatings *in vitro* revealed that they are active between 24 to 150 hours. Rauschmanna et al. demonstrated better biocompatibility and local antibacterial delivery for highly porous resorbable nanocomposites of calcium sulfate and HA in comparison with pure CaP (153). The open porosity allowed the uptake of antibiotics (i.e. gentamicin, vancomycin) in the materials, which then continued to release for ten days.

3. Chitosan

Chitosan is a linear polysaccharide containing randomly distributed β-(1-4)-linked D-glucosamine and N-acetyl-D-glucosamine groups that can be synthesized by treating crustacean shells with alkaline sodium hydroxide. Chitosan has proved to be an effective drug delivery system as it is non-toxic, biocompatible, has excellent absorbing properties, and is biodegradable. Chitosan is degraded easily in the human body when it comes into contact with lysozyme to form saccharide and glucosamine (154). Smith and coworker (154) loaded daptomycin and vancomycin in dehydrated chitosan films by submerging the films in 1mg/ml of antibiotic in phosphate buffered saline (PBS) solution for 1 minute. The antibiotic activity of the chitosan films prepared *in situ* was determined using *in vitro* turbidity assay. Eluate samples were tested at 48 and 72 hours and found to be effective in inhibiting bacterial growth of *S. aureus* (154). Preparation of the films *in situ* also resulted in significantly decrease coating degradation before implantation. De Giglio and coworkers developed a ciprofloxacin-loaded chitosan nanoparticulate coating for Ti implants and tested it *in vitro* against *S. aureus* and *P. aeruginosa* (155). The amount of ciprofloxacin released was estimated using HPLC and revealed that chitosan-loaded nanoparticles did not display any initial burst release profile and the relatively slow release rate (2.8 μg/ml) continued after for 120 hours and was effective in inhibiting bacterial growth.

4. Collagen

Much research has been done on the use of collagen due to its prevalence in the extracellular matrix (ECM). Drug release characteristics depend strongly on the porosity and method of preparation (156). Tu et al. produced layered HA and mineralized collagen on Ti implants by electrolytic deposition and studied the cytocompatibility and antibiotic release kinetics (157). They observed an initial burst release of vancomycin (80-85%) in

the first 10 to 16 hours followed by a slow release sustained over four days. Antibacterial testing was performed for 16 hours *in vitro* and showed good antibacterial efficacy. A detailed review on efficacy testing *in vivo* of prophylactic and therapeutic application of gentamycin-loaded collagen implants can be found elsewhere (158).

5. Bone grafts/Cancellous bone

Bone grafts, including cancellous bone, are occasionally used for replacing missing bone or used to stimulate fracture healing. They have high surface area-to-mass ratio, which makes them ideal for use as a drug carrier. In most cases, they are reabsorbed and replaced during the healing process. Zeolites are aluminum silicate minerals which are highly porous and can be used as absorbents. In addition to being biocompatible and non-toxic, zeolites have a significant number of functional groups that can combine with various drug molecules by hydrogen bonding. Guo et. al. have used zeolite to fabricate bone grafts (159). They demonstrated that the drug loading capacity of zeolite was almost three times that of HA while the drug release of gentamicin in phosphate buffer saline (PBS) using colorimetric techniques showed that the zeolite exhibited slow and sustained release of 62.2% in 6 days. In another study, human demineralized bone matrix (DBM) was loaded with gentamicin and used to prevent infection (160). The grafts were able to release drugs effectively *in vitro* for up to 13 days. Meanwhile, there were no adverse effects on osteoinductive or osteoconductive nature when tested *in vivo* in rat ectopic pouch models after 28 days. Other studies on antibiotic-loaded bone grafts and DBM can be found in detailed reviews elsewhere (161, 162).

The local application of antimicrobial-eluting agents is a well-known and accepted

tool in the treatment of implant-related infections (59). These materials inhibit bacteria both locally and remotely from the implant based on the technique used. However, some questions arise regarding the by-products of their use, like crystals and acids that are formed after degradation that cause inflammation (infection like reaction) (131). The use of antibiotics in high doses can also lead to antibiotic-resistant bacteria. Also, these coatings tend to have low strength. Further research needs to be done to understand the release mechanism of drugs into the body to optimize their usage.

2.4.4 Coatings that accelerate osteocyte adhesion

Another way of preventing implant-related infections is by promoting and speeding up the adhesion of desired eukaryotic cells so that tissue integration dominates over bacterial adhesion in the "race for the surface." Layering implants with desired tissue cells provides a defense mechanism that can prevent bacterial colonization (163, 164). Some of the techniques to promote osteocyte adhesion are given below.

2.4.4.1 Incorporation of growth factors

HA offers several advantages as an implant coating, which includes good bonding with the implant and the surrounding tissues. Such properties offer the opportunity for bone formation and prevent implant wear and release of metallic particles (165). Along with HA, CaP ceramic and octa-CaP coatings have also been explored and found to have desirable osteoconductive properties (166). Although these materials provide osteoconductive properties, they are themselves not osteoinductive and do not assist in osseointegration. Several studies have been conducted to show that the presence of enzymatic and nutritional growth factors aids in osteoinduction to achieve improvements in osseointegration (167). A bioactivity study in a rat model showed that ~60% of the incorporated growth factors

were consumed by the five-week follow-up. Transforming growth factor-β-1 enhances bone regenerative properties by stimulating the differentiation of pre-osteoblastic cells (168). Bone morphogenic proteins (BMPs) have also been identified as important growth factors (169, 170). Reyes et al. observed that coatings comprising type I collagen-mimetic peptide glycine-phenylalanine-hydroxyproline-glycine-glutamate-arginine (GFOGER) promote osseointegration and cell adhesion by binding to $\alpha_2\beta_1$ integrin (171).

2.4.4.2 Bioglass

Bioglass is a surface active member of the bioactive glass family composed of sodium oxide, calcium oxide, phosphates, and silicates. Effective bonding and ingrowth of bone depend strongly on the bioglass formulation. Naghib et. al. coated steel implants with 45S5 bioactive glass synthesized by sol-gel technique (172). The bioactive glass showed good adhesion to the metal due to its high thermal expansion and bioactivity after 14 days *in vitro* in simulated body fluid. More thorough reviews of sol-gel based biomaterials and bioactive glasses, which have been studied extensively, can be found elsewhere (173, 174).

2.4.4.3 Silicon carbide ceramics

Biomorphic silicon carbide (SiC) ceramics coated with a bioactive glass layer have shown excellent osteoconductive properties (175). SiC possesses excellent mechanical properties and low density, which is promising for use with load-bearing implants. The SiC-bioactive glass composite resulted in dense apatite layers after 72 hour testing *in vitro*. Dey et al. modified SiC biomaterial with 10-undecenoic acid methyl ester and studied CaP/HA formation on the surface for five days after converting the methyl ester to a carboxylic acid (176). They observed improved CaP/HA nucleation resulting in well-defined, highly crystalline multilayers.

2.4.4.4 Coating with extracellular bone matrix (ECM)

Coating implants with ECM components has been found to be an attractive solution because it does not lead to foreign body reactions and the ECM can interact with bone cells to facilitate bone growth and adhesion (177). Rammelt et al. found enhanced bone growth on Ti implants placed in rodent models that had been coated with several ECM components: collagen, RGD proteins, and chondroitin sulfate (177). Bernhardt et al. performed a similar study in a goat model (178). They observed enhanced bone growth on the ECM-coated implant that promoted subsequent implant stabilization.

Many cases of implant failure are due to loosening and improper osseointegration. Coatings that accelerate osteocyte adhesion enhance bone formation and healing. However, further research needs to be done in the various immobilization processes and their effects on osseointegration rates. In most cases, the coating manufacture process is tedious and yields poor coating-implant anchorage. Also, incorporating different materials induces drastically different cellular responses, which need to be studied to identify optimal materials for rapid healing and bone formation while ensuring patient safety.

2.4.5 Coatings with multiple modes of action

Several researchers have developed composite coatings combining the beneficial properties of more than one of the above methods to improve osseointegration and antimicrobial efficacy. Lee et. al. developed a dual drug-eluting heparin-based composite coating for Ti substrates (179). The antibiotic gentamicin sulfate and protein bone morphogenic protein-2 (BMP-2), which promotes osseointegration, were immobilized in a heparin matrix. They observed an initial burst release for one day followed by a sustained release of gentamicin and BMP-2 over four weeks. Alkaline phosphatase activity and

calcium deposition were also examined, and the composite coating was found to perform significantly better than an unmodified heparin coating. Tan et. al tested some composite bone cement for biocompatibility and infection inhibition and found that a composite quaternion chitosan derivative-loaded PMMA out-performed the PMMA control, chitosan-loaded PMMA, and gentamicin-loaded cement (180). Macdonald et. al. integrated BMP-2 growth factors in a multilayered chondroitin sulfate coating (181). Both *in-vitro* and *in vivo* studies showed bone growth at four and nine weeks, respectively. Cheng et al. used Ag-impregnated Ti nanotubes fabricated on Ti implants and found that the implants exhibited antimicrobial activity for 30 days against *S. aureus* (MRSA, ATCC43300) *in vitro* (182). The composite is also tested *in vivo* in rat models and showed satisfactory adhesion and integration with the implants. Svensson et. al. performed a similar study where nanoscale surface features were utilized in conjunction with noble metal additives (Au, Ag, and Pd) for the simultaneous promotion of bony ingrowth and bacterial inhibition at the implant interface (183). These coatings inhibited bacterial infection *in vitro* while osseointegration was observed *in vivo* using a rat model. Kazemzadeh-Narbat et. al. used electrolytic deposition of a thin CaP layer on Ti substrate to act as a carrier for antimicrobial peptides (106). Analysis of the coatings was performed *in vitro* against both gram-positive *S. aureus* and gram-negative *P. aeruginosa*. The coatings were effective in killing both strains of bacteria in less than 150 minutes. Bone growth analysis was done by implanting the coatings in rabbit models. Backscattered electron microscopy was done to confirm the formation and growth of bone, which was considerably higher on an uncoated Ti substrate.

Another effort to utilize multiple modes involved simultaneous testing of the zeolite anti-adhesive property derived from its super-hydrophilicity and ion exchange property for

hosting and regulating the release of Ag^0/Ag^+ antimicrobials (184). Wang et al. demonstrated *in vitro* that bacterial adhesion and proliferation of *S. aureus* was significantly inhibited using silver-doped zeolite coatings, evaluated both at the implant surface and in the surrounding culture medium. The antibacterial and anti-adhesive zeolite coatings show great potential for application in orthopedic implants and general wound care (184, 185).

Coatings with multiple modes of action prove to be a promising technique for preventing infection as well as enabling bone growth. Despite their multifaceted utilities, several questions need to be addressed. Firstly, the performance of these implants may be hampered by protein attachment to the surface blocking active sites or preventing diffusion of antimicrobial agents. The success of these implants depends on the host tissue response, and they are *in vivo* performance in overcoming adverse reactions. Secondly, the ease of manufacture and robustness of these coatings need to be considered. Further research needs to be done to prevent loss in functionality before osseointegration and implant stabilization is complete.

Table 2.2: A summary of the various coatings and surface modifications imparting antimicrobial activity to orthopedic implants and their duration of efficacy.

Mode of action	Type of antimicrobial coating	Duration of antimicrobial efficacy
Prevent bacterial adhesion via physical	(a) Sacrificial surfaces (74, 79)	9-10 weeks (*in vitro*)

effects	(b) Adhesion-resistant coatings (82, 91-93) (i) Unstructured polymer coatings (ii) Polymer brushes (iii) Diamond-like carbon coatings	90 days (*in vitro*)
Kill adherent bacteria	(a) Photoactive coatings (96)	Two days (*in vitro*)
	(b) Metal impregnated surfaces (99-101)	21 days (*in vitro*)
	(c) Surface-anchored antimicrobial peptides (66, 103, 106)	Seven days (*in vivo*)
	(d) Surface quaternary ammonium salts (108)	30 days (*in vitro*)
	(e) Nitric oxide (110)	48 hours (rat model)
Release antimicrobial agents to surrounding regions	(a) Antibiotic-loaded bone cement (117-120)	6-14 weeks (*in vivo*)
	(b) Polyhydroxyalkanoates (122, 123)	Up to two weeks (*in vitro*) and up to six weeks (*in vivo*)
	(c) Mesoporous materials (59, 125)	Up to 20 days (*in vitro*)

	(d) Hydrogels (127-129)	Up to 28 days (*in vitro*) 3-6 weeks (*in vivo*)
	(e) Drug-eluting degradable coatings (79, 133, 134, 136, 137, 151-155, 157, 159, 160) i. Polymer coatings ii. Calcium phosphate iii. Chitosan iv. Collagen v. Bone grafts/ Cancellous bone	2-3 weeks (*in vitro*) Up to six weeks (*in vivo*)
Accelerate adherence of desired cells	(a) Incorporation of growth factors (167, 169-171)	4-5 weeks (*in vivo*)
	(b) Bioglass (172)	14 days (*in vitro*)
	(c) Silicon carbide ceramics (175, 176)	3-5 days (*in vitro*)
	(d) Coatings with ECM (177, 178)	4-12 weeks (*in vivo*)
Coatings with multiple modes of action	Coatings with multiple ways of action (106, 179-185)	Up to four weeks (*in vitro*)

		4-9 weeks (*in vivo*)

2.5 Conclusions

Numerous approaches toward realizing robust, inexpensive antibacterial coatings have been described. Varying degrees of success at preventing the colonization of implant surfaces by bacteria have been achieved. However, bacteria are not only hardy but are continuously introduced and re-introduced into the bloodstream by daily activities (e.g. brushing teeth, scrapes, minor cuts) and by surgical procedures such as catheter insertion and gastrointestinal surgery. Under normal circumstances, the microorganisms that enter the bloodstream (i.e. transient bacteremia) are neutralized by the body's immune system. However, orthopedic implant surfaces provide a convenient "hideout" for bacteria and transient bacteria reaching the implant surface can develop into full-blown infections even months after implantation. Thus, it is highly desirable that coatings retain their antimicrobial activity for as long as possible. Methods/coatings employing a combination of the approaches described above may be more effective antimicrobials as they carry some redundant activity that is not easily bypassed. Also likely to prove effective are 'smart' materials: those that either release their active antimicrobial agents in a controlled manner or only in response to the presence of microbes. However, efficient reduction in microorganism loads alone will not ensure wide acceptance or commercial success of the special coating. For the latter, the coating will not only have to meet various mechanical criteria (e.g. bond strength of the implant coating interface, resistance to repeated mechanical loading) and biological constraints (e.g. demonstrate non-toxicity to humans,

promote osseointegration) but will also have to be cost-effective when manufactured in bulk. As all current coatings fail at one of these three criteria, the next-generation antimicrobial coating to be used in virtually all implants remains an elusive target.

CHAPTER 3

3 FOAMING BETADINE SPRAY AS A POTENTIAL AGENT FOR NON-LABOR-INTENSIVE PREOPERATIVE SURGICAL SITE PREPARATION

The material presented in this chapter was reviewed and published as "**Foaming Betadine Spray as a potential agent for non-labor-intensive preoperative surgical site preparation**"

Roli Kargupta,, Garret J Hull, Kyle D Rood, James Galloway, Clinton F Matthews, Paul S Dale and Shramik Sengupta

Annals of clinical microbiology and antimicrobials, 2015. 14(1): p. 20.

The Centers for Disease Control and Prevention's (CDC) National Healthcare Safety Network (NHSN) report published in 2009 shows that there were about 16,000 cases of surgical site infection (SSI) following ~ 850,000 operative procedures making SSI one of the most predominant infections amongst nosocomial infections. Preoperative skin preparation is a standard procedure utilized to prevent SSIs thereby improving patient outcomes and controlling associated healthcare costs. Multiple techniques/ products have been used for pre-operative skin preparation, like 2-step scrubbing and painting, 2-step scrubbing and drying, and 1 step painting with a drying time. However, currently used products require strict, time-consuming and labor-intensive protocols that involve repeated mechanical scrubbing. It can be speculated that a product requiring a simpler protocol will increase compliance, thus promoting a reduction in SSIs. Hence, the antimicrobial efficacy of a spray-on foaming formulation containing Betadine (povidone-iodine aerosol foam) that can be administered with minimum effort is compared to that of an existing

formulation or technique (Wet Skin Scrub).

In vitro antimicrobial activities of (a) 5% Betadine delivered in aerosolized foam, (b) Wet Skin Scrub Prep Tray and (c) liquid Betadine are tested against three clinically representative microorganisms (*S. aureus, S. epidermis,* and *P. aeruginosa,*) on two surfaces (agar-gel on petri-dish and porcine skin). The log reduction/growth of the bacteria in each case is noted, and ANOVA statistical analysis is used to establish the effectiveness of the antimicrobial agents, and compare their relative efficacies.

With agar gel as the substrate, no growth of bacteria is observed for all the three formulations. With porcine skin as the substrate, the spray-on foam's performance was not statistically different from that of the Wet Skin Scrub Prep technique for the microorganisms tested.

The povidone-iodine aerosolized foam could potentially serve as a non-labor intensive antimicrobial agent for surgical site preparation.

3.1 Background

Surgical site infection (SSI) is one of the major concerns associated with surgery (13, 186). SSIs can lead to severe complications, and also to patient mortality in extreme cases (16). A 2009 estimate of the annual direct medical costs of Hospital Acquired Infections (HAI) by the Centers for Disease Control and Prevention (CDC) estimated the number of SSIs in the USA to be >290,000 per year, with an estimated cost of resulting inpatient services of up to $ 10 Billion (8). A reduction in the incidences of SSI would thus significantly improve patient wellbeing with a significant decrease in healthcare expenses (12, 187).

Colonizing microorganisms often cause SSI. Microorganisms present in the skin and the operation room can readily enter a patient's body through the site of an incision (15). Transient bacteria present on the skin can and do cause SSIs, and reducing their number is of vital importance. This is achieved using a combination of processes: sterilization of the operating room, cleaning, showering and de-hairing of the surgical site, and scrubbing the surgical site with antimicrobial agents (15, 188).

Commonly used antimicrobial agents are alcohol, iodine, chlorhexidine and povidone-iodine solution (PVP-I) among others (16). They can be administered in the form of liquids and solutions (13). The choice of antimicrobial agent and the technique of preoperative skin preparation to be used depends on various factors like surgeon's familiarity with the technique, cost, efficacy of the agent used, ease of use, surgical site and possible bacteria present at the site (189). There are several techniques like 1-step paint and dry method (taking about 3 minutes) or only scrub and dry techniques (taking greater than 5 minutes) or scrub-paint technique (taking about 5 minutes) (190-193). We selected the wet skin scrub prep technique as it is a commonly used technique in the operating room and the technique of choice for some clinicians at our institution. Drawbacks of the current protocols of surgical site preparation techniques are; they are laborious, time-consuming, expensive and often require the user to follow certain strict protocols (16, 188, 194). It is speculated that a product sprayed directly at and near the surgical site would be able to overcome these disadvantages, resulting in a reduction in time, effort, and personnel needed for surgical site preparation, and hence cost incurred.

While there are multiple products available for surgical site preparation (with varying, but broadly comparable efficacies), a common preoperative surgical site

preparation technique involves a 5-minute scrub with povidone-iodine detergent (17). If the 5-minute scrub is replaced with a spray-on protocol taking 2 minutes, it could result in saving 3 minutes during every surgical procedure. Given average operating room charges of $62/minute, this three-minute reduction in surgical site preparation will lead to savings of $186/case if the cost of the spray-on product is similar to the existing technique (195). This increased efficacy would result in saving $0.93 million a year and also generate 15,000 minutes of extra procedure time for hospitals that annually perform about 5000 procedures. The time saved can be rightfully utilized for additional procedures. Also, SSIs have been estimated to increase hospital expenses per admission by $ 20,842 (196). So the reduction of both extra procedure time and incidence of SSI can lead to a decrease in the financial burden of the patient.

It is estimated that a large percentage of surgical site infections (up to 60%) can be prevented following proper SSP techniques (197). Therefore, any preoperative skin cleaning technique whose efficacy is at least equal to that of the existing methods, but which is less dependent on user skill is likely to improve overall outcomes.

3.2 Materials and Methods

3.2.1 Overview

The bactericidal efficacy of our spray-on formulation (povidone-iodine aerosol foam), is compared to that of the traditional sponge-based application method using the methodology schematically depicted in Figure 3-1. Details regarding individual steps in the protocol are described below. Standard 0.5 McFarland bacterial suspensions are spread on two different substrates: sterile nutrient agar and sterilized porcine skin. The substrates are incubated for an hour to allow sufficient time for the bacteria to adhere to the substrates.

Post incubation, the surfaces are exposed to the various preoperative skin preparation techniques: povidone-iodine aerosol foam, wet skin scrub prep tray, flood coverage with liquid Betadine (positive control) and flood coverage with Phosphate buffer saline (PBS) or no treatment (negative control). Post-exposure, the substrates are again incubated for 24 hours. After 24 hours, the number of surviving bacteria is estimated using colony counts, to estimate the bactericidal efficacy of the various techniques. 48 hours incubation of the plates is also done to validate if the bacteria are killed during the process or are merely injured and could grow if proper nutrients are provided to it (198).

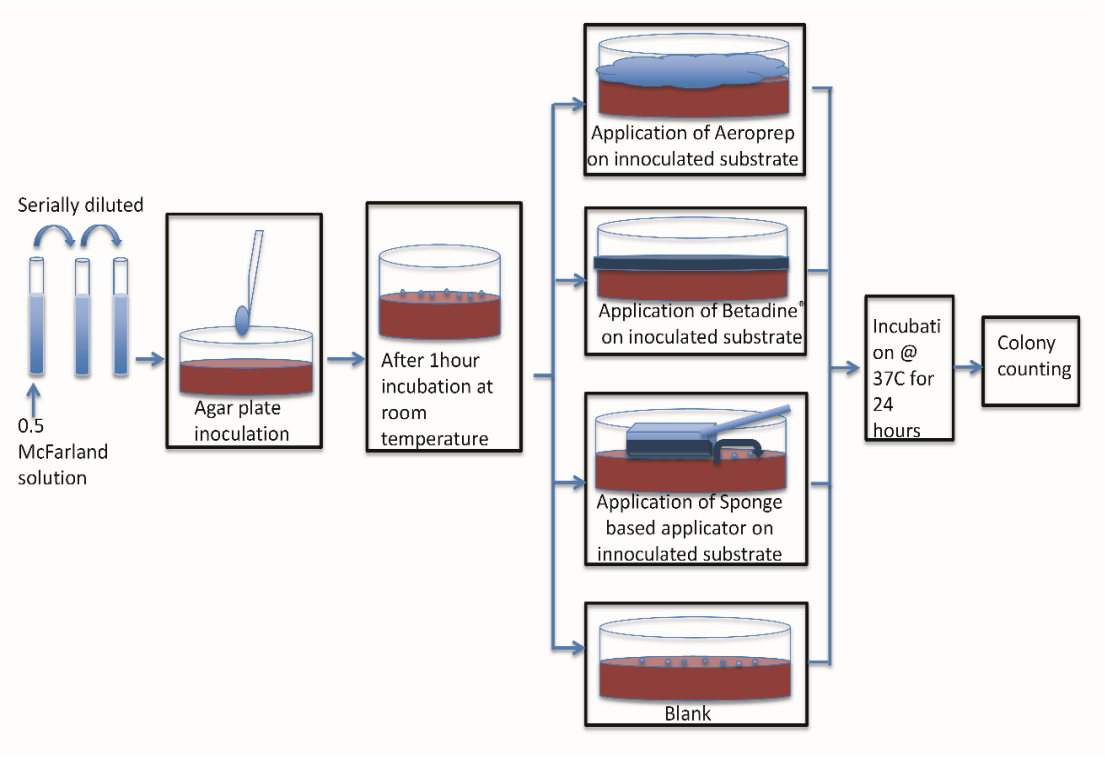

Figure 3-1 Schematic of the method of testing the bactericidal efficacy. This schematic details the methodology of screening the bactericidal efficacy using Povidone-iodine aerosol foam, sponge based applicator, and flood coverage with liquid Betadine.

3.2.2 Bacterial cell culture

The micro-organisms used in the study are gram-positive bacteria *Staphylococcus aureus* ATCC 29213 and *Staphylococcus epidermis* ATCC 12228 and gram-negative bacteria *Pseudomonas aeruginosa* ATCC 27853. The bacterial strains were chosen for the study contribute to about 42% of SSI (15). The strains are sub-cultured in Tryptic Soy Broth (TSB) and incubated for 20-24 hours at 37°C to obtain log-culture. Following which standard 0.5 McFarland bacterial suspension is prepared in TSB for use in the study using standard protocols (199).

3.2.3 Selection of substrates

The antimicrobial efficacy of the agents used for preoperative skin preparation is tested *in vitro* using both agar plates as well as porcine skin. Tryptic Soy Agar (TSA) plates are used for culturing the bacteria.

Porcine skin is chosen for its close resemblance to human skin, and has previously also been used for studying the effect of chemicals on human skin (200, 201). Porcine skin purchased from local grocery shops is cleaned, de-haired and cut into one square inch pieces and sterilized, before use. The sterilization protocol, described in detail elsewhere (202) involved treating the skin pieces with an aqueous solution of 1M sodium chloride and 0.1% (v/v) peracetic acid with continuous stirring of the solution at 225rpm for 30mins. It is followed by two times rinsing in PBS for 24hours each time by continuous stirring at 225rpm (202, 203).

3.2.4 Selection of antimicrobial agents for testing

Liquid, 5% Betadine, is used for flood coverage of the substrates. Preoperative wet skin scrub prep kit containing sponge applicators are used for the study with the applicators

wetted with 5% Betadine before scrubbing. The aerosolized foam of povidone-iodine, 5% Betadine is used. The product is designed to be sprayed on the surgical site from a distance of 4-8 inches, resulting in the site being covered with foam. The propellant gasses present in the aerosol foam canister mix with anti-microbial agents like povidone and iodine to produce a layer of foam. It requires less manual labor, unlike scrubbing or painting. After predetermined contact time, the foam can be removed from the site with a sterile cloth thus making the site ready to be operated.

Also, to prove that there is no mechanical washing away of the bacteria on being flooded with 5% Betadine, the experiment was repeated with 1X PBS instead of 5% Betadine.

3.2.5 Evaluation of bactericidal activity

For each bacterial culture, both agar plates, and porcine skin is used. Five agar plates are utilized for each case: control, flood coverage by 5% Betadine, sponge-based applicator and povidone-iodine aerosolized foam (our product). Similarly, for porcine skin, a group of 5 one-inch square skin pieces is used for each case, control, flood coverage with 5% Betadine, sponge based applicator, and our product.

Each bacterial culture is diluted to ~$1*10^4$ CFU/ml and 100µl is of the diluted bacteria is used for inoculation. It is thus expected that there will be ~10^3 CFU on agar plates and porcine skin before disinfection. Post-inoculation, the agar plates, and the porcine skin are allowed to incubate at room temperature for 1 hour. After this incubation time, the control samples of agar plates are allowed to incubate at 37°C for 24 hours. The imprint of the control samples of the porcine skin is taken on agar plates with the plates being incubated at 37°C for 24 hours. It may be noted that samples were incubated for 48

hours in the hope of detecting bacteria that were only injured, but not killed by the disinfecting techniques (198).

The steps involved in treating the agar plates and the porcine skin with flood coverage of Betadine, aerosolized foam and sponge based applicator are depicted in Figures 3-2 and 3-3, respectively.

For agar plates and skin pieces serving as a substrate for 5% Betadine about 5-10ml of liquid 5% Betadine, is poured on the surface. This ensures flooding and complete coverage of the entire surface of the agar plates/porcine skin with 5% Betadine. After 2

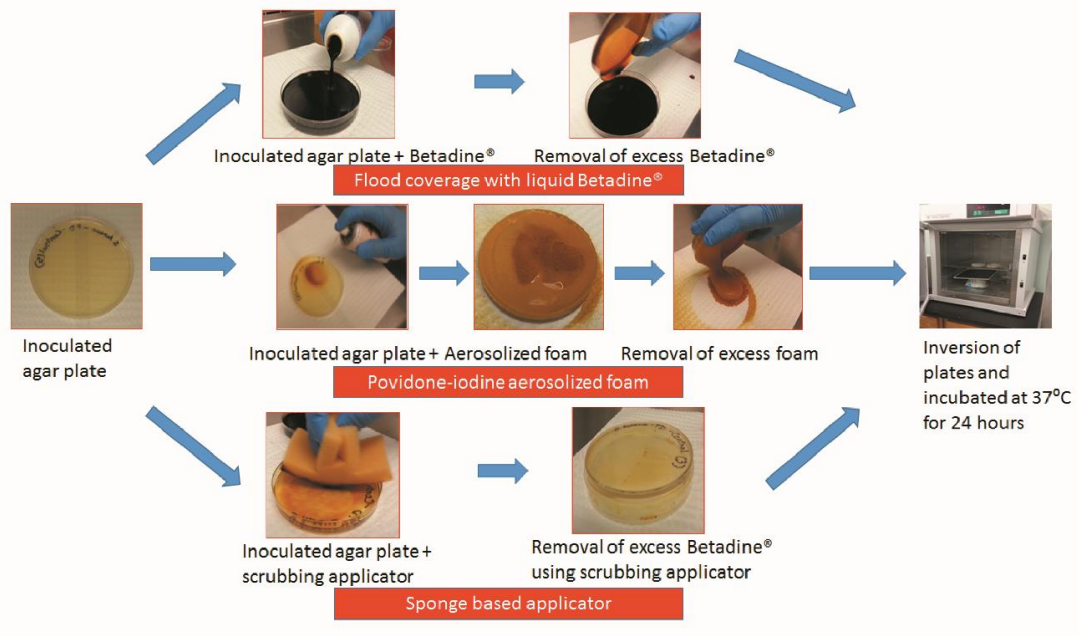

Figure 3-2 Steps involved in evaluating bactericidal activity on nutrient agar plates. Steps involved in treating the agar plates with flood coverage of Betadine aerosolized foam and sponge based applicator and evaluating its bactericidal activity.

minutes of contact, the agar plates are flipped upside down to remove excess solution. In the case of porcine skin, the skin is taken out and shaken well to remove excess solution and imprinted on agar plates.

For groups of agar plates and skin pieces being used for our product, the aerosolized foam is sprayed on the surface. After two minutes of contact time, the aerosolized foam is removed from the surface and in the case of porcine skin the imprints of the skin are taken on agar plates. Similarly, for the agar plates and porcine skin pieces used for sponge based applicator, the sponge post wetting with liquid 5% Betadine is gently rubbed on the

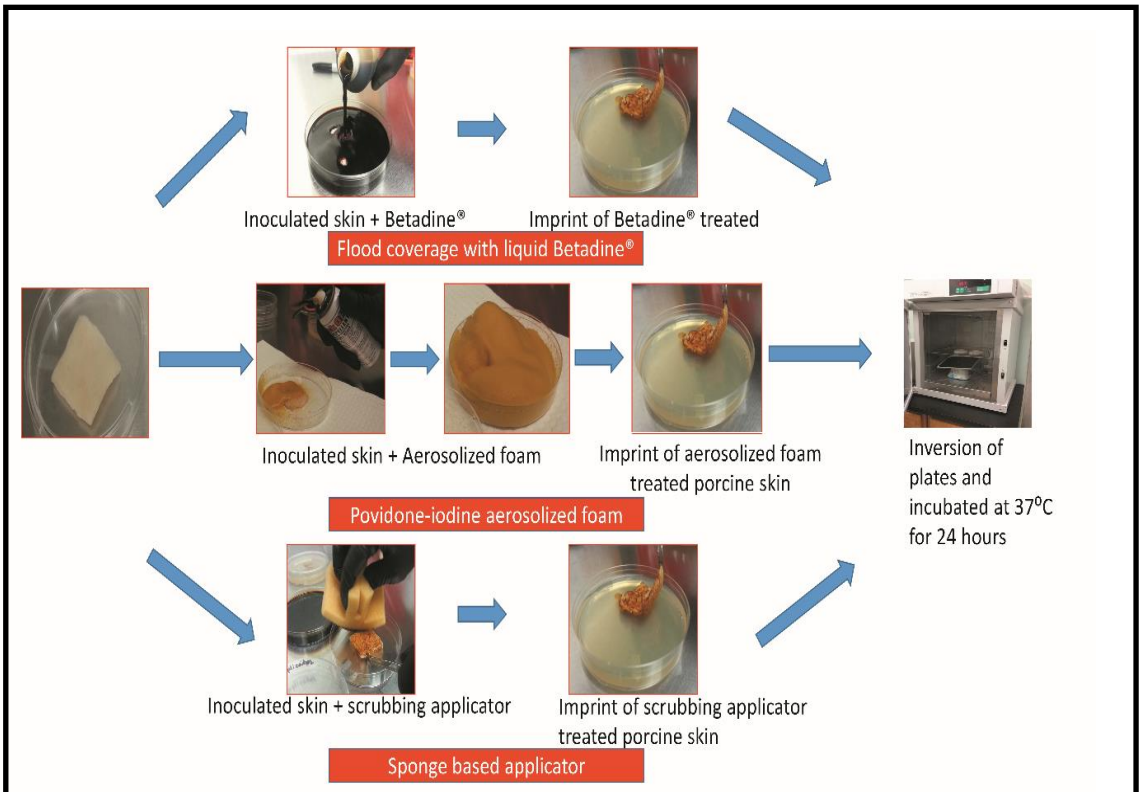

Figure 3-3 Steps involved in assessing bactericidal activity on porcine skin. Steps involved in treating the porcine skin with flood coverage of Betadine aerosolized foam and sponge based applicator and evaluating its bactericidal activity

inoculated surface in natural motion. The porcine skin is held firmly with a sterilized forceps to enable researchers to scrub the surface thoroughly, like the real world situation. Damaged plates resulting from scrubbing were discarded. Post surface rubbing with the wet sponge for two minutes; a dry sponge is used to remove the excess liquid. In the case of the porcine skin, they are taken out and imprinted on an agar plate.

3.2.6 Statistical analysis

Statistical analysis was performed in Microsoft Excel using analysis of variance (ANOVA) single factor to establish the efficacy of the antimicrobial agents used. A measure of the significance of differences is the p-value. The p-value thus provides a more intuitive feel of the degree of difference between the two quantities being compared. For our case, the null hypothesis is that the number of surviving bacteria (colonies) remaining is equal for the two processes that we compare, namely, aerosolized foam and sponge based applicator.

3.3 Results

Figure 3-4 shows the number of live bacteria remaining on the surface of the agar plate after addition of 100µl suspension with 10^4 CFU of bacteria/ml on a TSA petri-dish and subsequent treatment with the disinfection protocols of interest. For the control (no disinfectant applied), this number starts at 1000 CFU and increases over 24 and 48 hours. More importantly, all the disinfection protocols, like povidone-iodine the aerosol foam, sponge based applicator, and flood coverage with liquid 5% Betadine (positive control) are equally effective for all three bacterial species the tested (*S. aureus*, *P. aeruginosa*, and *S. epidermis*). All bacteria are eliminated (no colonies are seen after 24 or 48 hrs of incubation, post-treatment).

Figure 3-5 show the results of the tests conducted on porcine skin subjected to the same preoperative skin preparation (disinfection) techniques tested against the same set of bacteria. In this case, different disinfection protocols have different outcomes. It is noteworthy that (as expected for a positive control), the flood coverage with liquid Betadine can eliminate all bacteria present in this case as well. For the applicator sponge

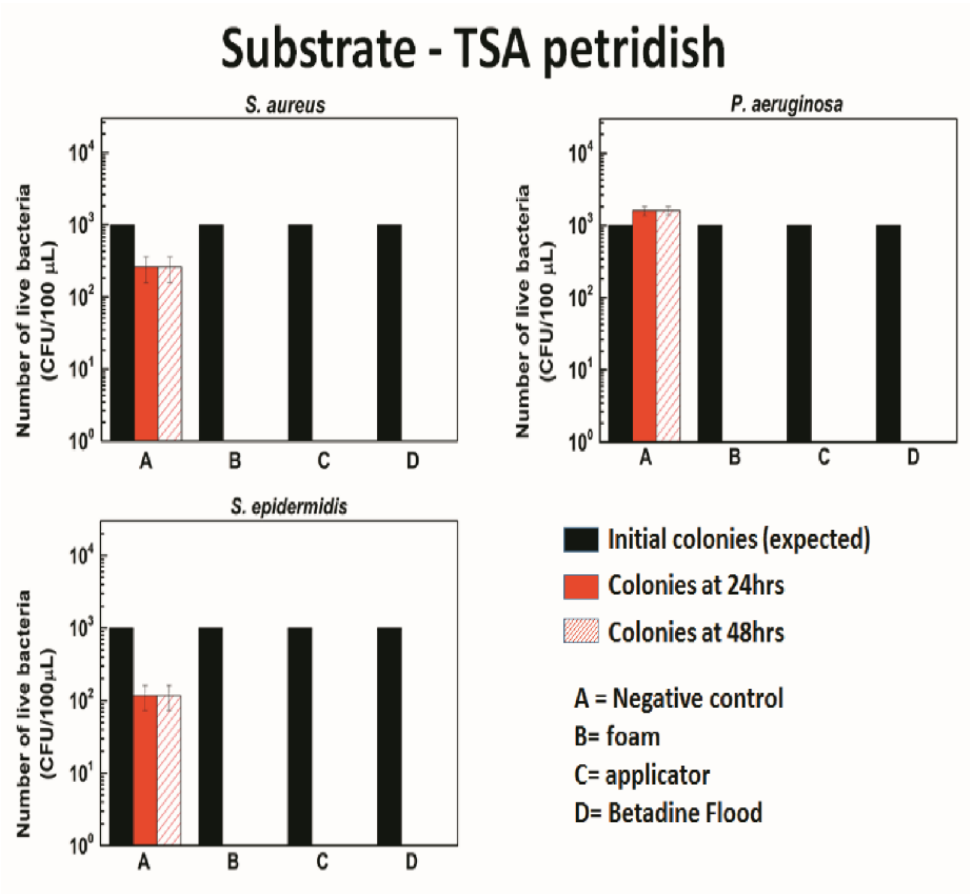

Figure 3-4 Viable bacterial count for different bacteria tested on agar plates. Number of live bacteria (CFU/100µL) observed on agar plate after 24 hours and 48 hours for negative control (no treatment done), application of aerosolized foam, application of sponge based applicator and positive control (application of 5% Betadine) for *S. aureus* (top left)[n=4], *P. aeruginosa* (top right)[n=5] and *S. epidermis* (bottom left)[n=5].

(currently used method for pre-operative skin disinfection), none of the bacteria tested were eliminated, although in 2 of the 3 cases (for *S. aureus* and *P. aeruginosa*) all were at least injured (no colonies seen at 24 hrs). With the foaming betadine suspension (new product

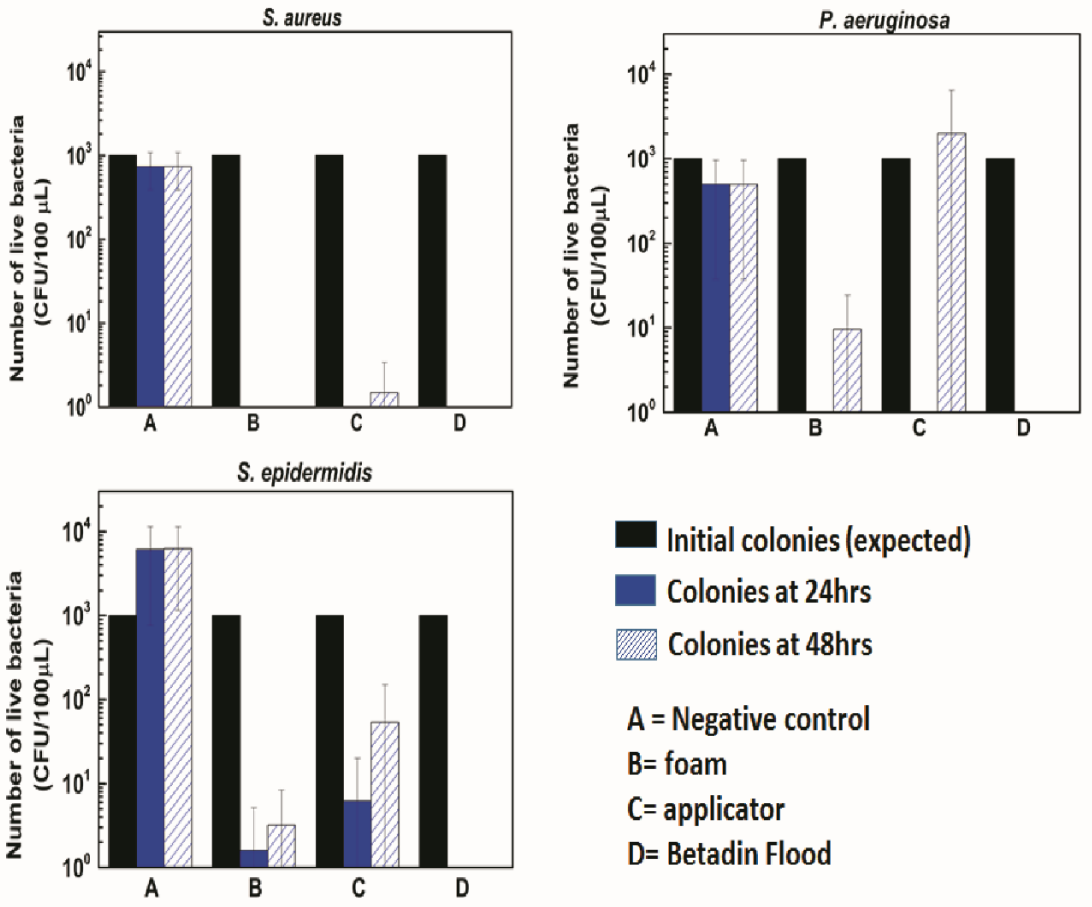

Figure 3-5 Viable bacterial count for different bacteria tested on porcine skin. Number of live bacteria (CFU/100µL) observed on porcine skin after 24 hours and 48 hours for negative control (no treatment done), application of aerosolized foam, application of sponge based applicator and positive control (application of 5% Betadine) for *S. aureus* (top left)[n=4], *P. aeruginosa* (top right)[n=5] and *S. epidermis* ((bottom left)[n=5]

being investigated), the results obtained did not show statistically significant difference when compared to the sponge applicator for all the bacteria tested. *S. aureus* was eliminated, and the number of colonies observed for the two other bacteria was lesser than the corresponding number for the sponge applicator at both 24 and 48 hrs. The p-values obtained when comparing similar readings (same bacteria, same duration of incubation) are shown in Table 3.1.

When the experiment was repeated by flood coverage of the plates with 1X PBS, it was observed that the plates showed bacterial growth similar to that of the control samples for both the substrates. This clearly indicated that there was no mechanical washing of the bacteria when flooded with Betadine but antimicrobial effects arose due to the chemical activity of 5% Betadine.

Table 3.1. p-values calculated using null hypothesis for all applications**.** List of p-values, as calculated for the null hypothesis that the two disinfection protocols (aerosolized foam and sponge based applicator) are equally effective. (n = 4 for *S. aureus*; n=5 for *S. epidermis* and *P. aeruginosa*).

Bacterial species	**Observation time period**	**Porcine skin**
S. aureus	24 hrs	-
	48 hrs	0.1682
P. aeruginosa	24 hrs	0.4876
	48 hrs	0.3486
S. Epidermis	24 hrs	0.4929
	48 hrs	0.2819

3.4 Discussion

For agar plates as a substrate, the aerosolized foam, like the other existing methods of application, has a very strong bactericidal effect, as observed from the lack of colonies even after 48 hours for all the disinfection methods examined. Given that these plates provide a smooth surface for the antimicrobial agents to come into contact with the bacteria, it can be considered as an ideal case.

Porcine skin can be regarded as a more realistic model for studying human skin *in-vitro*. Here, the bactericidal effect of the agents tested is mitigated by pores, folds and other structures in the skin that prevent the antimicrobial agents from sustained contact with the bacteria. Though all agents show approximately 2-log reductions in bacterial number, the tested foam did not have any statistically significant difference in efficacy when compared with the other agent/method tested as seen from the statistical analysis. It may be noted that none of the current surgical site preparation practices can completely sterilize skin.

Further, this is a preliminary study that merely looks at the efficacy of the foam against three bacterial species *in-vitro*, and it only suggests that the foam can be used for the surgical site preparation. Additional studies on live animals and humans in a "real-world" setting may be needed before one can accurately establish how effective it is compared to other formulations/ methods available in the market, and whether there are any conditions under which it may not be as effective.

3.5 Conclusion

This study shows that using a new delivery system (aerosolized foam) for an established antiseptic (Betadine) achieved bactericidal results comparable to a traditional system that is currently used when tested *in-vitro* on both agar plates and porcine skin.

Given the limitations of this preliminary study, further studies venturing into clinical trials will be needed to obtain substantial evidence for SSI prevention using this product. Such studies will also explore how the aerosolized foam compares with many other kinds of surgical skin preparation products/techniques and whether the anticipated advantages of using the aerosolized foam (lower "error" rate due to its ease of use, and saving health care costs by virtue of requiring less time compared to the standard method) can be realized in a "real world" clinical setting.

CHAPTER 4

4 MICROCHANNEL ELECTRICAL IMPEDANCE SPECTROSCOPY

The impedance of a system is measured by applying an alternating voltage to the system and then measuring the alternating current through the system. Any chemical system can be represented as an equivalent circuit composed of resistors, capacitors, and inductors. This equivalent circuit describes the "complex resistance" or Impedance that the alternating current encounters when passing through the system (204). Electrical impedance is a non-destructive and non-invasive technique.

Sengupta et. al used electrical impedance spectroscopy (EIS) to detect the presence of living and viable bacteria in a suspension (205). Bacteria are prokaryotes and are surrounded by a cell membrane that encloses the contents of a cell. That is, the membrane of the cell acts as an interface that separates the cell interiors from the external broth media. Bacterial cells can store charges (capacitance) when exposed to an alternating field due to the presence of cell membrane (206). These cells, therefore, act as capacitors and contribute towards the capacitance of the suspension.

A capacitor is an electrical component that can store electrical energy (store charges) in an electrical field. The most commonly used capacitor involves two electrical conductor plates separated by an insulating material. On application of an electric field, the positive charges tend to collect on one plate while the negative charges collect on the other plate resulting in the formation of an electric field. Capacitance is measured as

$$C = \frac{\mathrm{Q}}{\mathrm{V}}$$

Where,

C = Capacitance (Farads)

Q = electric charge on each conductor (Coulombs)

V = potential difference between the plates (Volts)

For parallel plate systems, where A gives the area of the plates and a distance of d separates the plates, the capacitance of the system is given by

$$C = \frac{\varepsilon A}{d}$$

Where,

ε = permittivity = $\varepsilon_0\varepsilon_r$

ε_0 = permittivity of vacuum

ε_r = relative permittivity

Bacterial cells act as dielectric particles and have both capacitive and resistive properties. However, if the cell is dead or unviable, the cell membrane of the bacteria is disrupted, and it loses its ability to store charges (206). Hence, any change in the number of cells in the suspension can be easily monitored by EIS. Thus, EIS technique can be used to distinguish the bacterial capacitance from a dead or unviable and alive or viable cell.

The presence of a microorganism in a suspension affects the impedance of the broth in two ways. Firstly, there may be a change in capacitance of the media due to the metabolites produced by the bacteria during its growth like carbon dioxide and organic acids; secondly, the charge storing capacity of a cell itself adds to the capacitance of the

media (205, 207). In a bacterial solution, other parasitic capacitors like the interfacial double layer capacitor can overwhelm the capacitance signal obtained from the bacterial cells in the bulk capacitance. However, prior work has been shown that by application of microfluidics and using a very thin capillary, the time constant for impedance effects of the bacteria can be significantly enhanced and recorded (205).

The microfluidic cassette employed by us has long thin capillary channels having a radius of 1mm with two gold electrodes inserted into the channel at a distance of 1cm (as shown in figure 4-1(a)). The bacteria suspension is inserted into the channel and an AC voltage across a frequency ranging from 1 kHz to 100 MHz is applied across the bacterial

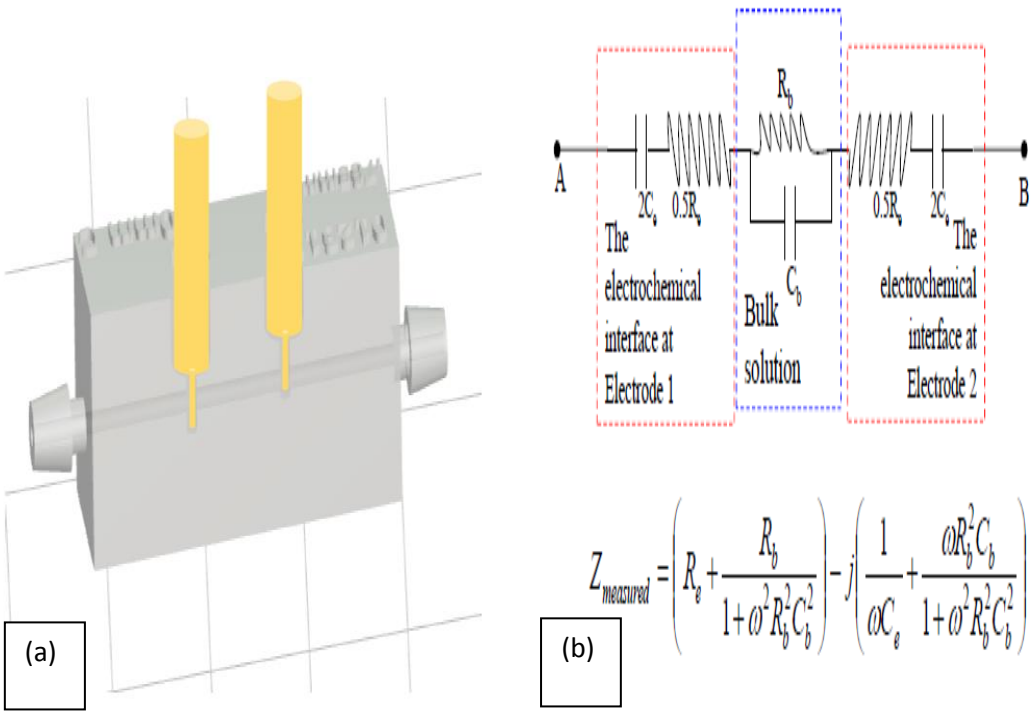

Figure 4-1 (a) Microfluidic channel with gold electrodes inserted at 1cm interval used for EIS analysis of bacterial solution. (b) Electrical circuit model to represent the presence of bacteria between two electrodes when a voltage is applied across them (205).

suspension captured in the channel. An Agilent 4294A Impedance Analyzer is used to detect the impedance change of the system. A sinusoidal potential is applied to the system and when expressed as a function of time,

$$V = V_0 \sin(\omega t)$$

Where,

V_0 = amplitude of the potential applied

ω = radial frequency

t = time

The response current generated is also in sinusoidal form but shifted in phase and can be denoted by

$$I = I_0 \sin(\omega t + \Phi)$$

Where,

I_0 = amplitude of the current

Φ = phase shift

The impedance of the system, thus, is dependent on the applied frequency and can be expressed analogously to the Ohm's law as

$$Z = \frac{V_0 \sin(\omega t)}{I_0 \sin(\omega t + \Phi)}$$

Where,

Z= impedance of the system,

$V_0 \sin(\omega t)$ = Voltage applied as a function of time

$I_0 \sin(\omega t + \Phi)$ = Response current as a function of time

ω = radial frequency

Φ = phase shift

The impedance can also be expressed as a complex number using Euler's relationship,

$$Z(\omega) = Z_0 \, (\cos\Phi + j\sin\Phi)$$

The real part denotes the resistance while the imaginary part denotes the reactance of the system.

As the bacterial number changes over time, there is a significant shift in the impedance of the suspension. The use of long and narrow microfluidic channels results in increasing the bulk resistance of the system. As seen in figure 4-1b, the reactance of the system is obtained by multiplying the bulk capacitance with the bulk resistance. Hence, any change in the reactance value gets magnified. In addition, operating in high frequencies >1MHz, further magnifies the effect. This system can also be applied to blood samples as the number of blood cells in a sample do not change with time, and hence any capacitive change in the system can be attributed to the change in the bacterial population in the suspension.

The circuit diagram of the device architecture is shown in figure 4-1(b). In the circuit, as illustrated in figure 4-1(b), the resistance due to the charge transfer is negligible and neglected as we are working with non-faradaic reactions. The screening effects arising from the electrode-solution interactions are accounted by the electrode interference

capacitances (C_e), while the charges stored by the bacteria is denoted by the bulk capacitance (C_b). Thus the equivalent circuit of our system is

$$Z_{measured} = \left(R_e + \frac{R_b}{1+ \omega^2 R_b{}^2 C_b{}^2}\right) - j \left(\frac{1}{\omega Ce} + \frac{\omega R_b{}^2 C_b}{1+ \omega^2 R_b{}^2 C_b{}^2}\right)$$

The number of bacteria present in the system modifies the bulk capacitance of the media. Hence any changes in the bacterial number is reflected by a concomitant change in the impedance of the system.

It is worthwhile to note that for all practical purposes, the equivalent circuit often has components like an inductor, L_e which accounts for the noise in the overall circuit. Resistance, R_e accounts for the resistance of the electrode due to the electrodes and connectors present. R_b is the resistance due to the media and bacterial cells. The bacterial C_b is overshadowed by C_e, the parasitic capacitance of the electrical double layer at the electrodes. C_e is a function of the ionic strength of the suspension only. However, using an optimized geometry of the capillary channel the relaxation time constant of the bulk, R_bC_b, becomes comparable to that of the interface, R_eC_e (205). Suitable modifications of the electrode geometry and the microfluidic architecture like a long and narrow channel and use of high frequencies allow us to detect any changes in C_b.

This allowed the researchers to study the changes in measured impedance chiefly due to the change in the bulk capacitance. The change in the bulk capacitance reflects the change in the number of the bacteria. It is well known that bacteria in a solution do not behave as ideal capacitors and hence the capacitance of the bacteria is better represented by constant phase element (CPE) in the equivalent circuit (3, 204). This non-ideal behavior

of cells results in semicircles with centers at the x-axis to be slightly depressed. Hence a circuit element CPE is introduced to account for the non-homogeneity of the system. The impedance of CPE is a combination of two values – CPE-T measured in $Fs^{(\alpha-1)}$ and CPE-P (phase component) which has numerical values less than 1. Mathematically, the impedance of a CPE is given by,

$$Z_{CPE} = \frac{1}{(j\omega)^{\alpha}C}$$

Where,

C = capacitance

α = values less than 1

It is worthwhile to note that here, the phase component of the bulk is strictly a measure of the type of bacteria and the media. It is independent of the bacterial concentration as has been shown elsewhere (3). On the other hand, bulk CPE-T is a measure of the concentration of bacteria in the solution. For most bacterial and media combination the bulk CPE-P is found to deviate slightly (approx. 0.95-0.97) from an ideal capacitor (CPE-P =1). Hence for all purposes, we use the unit Farad to represent the bulk CPE-T even though ideally the units should be Farad x $second^{(\alpha-1)}$ (3). For our system, the impedance response tends to be a capacitor at higher frequencies [$Z \sim (\omega C)^{-1}$] while it tends to be a resistor at lower frequencies [$Z \sim R$].

The experimentally obtained data is fit on a circuit built using the various electrical parameters, known as the equivalent circuit model to analyze and interpret the impedance data. It is worthwhile to note that an increase in bacterial growth leads to a concomitant

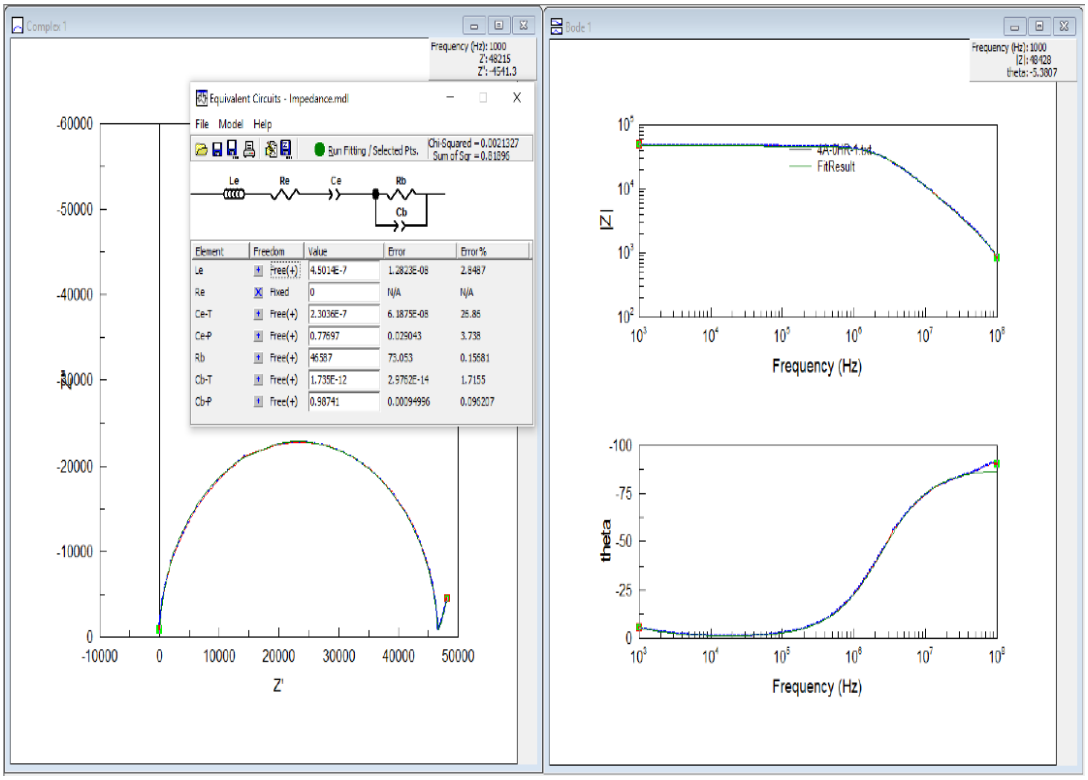

Figure 4-2 Z-view® software used for EIS data fitting. Inset (Equivalent circuit model)

increase in impedance while a decrease in the impedance is recorded as a measure of the death of cells. On modeling, the observed impedance data to an equivalent electrical model, the increase in the impedance of the solution appears as an increase in bulk capacitance. A commercial software called Z-view® is used to fit the equivalent circuit models with the impedance values obtained from the EIS of the bacterial culture as shown in figure 4-2. This allows us to find the values of individual parameters in the circuit, C_e, R_e, L_e, R_b and C_b, as shown in figure 4.2. A plot of C_b-T with time denotes the change in capacitance of the bacterial population over time.

Here, we have applied the same principles to acid-fast bacteria like *Mycobacterium bovis BCG* (*M. bovis BCG*) and *Mycobacterium smegmatis* (*M. smegmatis*) to analyze their

time-to-detection. The automated culture-based systems using impedance technology measures the discernable change in impedance chiefly by the change in the resistance of the growth media/conductivity of the double layer resulting from the generation of metabolites. However, our technique is not based on the changes caused by the bacterial metabolism but by directly measuring the number of bacteria present in the media. Some examples of currently available automated culture-based systems that are based on impedance changes occurring at the double layer involve the Bactometer (Bio Merieux, Nuertingen, Germany), the Malthus systems (Malthus Instruments Ltd., Crawley, UK), rapid automated bacterial impedance technique (RABIT) (Don Whitley Scientific Ltd., Shipley, UK), and BacTrac (Sy-Lab, Purkersdorf, Austria) for blood culture purposes (207). Till date, no culture based systems using impedance spectroscopy exists that uses just change of impedance resulting from the change in the bacterial concentration in the media to detect the presence or absence of bacteria in a system.

CHAPTER 5

5 MYCOBACTERIA

5.1 Background

The genus Mycobacterium mostly appears as saprophytic inhabitants. However, it also includes several disease-causing pathogens that can cause diseases in humans and animals. Most of them are aerobic, non-spore forming and non-motile bacteria that can be found in air, water, and soil. The manifestation of these pathogens may be in pulmonary, skin or soft tissue lesions and some of the serious, chronic diseases which result from mycobacteria are tuberculosis, leprosy (208). Preventing the transmission of mycobacteria is difficult as they are resistant to drying, alkali treatment, frozen section preparation and many chemicals (26, 209). Also, they have been found to be resistant to several antibiotics and chemotherapeutic agents (209). The drug resistance in mycobacteria is attributed to its hydrophobic cell envelope as well as due to the presence of hydrolytic or drug modifying enzymes (210).

Tuberculosis (TB), is the second deadliest disease amongst infectious diseases, caused by *Mycobacterium tuberculosis*. Even with all advances and better detection techniques, the detection rate is very low. This is so as in most cases, a patient afflicted with TB is asymptomatic and noninfectious. This compounded by the fact that *M. tuberculosis* has a long generation time, extended dormancy periods, complex cell envelope and intracellular pathogenesis (210).

Based on their generation times mycobacteria are divided into slow and rapid grower species. Species that need more than seven days to form colonies on solid media

under optimum conditions are known as slow growing species (*like M. tuberculosis, M. bovis BCG*) while species which take less than seven days are known as rapid growers (like *M. smegmatis, M. fortuitous*) (211).

The generation time of M. tuberculosis is ~24 hours. Low concentrations of bacteria and long generation periods and long incubation times lead to diagnostic delays. Also, its state of dormancy and its ability to remain in the infected tissue inactive further aggravate the situation. Failure to detect the disease in time leads to secondary drug resistance, continued transmission and ultimately to death (212). Mycobacterial cell structures are very different from other bacterial cells that further complicate matters.

5.2 Transmission

M. tuberculosis is unable to replicate in inanimate environments, and it spreads from one human to another through the air. When an infected person coughs, sneezes or talks, the aerosolized sputum containing the bacilli is generated. Droplet nuclei containing organisms may also be produced during sputum processing. When these droplet nuclei containing organisms are inhaled by another person, and they reach the alveoli within the lungs, they can replicate (213). For healthy humans, the host immune systems kick in and prevent such replication. However, if the bacilli remain viable but dormant, they result in latent TB. For immunocompromised humans, the mycobacteria can replicate in the lungs and result in the spread of TB. After inhalation of the organisms, viable bacteria can multiply within the alveolar macrophage every 25 to 32 hours (213). As it reaches a concentration of 10^3 to 10^4 in number in about 2 to 12 weeks, it elicits host immune response (213). The transmission of TB is determined by the following factor – (a) duration of for which a person is exposed to the infecting bacilli, (b) the immune system of the

exposed person, and (c) the number and concentration of the causative organism in the air.

5.3 Staining

Both gram-positive and gram-negative bacteria contain peptidoglycan which is composed of repeating N-acetyl-β-D-glucosaminyl-(1-> 4)-N-acyl-muramic acid units cross-linked by short peptide chains (209). Gram-positive bacteria have thick peptidoglycan layer in the cell walls while gram-negative bacteria contain an outer membrane outside the thin peptidoglycan layer (209). As a result, when gram-staining is done, gram-positive bacteria retain the color of crystal violet and appear purple in color when looked under a microscope. However, when gram staining (using alcohol), gram-negative bacteria do not retain the color of crystal violet during the decolorization step. The outer membrane of a gram-negative cell degrades, the cell wall becomes porous, and the counterstain can penetrate the cell wall. As a result, gram-negative bacteria appear red when observed under a microscope. However, mycobacterial species differ from other bacteria cells; gram staining cannot be done for them. Unlike other bacteria, the mycobacteria cell wall is much thicker and waxy, and rich in mycolic acid. They contain several fatty acids like waxes, phospholipids, mycoserosic and phthienoic acids. The presence of mycolic acid (having carbon atoms ranging from 70-90) and other free lipids provide hydrophobicity to the cells (209). They have a unique IV cell wall structure which consists of a hydrophobic mycolic acid and peptidoglycan layer held together by arabinogalactan (209). The mycobacterial organisms do not stain by gram staining and appear as ‘ghosts.' To visualize mycobacteria under a microscope, they need to be acid-fast stained. Carbol fuchsin forms stable complexes with mycobacterial cell walls and can retain the stain as seen in figure 5-1(a) and (c). When decolorization is done using acid-

alcohol solution, the cell walls retain the stain. As these organisms can resist decolorization even with acids, they are known as acid-fast bacteria. Further, when counter stains like methylene blue are used, they make the visualization, of the acid-fast organism under the microscope, much easier. Techniques like Ziehl-Neelson, Kinyoun staining, are used. Upon staining the mycobacteria appear as pink or bright red and have long, rod-shaped structure (211).

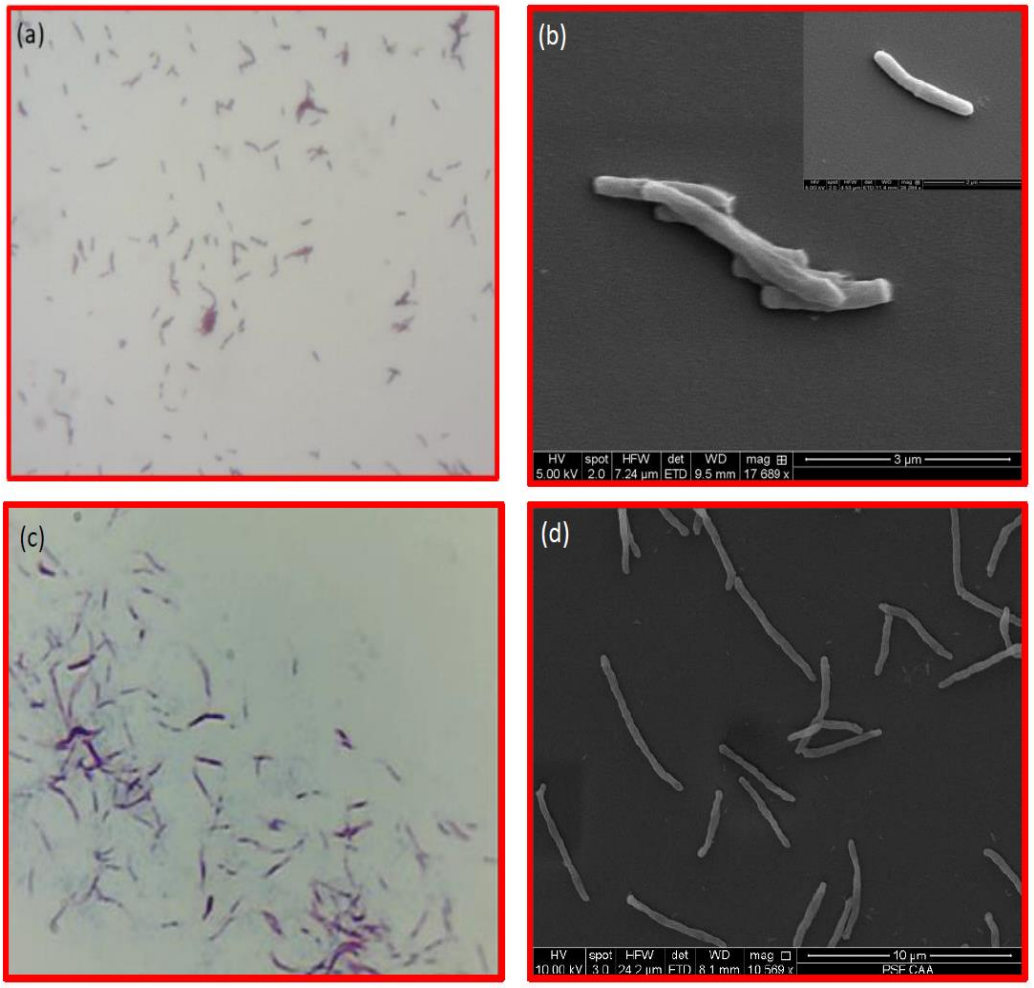

Figure 5-1 (a) Kinyoun acid fast staining of *M. bovis BCG* (b) SEM image of *M. bovis BCG*, (c) Kinyoun acid fast staining of *M. smegmatis* (b) SEM image of *M. smegmatis*.

5.4 Structure

Mycobacteria are long, rod-shaped organisms (1-10μm long X 0.2-0.6 μm wide) (26, 211). They may be slightly curved or straight as seen the SEM images of *M. bovis BCG* and *M. smegmatis* in figure 5-1 (b) and (d) respectively. The colony morphology varies with the species. The colonies range from being smooth to rough. *M. tuberculosis* (on Middlebrook 7H10 agar) have dry, rough-edged colonies with a wrinkled surface. Mycobacteria tend to clump to one another producing strand-like structures as shown in figure 5-1(b).

5.5 Digestion and Decontamination

Clinical samples obtained from patients are rarely pure samples (that is, they usually have a mixture of two or more microorganisms). For example, a clinical sputum sample from a patient suffering from TB will have, in addition, to *M. tuberculosis* has *S. aureus, P. aeruginosa, S. epidermidis* etc (214, 215). As the mycobacteria have long generation periods, other bacterial species tend to overgrow in the samples. Hence, for proper identification and detection of mycobacteria, the clinical samples need to be pretreated (digested and decontaminated) to kill all non-mycobacterial species before being subjected to any form of processing/ detection technique. The process of digestion and decontamination enable us to eliminate the contaminants (all bacteria other than mycobacteria) and isolate mycobacteria from the samples.

There are several methods proposed for decontamination. Sodium hydroxide (NaOH), is commonly used for decontamination. However, it has been found that strong alkali tends to affect the mycobacteria as well during decontamination. Hence, one should target to achieve milder decontamination technique with effective control over the

contaminating bacteria. A combination of N-Acetyl-L-cysteine (NALC) and NaOH is preferred by several researchers as an effective decontaminant and is considered as a gold standard (215, 216). NALC also serves as an effective mucolytic agent and help in reducing the viscosity of the sputum samples. Liquefying the sputum ensures that the chemicals can reach all the contaminants and eliminate them. The use of NaOH-NALC solution for 15 mins followed by addition of phosphate buffer solution (PBS) dilutes the harsh effect of NaOH. Following this steps, the sample is centrifuged to ensure homogenization. The supernatant is discarded, and the pellet is resuspended in appropriate culture medium for the mycobacteria to grow.

CHAPTER 6

6 RAPID CULTURE-BASED DETECTION OF LIVING MYCOBACTERIA USING MICROCHANNEL ELECTRICAL IMPEDANCE SPECTROSCOPY (M-EIS)

The material presented in this chapter is under review as "**Rapid culture-based detection of living Mycobacteria using microchannel Electrical Impedance Spectroscopy (m-EIS)**"

Roli Kargupta, Sachidevi Puttaswamy, Aiden J. Lee, Timothy E. Butler, Zhongyu Li, Sounak Chakroborty and Shramik Sengupta

in Biological Research.

Multiple techniques exist for detecting mycobacteria, each having its advantages and drawbacks. Among them, automated culture-based systems like the BACTEC-MGIT^{TM} are popular because they are inexpensive, reliable and highly accurate. However, they have relatively long "time-to-detection" (TTD). Hence, a method that retains the reliability and low-cost of the MGIT system, while reducing TTD would be highly desirable. Living bacterial cells possess a membrane potential, on account of which they store charge when subjected to an AC-field. This charge storage (bulk capacitance) can be estimated using impedance measurements at multiple frequencies. An increase in the number of living cells during culture is reflected in an increase in bulk capacitance, and this forms the basis of our detection.

M. bovis BCG and *M. smegmatis* suspensions with differing initial loads are cultured in MGIT media supplemented with OADC and Middlebrook 7H9 media respectively, electrical "scans" taken at regular intervals and the bulk capacitance estimated

from the scans. Bulk capacitance estimates at later time-points are statistically compared to the suspension's baseline value. A statistically significant increase is assumed to indicate the presence of proliferating mycobacteria. Our TTDs were 60 and 36 hours for *M. bovis BCG* and 20 and 9 hours for *M. smegmatis* with initial loads of 1000 CFU/ ml and 100,000 CFU/ml respectively. The corresponding TTDs for the commercial BACTEC MGIT 960 system were 131 and 84.6 hours for *M. bovis BCG* and 41.7 and 12 hours for *M smegmatis,* respectively. This proves that our culture-based detection method using multi-frequency impedance measurements is capable of detecting mycobacteria faster than current commercial systems.

6.1 Introduction

Tuberculosis (TB) is a chronic disease with a high mortality rate. According to a recent WHO report, it is estimated that about 1.5 million people died from TB in 2013 (217). However, proper and timely diagnosis and treatment can reduce the mortality rate and the economic burden associated with TB (217, 218). An early diagnosis of TB would yield two benefits. Firstly, clinical intervention (treatment with first-line antibiotics) is initiated sooner and secondly, drug susceptibility testing (DST) can be completed earlier, leading to tailored treatment of patients according to the DST results (219) and prevent the widespread transmission of drug resistant strains.

Various diagnostic techniques are available to clinicians to identify patients with TB and/or detect mycobacteria in patient samples. Common diagnostic techniques include serial sputum smear microscopy and chest X-ray. However, these techniques suffer from poor specificity and/or sensitivity (have high rates of false negatives) and information on drug susceptibility is lacking (217, 219-221). An alternative testing method is the Mantoux

tuberculin skin test (TST). In Mantoux TST, the response to the injection of a small dose containing *M. tuberculosis* derivatives is observed at different time intervals. However, this test suffers from low specificity and the interpretation of the obtained test results is subjective (218). Other techniques include polymerase chain reaction (PCR) based rapid diagnostic tests (222-224). The Xpert MTB/RIF is a nucleic acid amplification technique that can detect the presence of mycobacteria in less than 2 hours, and has a limit of detection of 131 CFU/ml in sputum (225). However, it suffers from a couple of limitations when compared to automated culture based systems. Firstly, the limit of detection of culture-based systems is 1 CFU in the sample (226, 227). Second, the reagents/chemicals used are sometimes unstable in "real-world" situations (220), which is not the case for disposables of the culture-based systems (growth media). Finally, whereas a hardware unit for culture-based system (BD Bactec 9120 that handles 120 Myco/F-lytic bottles simultaneously) costs ~$20,000 and disposables cost < $10 per test, the costs are significantly higher for the Xpert (228). The XpertMTB/RIF instrument (with 4 modules that can run 16-20 tests per 8 hr shift) has an unsubsidized cost of ~$34,000 and each single use cartridge has a cost of ~$40 (229). The high cost is especially daunting to end-users (hospitals) in low to mid-resource environments, where the great majority of TB cases occur. While, a consortium of charitable organizations that include the Foundation for Innovative New Diagnostics (FIND), the Gates Foundation, USAID and UN agencies, provide a 50% subsidy on the instrument and a 75% subsidy on the disposables, making the Xpert^{TM} instrument available for $17,000 and disposables available for ~$10 a test, such funding is limited and available to only a few select "approved" users. Hence, culture based testing is still considered the gold standard (217) because of its limit of detection of 1 CFU and still widely used (230)

due to their relatively low cost.

Culture based detection is cheap, reliable, highly accurate and can be used for DST against multiple drugs and drug combinations (217). It has been found that in comparison to solid media, mycobacteria grow much faster in liquid media (231). Currently a number of culture-based methods for detection of TB is available such as broth micro-titer based microscopic observation drug susceptibility (MODS) assay and automated liquid culture based diagnostic systems such as the BD BACTEC 960 MGIT fluorometric system, BACTEC 460 TB System and Biomerieux's BacT/ALERT 3D system for detecting mycobacteria in samples. MODS assay, though inexpensive and has an average time-to-detection (TTD) of ~8 days (232), requires training and technical expertise of the personnel (231). On the other hand, automated liquid culture-based systems only need sample to be prepared and loaded into the instrument. A major drawback of these broth based culture systems (automated, or otherwise) is that they are time consuming, with most positive clinical samples having TTDs of ~ 14 days (for MGIT system) (233). Also samples are typically incubated for at least 6 weeks before being deemed negative (234, 235). Hence, a system for detecting mycobacteria that retains all the advantages of current automated culture-based systems like the MGIT system while requiring less time for results, is likely to be welcomed by users.

In 2010, Association of Public Health Laboratories (APHL) and the US Centers for Disease Control and Prevention (CDC) launched a 118- questions survey to assess the capabilities and capacities of TB testing facilities in United States (230). Of the 656 respondents, 580 (~88%) of them had know-how for implementing TB testing. Out of them, 466 facilities used primary broth based culture and 356 (~76%) of them used

semi/fully automated culture base systems. (The University of Missouri Hospital also uses a fully automated culture system viz. the BACTEC™ MGIT ™ 960 System from BD).

TB detection in bacterial suspensions by automated broth-based culture system takes a long time, chiefly because of the mechanism by which these systems operate. The semi-automated BACTEC 460 TB system uses Middlebrook 7H12 broth medium containing radioactive ^{14}C radioisotopes, and uses radiometric detection of $^{14}CO_2$ released to detect the presence of active microorganisms (mycobacteria) (236, 237). MGIT 960 systems, on the other hand, contain an oxygen-quenched fluorochrome that changes color as oxygen levels in the media change. MGIT 960 systems, hence, detect the depletion of oxygen inside the tubes as living mycobacteria consume oxygen (238). Similarly, systems like Versa TREK and MB/BacT-Alert are based on monitoring headspace pressure changes of sealed bottles/tubes (237) and monitoring the pH change of the media, respectively (239). Thus, all these automated culture-based systems share a basic operating principle viz. they sense changes in medium properties (O_2/CO_2 levels, pH etc.) brought about by mycobacterial metabolism as a marker for actively respiring/proliferating microorganisms. In this respect, they are similar to automated systems used for other applications such as blood culture (BACTEC™ and BacT/Alert™) or food quality testing (RABIT, Malthus 2000 etc.) (205).

The term “Impedance Microbiology” is often used to describe techniques that are based on the ability of microorganisms to alter the electrical properties of their growth media. The fact that microbial metabolism causes an increase the conductivity of the medium by breaking down less conductive species like sugars and proteins into more conductive ones such as lactic/pyruvic/carbonic acids and urea/ammonia was first reported

by Stewart in 1899 (240), and was studied in a quantitative manner by Cole (241).

After the development of more accurate and robust instruments to measure and monitor impedance, this approach became more feasible to implement in a lab setting. A number of researchers began investigating this method more rigorously and started to explore the use of this technique as a means to detect the presence of bacteria in various settings. In particular, it was discovered (242) that two distinct sources contribute to any measured electrical signal (impedance): the bulk solution and the electrochemical interface of the solution and the electrodes in direct contact with it. The bulk solution typically contains two types of species: (a) relatively mobile ions (such as Na^+, K^+, Cl^-, PO_4^{3-} etc.) that move through the solution overcoming drag by the solvent molecules on the application of an electric field, and (b) larger, relatively immobile species such as proteins and cells that either carry native charge or on which charges could be induced on applying an electric field. Thus, as shown in Figure 6-1(a), the bulk could be represented by a resistor and capacitor in parallel, and the electrochemical interface of the electrode and solution, which consists largely of ions in chemical equilibrium with the bulk, could be represented by a capacitor in series with the resistance of the electrode itself (205, 242). By increasing the number of ionic species present, bacterial metabolism is found to affect not only the bulk resistance (243), but also the surface capacitance (244, 245) since the latter arises from ions in chemical equilibrium with those present in the bulk . A more rigorous analysis of the relative quantitative contributions of the bulk and the interface to the overall capacitance (246) found that at operating frequencies of 1 MHz and lower, the contributions from the bulk capacitance (a.k.a. the geometric capacitance) and the interfacial capacitance were of the order of picofarads (10^{-12} F) and micro to nano farads

(10^{-6} to 10^{-9} F), respectively. Thus, while it is known that exposure to an AC field causes charge accumulation at the membrane of cells with non-zero membrane potential (living cells) (206), it logically follows that an increase in the number of cells in suspension would result in increased charge storage (bulk capacitance). Measuring changes in bulk capacitance brought about by an increase in the number of suspended cells, however, was not considered feasible. The consensus was explicitly stated in a review article by Munoz-Berbel et al.(247), who wrote that

"Geometric capacitance… due to the solution between the electrodes …. Because of its small value, in the picofarad range, it can usually be neglected in the measurement frequencies used in biosensor applications"

Our early work (205) at attempting to measure changes in bulk capacitance (C_b) relied on using geometric effects to enhance the effect of changes in C_b to the measured reactance (X) (the "imaginary" or "out-of-phase" component of the impedance). As shown in Figure 6-1(b), the use of long narrow microfluidic channel causes a larger fraction of the electrical flux lines to interact with the (few) microorganisms present. Another way to look at the effect is to study the equation embedded in Figure 6-1(a). Since for any given material, the resistance is inversely proportional to cross-sectional area and directly proportional to length, the long narrow geometry results in an increase in bulk resistance (R_b). It can be seen that for the reactance (X), the C_b is always multiplied by R_b. Thus, any changes to the value of X due to a change in C_b will be "magnified" by the higher R_b. Since the R_bC_b is also multiplied by the frequency (ω), this effect is further enhanced at high frequencies. The geometric effect alone allowed us to detect changes in C_b that was previously considered too small to measure.

We further enhanced the sensitivity of our measurement technique by using AC signal with higher frequencies (ω) as high as 100MHz. At these frequencies, the charge on the electrode reverses every ~10nsec (as opposed to 1 μsec or longer for signals of frequency 1 MHz or lower). A consequence of this is that, certain assumptions that we had previously made regarding the electrical behavior of the solution, no longer hold. For instance, the model shown in Figure 6-1(a) assumes that the capacitances (bulk and interfacial) were ideal. In an ideal capacitor, charges accumulate instantaneously. However, in cases like ours charge carriers are ions that are slow and bulky compared to electrons, and may take as long as hundreds of nanoseconds to complete the process of accumulation at the electrode (248). Hence, when fitting data, we replace the ideal capacitors in equation in Figure 6-1a with Constant Phase Elements (CPEs)(as shown in figure 6-1c).The impedance of a CPE is mathematically given (204) by

$$Z_{CPE} = 0 + 1/(j\omega)^{\alpha}Q$$

……..….(1)

as opposed to an ideal capacitor, whose impedance is given by

$$Z_{capacitor} = 0 + 1/j\omega C$$ ……..…..(2)

Q is the magnitude of the CPE and α is its phase. It can be seen that when α equals 1, the two equations are identical. In addition, at the high frequencies we deal with (up to 100MHz), the inductance of the wires connecting to the test circuit (the electrodes in contact with the aqueous suspension) can no longer be neglected. It is given by

$$Z = 0 + j\omega L,$$ ……..(3)

where, L is the inductance and ω is the angular frequency of the applied voltage. While this results in a more complicated circuit model with 7 parameters (the resistances of the

electrode and solution, the magnitudes and phases of the CPEs at the electrode and in the bulk, and the connection inductance), we use a large number of data points (Z at 200 different frequencies) and commercially available software for electrochemical analysis (Z-view ™) to obtain the values of our parameters.

By being able to detect small changes in C_b, our measurement method can tell us when the bacterial numbers in suspension are increasing, even when their values are

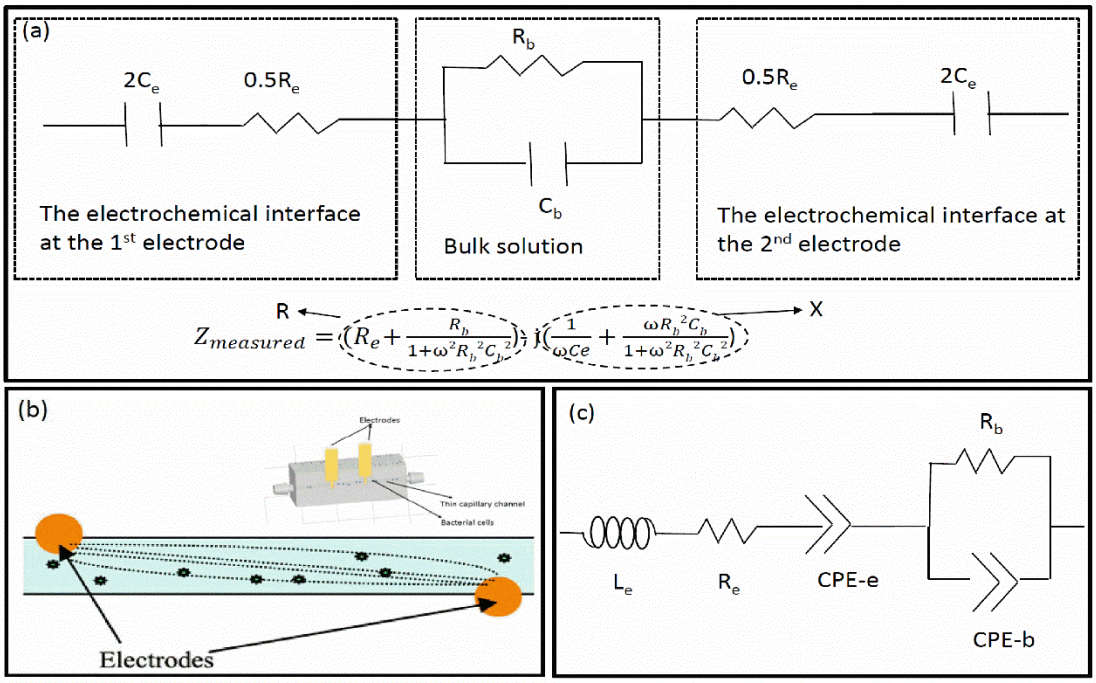

Figure 6-1 Electrical model and cassettes used for impedance measurement. (a) Electrical model representing two electrodes submerged in a microorganism suspension enclosed in a thin capillary channel (b) 3D printed long and narrow microfluidic channels with two gold electrode inserted for impedance measurement (inset) and schematic showing electrical lines of forces between two electrodes in the channel [205] (c) Modified electrical model which uses CPE instead of ideal capacitors to detect the presence of microorganisms in a suspension.

extremely low (~1000 CFU/ml). It can hence serve as a faster alternative to traditional automated culture-based detection methods like those discussed earlier. We have earlier demonstrated that our method is able to achieve faster times-to-detection (TTDs) in suspension with low initial loads (< 100 CFU/ml) for applications such as food quality testing (3) and blood culture(249). In both cases, we obtained 4-10 fold reductions in TTD, when compared to commercially available culture based systems like BACTEC etc. (249). In this work, we seek to demonstrate (a) a similar approach can also be used to detect/ rule out the presence of mycobacteria in broth based culture systems, and (b) that systems using our approach would have a lower TTD than state of the art culture-based detection systems like MGIT 960 system, Versa TREK and MB/BacT-Alert. We believe that shorter TTDs may turn out to have clinical relevance in the early diagnosis (and hence treatment) of persons with TB.

6.2 Method

6.2.1 Background and Overview

Mycobacterium bovis BCG and *Mycobacterium smegmatis* is used instead of *Mycobacterium tuberculosis* (Mtb) to demonstrate the applicability of our method *in-vitro* since they are easier and safer to handle under BSL-2 laboratory condition (250, 251). *M. bovis* BCG, like Mtb, is a slow growing mycobacterium with a doubling time of ~20 hours (252). *M. smegmatis*, on the other hand, is a rapidly growing mycobacterial species having a doubling time of ~3 hours, but has membrane properties similar to Mtb (253, 254).

To ensure absence of other bacterial contaminants all suspensions are frequently stained by Kinyoun staining. To visualize mycobacteria, acid-fast staining is used as the presence of mycolic acid in the cell walls prevent other staining protocols from working

(26, 255).

Figure 6-2 shows the broad outline of the experimental protocol. Individual

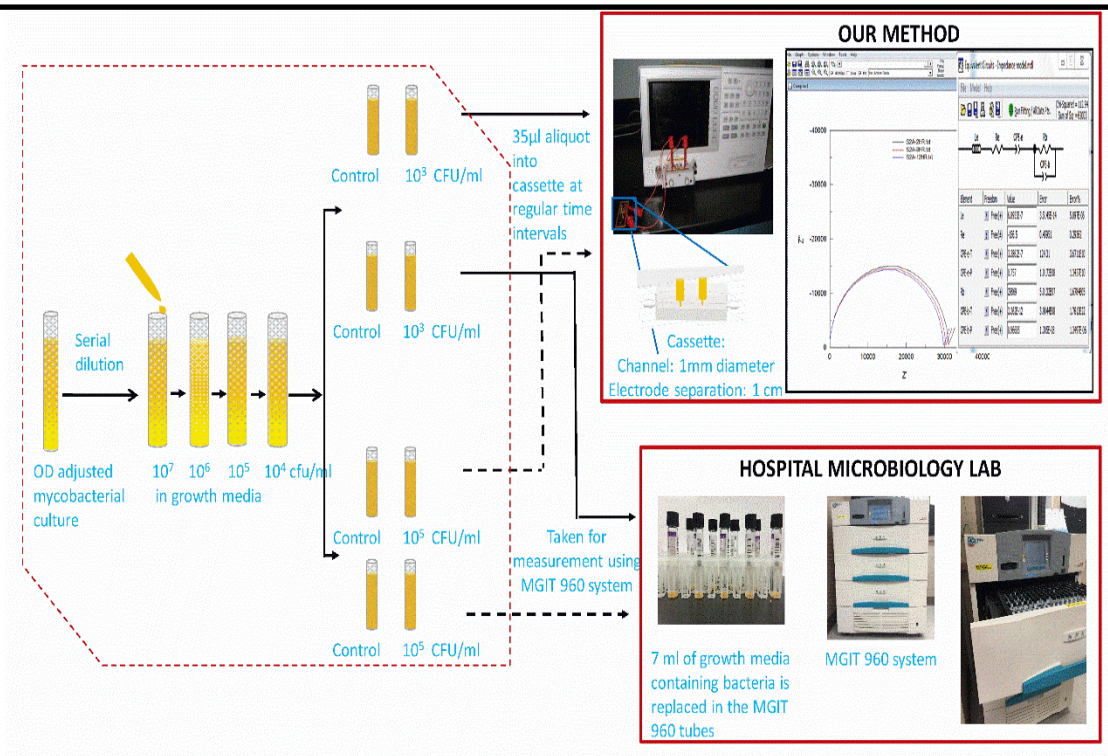

Figure 6-2 Experimental set-up for determining TTD of mycobacteria. 2 sets of similar samples are prepared by inoculating with mycobacteria and incubated at 37C. One set is sent to the Hospital microbiology lab for detection using MGIT 960 automated culture-based system while the other set of sample is tested using our technique. For our technique, at regular intervals of time, small aliquots of sample are drawn and its impedance is tested using impedance analyzer. The data is fitted to an equivalent circuit to generate a Nyquist plot [259] and thereby estimates the values of the desired circuit parameters. We show on the graph three sets of data: those obtained at 2 hr, 8hr, and 12hrs for a culture of *M. smegmatis* (large, medium, and small semi-circles). The inset shows the software output for circuit parameters obtained by fitting the data at 12 hrs to the circuit.

steps/procedures are described in detail later. Briefly, active cultures of *M. bovis* BCG and *M. smegmatis* are created in BD MGIT media and Middlebrook 7H9 media respectively with initial loads of $1X10^3$ and $1X10^5$CFU/ml. One set of cultures is sent to an external lab for analysis using an automated system (BD BACTEC MGIT 960). The automated system records when individual culture-tubes are placed into it, and when growing mycobacteria are detected by it for each individual tube, thus allowing us to easily obtain the time-to-detection (TTD). The other set is analyzed in our lab using our method.

In our method, tubes containing the cultures are incubated at 37°C. Periodically, aliquots from these growing cultures are withdrawn and placed within a 3D printed microfluidic cassette with 1 mm diameter micro-channels (Figure 6-1b). Microchannel Electrical Impedance Spectroscopy (m-EIS) data is obtained from the cassette and analyzed to obtain the bulk capacitance (C_b). Multiple sampling is done to ensure repeatability. C_b values are compared with the baseline (initial) values, and the time taken for the measured values to become larger than the baseline (with statistical significance) is our TTD.

Control samples containing growth media but no microorganisms are also analyzed similarly. TTDs of similarly prepared samples (containing approximately the same initial load of microorganisms) for the two methods (ours and that of the MGIT system) are compared.

6.2.2 Mycobacterial cell culture

Slow growing acid-fast organism *M. bovis BCG* (ATCC® 35734™) and rapid growing mycobacteria *M. smegmatis* (ATCC 700084) are used. Colonies of these mycobacteria are obtained by plating on egg based Löwenstein-Jensen plates for *M. bovis BCG* and 7H10 agar plates for *M. smegmatis*. Suspension cultures of the same are obtained

by inoculating BD MGIT media supplemented with mycobacteria growth supplements in the case of *M. bovis BCG,* and Middlebrook 7H9 broth supplemented with 0.05% Tween 80 and Middlebrook Albumin Dextrose Catalase supplements (ADC) in the case of *M. smegmatis*. During sub-culturing, the bacterial suspension is incubated at 37^0C with continuous agitation. The optical density (OD) mid-log cultures of the microorganisms are then adjusted to OD_{600} = 0.05 for *M.bovis* BCG and OD_{600} = 0.1 for *M. smegmatis* using a spectrophotometer which corresponds to a value of $5*10^6$ CFU/ml and $1\text{-}5*10^7$ CFU/ml respectively for use in the study (256-258).

6.2.3 microchannel Electrical Impedance Spectroscopy (m-EIS)

The basic principles governing the use of m-EIS to detect microorganisms have been described in our prior work (3, 249, 259). Briefly, the protocol requires us to periodically (every 12-24 hours for *M. bovis BCG,* and 2-4 hours for *M. smegmatis*) perform an electrical "scan" of sample aliquots in a microfluidic cassette, wherein we measure electrical impedance at multiple (200) frequencies ranging from 1 kHz to 100 MHz. The cassette contains a 1mm diameter microchannel with two gold electrodes, 1 cm apart in the channel. An AC voltage of 500 mV is applied across the two gold electrodes, using an Agilent 4294A Impedance Analyzer. At each frequency (ω), both the in-phase and out-of-phase components of the electrical impedance, Z, (resistance (R) and reactance (X)) are measured. In order to take the EIS measurements (scans), all aliquots from a given culture (across the different points in time) are introduced into the same individual cassette. As the cassettes used are handmade their readings vary from each other slightly and hence the data (values of bulk capacitance obtained) is scaled with respect to the value at the initial point in time (on the same cassette) to account for the cassette to cassette

variation.

The Z vs. ω data is fitted to an equivalent electrical circuit shown in Figure 6-2 using a commercially available software package (Z-view^{TM}). The software provides an estimate for the various circuit parameters, including the "bulk capacitance", which happens to be our parameter of interest – that provides a measure of charges stored in the interior of the suspension (away from the electrodes). It may be noted that the bulk capacitance is represented as a constant-phase element (CPE) to account for the non-ideal nature of the capacitance at cell membranes. The magnitude of the CPE, thus, reflects the amount of charge stored at the membranes of living microorganisms in suspension. Any increase in the number of microorganisms in suspension should hence, in theory, lead to larger amounts of charged stored in the interior of suspensions, and hence lead to a higher bulk capacitance (CPE_b-T) over time.

When observing a given suspension suspected of harboring proliferating microorganism, our problem reduces to asking the question of "Is the current value of the bulk capacitance *significantly g*reater than its value at the initial point in time?" To enable us to answer this question with a greater degree of confidence, for each sample, capacitance of 4-5 replicates are measured at specified time interval and statistically compared to baseline using Mann-Whitney U test. The earliest time point at which a significant difference is found, is defined as the TTD by m-EIS. Details of the statistical method are provided below.

6.2.4 Statistical analysis

Statistical analysis is performed in Microsoft Excel using Mann Whitney U-test. This non-parametric test compares if the population average between two groups is

significantly different or not (260). We chose to adopt the Mann-Whitney U-test over the more popular tools like t-test since we have only a few data points (bulk capacitance readings) per time point (5 for *M. bovis* BCG cultures, 4 for *M. smegmatis* cultures). More importantly, the normality assumption of the reading which is required for a t-test is not appropriate for our data. To check if the average of the bulk capacitance obtained at a time interval is significantly different from the bulk capacitance reading obtained in the first reading, the mean of the readings taken at the latter point in time is compared with the mean of the readings at the beginning of the culture (baseline values) and the U values corresponding to a p -value of 0.05 (level of significance of 5%; two tailed test) are calculated. Our null hypothesis is that the two bulk capacitance values are equal and the alternate hypothesis is that there is a significant difference between the bulk capacitance values. The Mann-Whitney U value obtained for our readings is compared to the critical U value (2 in the case of *M. bovis* BCG cultures where we had 5 readings at each time point and 0 in the case of *M. smegmatis* cultures where we had 4 readings at each time point) (260). If the Mann-Whitney U value obtained is equal to or less than the critical value, the null hypothesis is rejected, which means that there is a significant difference between the bulk capacitance values at the two time points. The earliest point in time where the U values obtained are equal to, or lower than, the critical U value is our time-to-detection (TTD) for a given sample.

6.3 Results

Six different kinds of suspensions are studied: Two of them contained *M. bovis* BCG in MGIT media with initial loads of ~10^3 CFU/ml and ~10^5 CFU/ml, respectively. Two other suspensions contained *M. smegmatis* in 7H9 media, again with initial loads of

~ 10^3 CFU/ml and ~10^5 CFU/ml. The other solutions are controls, consisting of sterile MGIT and 7H9 media. One sample each of the controls, three samples each of the suspensions with *M. bovis BCG*, and two samples each of the suspensions with *M. smegmatis* are analyzed using our m-EIS method. In parallel, one sample of each of the suspensions is sent to the University of Missouri Hospital Microbiology lab for analysis using the BD BACTEC MGIT™ system. Times-to-detection (TTDs) for our method are compared to those of the MGIT system.

Table 6.1: Comparison of TTD values obtained by our technique to BD BACTEC MGIT 960 system. Compares the TTD values obtained for the various concentrations of *M. bovis BCG* and *M. smegmatis* by our technique and that obtained by the commercially available automated system BD BACTEC MGIT 960.

M. bovis BCG			*M. smegmatis*		
Bacterial concentration used (in CFU/ml)	Our technique TTD (in hours) (n=3)	Hospital TTD (in hours) (n=3)	Bacterial concentration used (in CFU/ml)	Our technique TTD (in hours) (n=2)	Hospital TTD (in hours) (n=2)
Control - no bacteria added	No growth	No growth	Control - no bacteria added	No growth	No growth
100,000	36 ± 0	84.6 ± 0.58	100,000	9 ± 1.41	12 ± 0.71
1,000	60 ± 0	131 ± 11.79	1,000	20 ± 0	41.7 ± 0.35

Bulk capacitance values obtained on studying cultures initially containing ~10^3 CFU/ml and 10^5 CFU/ml of *M. bovis* BCG are shown in figure 6-3 (a) and (b) (along with the corresponding control). As shown in the table included as part of the figure, a statistically significant increase in the value of the bulk capacitance is seen at 60 hours for 10^3 CFU/ml and 36 hours for 10^5 CFU/ml in all three cases. Similar plots are shown for the suspensions with initial loads of ~10^3 CFU/ml of *M. smegmatis* and ~10^5 CFU/ml of *M. smegmatis* are shown in figures 6-4 (a) and (b) respectively. The TTDs obtained for each type of suspension using our method, and the TTD for similar solutions using the commercially available system (MGIT) is shown in Table 6.1.

6.4 Discussion

For both mycobacterial species, and for both initial loads in each, our times-to-Detection (TTDs) are lesser than the corresponding TTDs obtained by the hospital using a Bactec MGIT 960 system. Also, the lower the initial load, and the longer the organism's doubling time, more is the time saved. It is thus anticipated that the difference in TTDs with our method and the commercially available culture based methods similar to those employed by the MGIT system, will be even greater for clinical samples containing *M. tuberculosis* (Mtb), since the doubling time of Mtb is even greater than that of *M. bovis BCG*, and the initial loads can be an order of magnitude lower than what we tested (~1000 CFU/ml). There are non-culture based systems like Xpert MTB/RIF which have a low limits of detection and can do rapid detection of mycobacteria (~2hrs), these devices and reagents used are expensive. However, our technique, based on using the same reagents as that of the BACTEC MGIT 960 (and compatible with other reagents used for growing mycobacteria) will be cost-effective and will cut down the TTD considerably when

compared to automated culture-based system.

We believe that our technique of detection, though faster, will have similar sensitivity and specificity as the existing culture based automated system. Human sputum from patients with TB contain not only mycobacteria, but also a large number of other gram-positive and gram-negative bacteria (214). The current protocol for detecting mycobacteria using MGIT and similar automated culture based systems requires the user to first carry out a "decontamination" step that eliminates all the non-mycobacterial pathogens while preserving *M. tuberculosis*. Standard decontamination protocols exist**,** whose efficacy at killing non-mycobacterial pathogens while keeping *M. tuberculosis* cells viable and culturable has been extensively documented (211, 216, 261, 262). Nevertheless, it is not unheard of for non-mycobacterial species to survive decontamination, or for the process to kill or render unculturable some or all of the mycobacteria present (215, 263). The former case leads to false positives, and the latter to false negatives in currently used automated culture-based systems like the MGIT. Another source of false positives is contamination during handling and processing, either with mycobacteria or with non-mycobacterial species (264). On the other hand, false negatives can also arise due to inefficient sampling, wherein the sample of sputum used does not contain any *M. tuberculosis* cells (although the patient does have TB). This is more likely for patients with low mycobacterial loads (264). When deployed for handling clinical samples, our system will also require the user to perform the same decontamination process that is used before placing the sample in other culture-based systems, and hence we will face the same potential pitfalls (mentioned above) that other systems face. Hence, we expect our diagnostic sensitivity and specificity to be similar to that of current systems like the MGIT

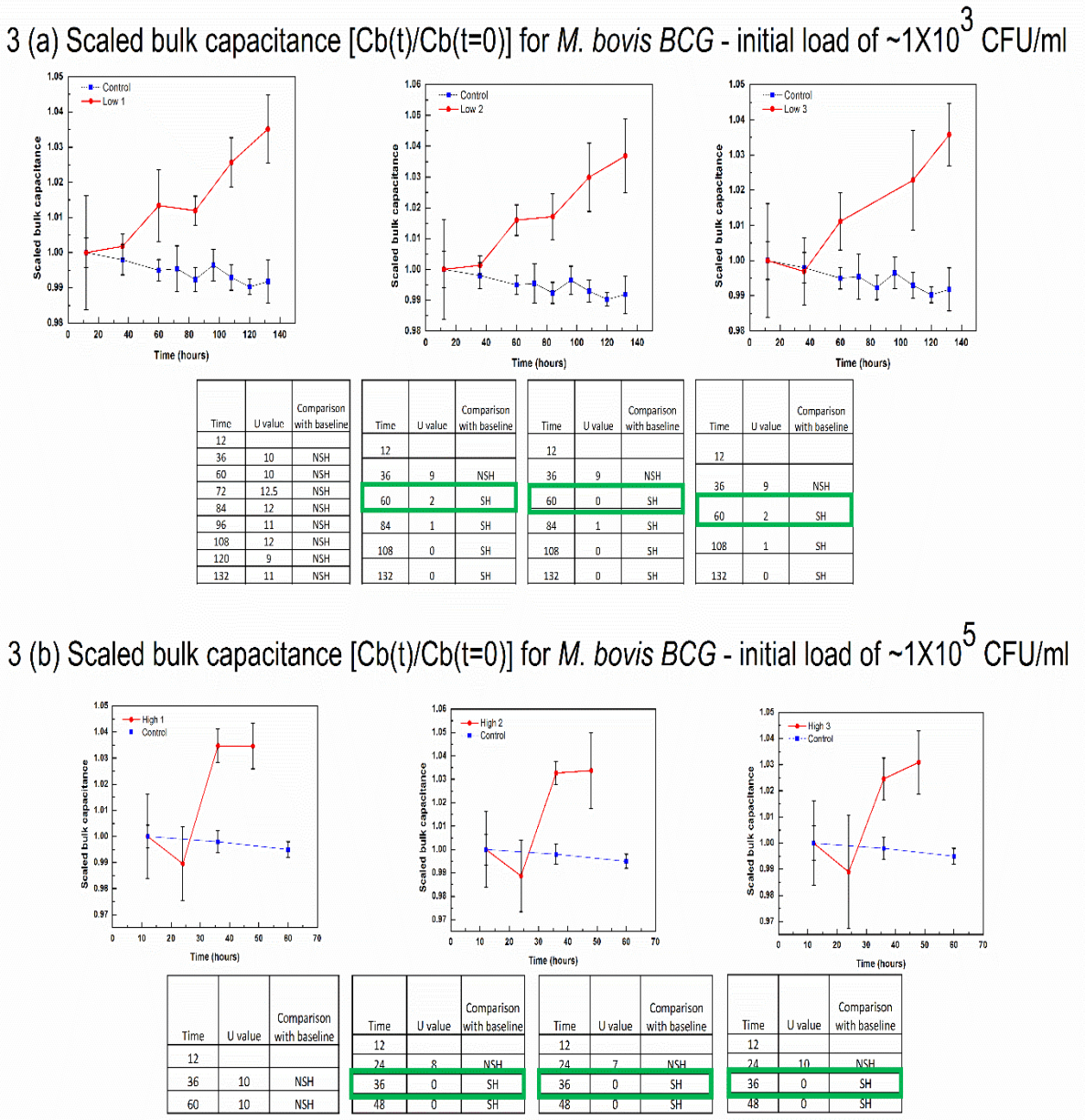

Figure 6-3 TTD of M. bovis BCG samples. The plot of bulk capacitance obtained over time for samples with (a) low initial loads (~1x10^3 CFU/ml) and (b) high initial loads (~1x10^5 CFU/ml) for M. bovis BCG. The error bars indicate the standard deviation of the readings (n=5) taken at each time interval. Statistical analysis is used to compare the baseline reading with the various time interval readings ($U_{critical}$=2). [Note: NSH = Not significantly higher, SH = Significantly higher]

4 (a) Scaled bulk capacitance [Cb(t)/Cb(t=0)] for *M. smegmatis* - initial load of ~1X10^3 CFU/ml

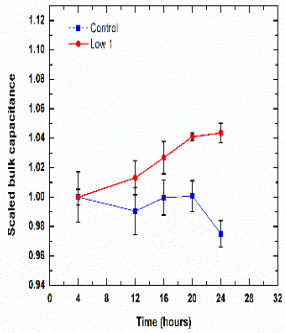

Time	U value	Comparison with baseline
4		
12	4	NSH
16	8	NSH
20	6	NSH
24	0	NSH

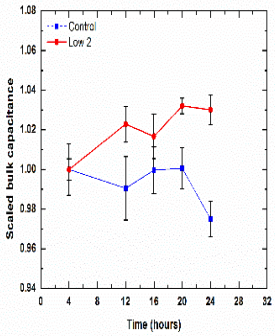

Time	U value	Comparison with baseline
4		
12	5	NSH
16	1	NSH
20	0	SH
24	0	SH

Time	U value	Comparison with baseline
4		
12	1	NSH
16	2	NSH
20	0	SH
24	0	SH

4 (b) Scaled bulk capacitance [Cb(t)/Cb(t=0)] for *M. smegmatis* - initial load of ~1X10^5 CFU/ml

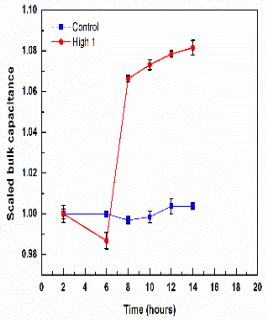

Time	U value	Comparison with baseline
2		
4	5	NSH
6	7.5	NSH
8	4	NSH
10	6	NSH
12	5	NSH
14	3	NSH

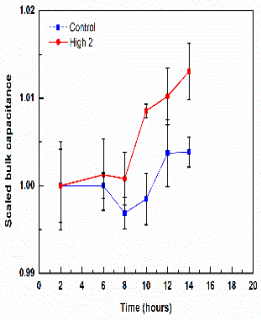

Time	U value	Comparison with baseline
2		
6	0	NSH
8	0	SH
10	0	SH
12	0	SH
14	0	SH

Time	U value	Comparison with baseline
2		
6	8	NSH
8	7	NSH
10	0	SH
12	0	SH
14	0	SH

Figure 6-4 TTD of M. smegmatis samples. The plot of bulk capacitance obtained over time for samples with (a) low initial loads (~1x10^3 CFU/ml) and (b) high initial loads (~1x10^5 CFU/ml) for M. smegmatis. The error bars indicate the standard deviation of the readings (n=4) taken at each time interval. Statistical analysis is used to compare the baseline reading with the various time interval readings ($U_{critical}$=0). [Note: NSH = Not significantly higher, SH = Significantly higher]

culture broth (249). Like sputum, blood drawn from different people have different bulk capacitance values to start with. By looking for a significant increase in the C_b value from their respective initial values, we are able to account for sample-to-sample variations. Therefore, any change in the C_b value will be due to the change in the number of mycobacteria present in the sample.

An important limitation of the system as implemented in the work presented here is that aliquots are manually withdrawn at select points in time. With support from the NIH via a Phase II SBIR award (No R44-AI096572-02), our industry partners (Techshot Inc., and ImpeDx Diagnostics), are currently developing an automated blood culture system that includes an automated sampler. Such a system, which could be readily adapted for detecting mycobacteria in cultures as well, will be tested against standard of care equipment (Bactec and similar) in multiple locations.

When trying to detect mycobacteria via culture, our times-to-detection (TTDs) are much lower than those obtained using currently available culture-based detection systems like the MGIT™ by a factor of ~2. Since clinical samples take up to 4 weeks to yield a positive result, an automated system implementing our method (which we plan to develop and optimize) could potentially obtain results many days (and sometimes even 1-2 weeks) faster than currently available automated culture-based systems. This is likely to yield significant clinical benefits in terms of improved patient outcomes.

CHAPTER 7

7 DETECTION BY DEATH: A RAPID WAY TO DETECT VIABLE SLOW-GROWING MICROORGANISMS ACHIEVED USING MICROCHANNEL ELECTRICAL IMPEDANCE SPECTROSCOPY (M-EIS)

The material presented in this chapter will be submitted as "**Detection by Death: a rapid way to detect viable slow-growing microorganisms achieved using microchannel Electrical Impedance Spectroscopy (m-EIS)**"

Roli Kargupta, Yongqiang Yang, Sachidevi Puttaswamy, Aiden J. Lee, Nicholas A. Padilla, Alec P. Foutch and Shramik Sengupta

in a peer reviewed academic journal in the area of Bioengineering.

Based on the insight that only living organisms can be killed (and that killing can proceed much faster than cell-growth), we present an approach for the detection of viable microorganisms that is much faster than currently used culture-based methods. We do so by using microchannel Electrical Impedance Spectroscopy (m-EIS) for real-time detection of cell-death on exposure to a killing-agent.

m-EIS relies on the fact that when living-cells with non-zero membrane potentials are exposed to high-frequency AC-field, induced-charges accumulate at the membrane-interface. Cell-death is accompanied by a loss of membrane-potential, and hence charge-storage (capacitance).

A proof-of-principle for a clinical-application (detection of living mycobacteria in sputum) is demonstrated. *Mycobacterium smegmatis* (doubling-time ~3hrs) and

Mycobacterium bovis BCG (doubling-time ~20hrs) in artificial-sputum are both detected in <3hrs when exposed to amikacin. Times-to-detection (TTDs) are ~12hrs and ~84hrs (3½days), respectively for culture-based detection using current technologies (BD-MGIT-960^{TM}) for samples containing similar loads of *M. smegmatis* and *M. bovis BCG*.

7.1 Introduction

In many real-world situations, one seeks to detect ***viable*** (live) microorganisms present. Often, it is known or expected that there will be non-viable microbial cells also present in the material being investigated. In many cases, it is also of utmost importance that this information be obtained as quickly as possible. Examples include (but are not limited to) (a) the need to detect the presence of viable bacteria and/or yeasts in blood for patients suspected of having an active bloodstream infection (septicemia), where it is possible that other non-viable bacteria are also present (265, 266), (b) the need to check for the presence of coliforms and other bacteria in food or water samples after they have been subjected to procedures such as pasteurization or disinfection (267), and (c) the need to detect viable cells of *Mycobacterium tuberculosis* in the sputum of patients suspected of having an active infection (given that dormant *M. tuberculosis* cells may be present in cases of "latent" TB (268), or previous treatment may have left behind some dead cells of *M.tuberculosis* (262).

In such cases, the need to prevent false positives due to the presence of dead cells excludes some technologies such as DNA based methods like PCR and antibody based approaches like ELISA as viable options (266). Given the above limitation (presence of dead cells) and added constraints brought about by the desire to contain costs, and make the detection automated and not dependent on human judgement, automated culture-based

systems currently serve as the work-horses of the microbiology laboratory for these types of applications. Some commonly encountered automated culture based detection systems include blood culture systems like the BACTEC ™ from Becton-Dickinson (BD), the BacT/Alert ™ from Biomerieux and Versa-TREK from Thermo-Scientific, specialized culture systems for mycobacteria like the Mycobacteria Growth Indicator Tube (MGIT) from BD, and Trek-ESP from Thermo-Scientific, and products like RABIT, BacTrac, Malthus 2000 that are used primarily for food and water testing.

In general, the protocol followed in automated culture-based systems require the user to add an aliquot of the sample of interest (blood, sputum, food etc.) into a bottle containing nutrient broth conducive to the target microorganisms. These microorganisms, if present, metabolize compounds such as sugars and proteins/peptides present in the nutrient broth and grow in number via reproduction. As they do so, they change the properties of the medium such as O_2/CO_2 levels, pH, electrical conductivity etc. While the specific membrane property that is monitored differs from instrument to instrument, all automated culture based systems monitor these properties continually (every few minutes at the longest) and generate a notification for the user when the property has changed significantly from the baseline (time t=0) value. Thus, they not only provide for a "load and forget" user experience, but also are reliable due to their rather straightforward detection methods and low-cost due to their not needing expensive specialized chemicals. The main drawback of these instruments is the long time that they need to detect the presence of microorganisms. The time-to-detection (TTD) can range from 1-5 days for blood culture (249, 269) to up to 6 weeks for tuberculosis (234). Two factors (low initial load and long doubling time of the microorganisms present) adversely affect TTD.

Typically, due to the low absolute rate of metabolism of a small bacterial cell (it is estimated that even a fast-growing bacteria like E. coli consumes only $2x10^{14}$ moles of O_2/hr (205) and hence has correspondingly low rates of CO_2/acid production), the bacterial load in the culture tubes being monitored must rise to ~10^8 CFU/ml in instruments like the BACTEC before they are detected (270).

Other approaches have being tried to reduce the TTD in culture-based systems. Gomez-Sjoberg and co-workers (271) concentrated the bacteria present in relatively larger volumes into a small volume using dielectrophoresis (DEP), and thus raised the effective starting concentration of the bacteria before trying to detect changes in solution conductivity brought about by the bacterial metabolism. By doing so, they obtained times to detection (TTDs) of ~ 2hrs for suspensions of *Listeria monocytogenes* with initial loads of ~10^5 CFU/ml (concentrated using DEP to effective initial loads of ~10^7 CFU/ml) as opposed to ~ 8 hrs to detect samples with similar loads without pre-concentration. It may be noted that in this case, the "threshold" concentration that must be reached for the system to flag the sample as positive remains similar to that of the current instruments on the market. The 4-fold reduction in TTD is obtained due to pre-concentration alone. On the other hand, in our earlier work (3, 205, 249), we developed a method that we call microchannel Electrical Impedance Spectroscopy (m-EIS), wherein we measure a parameter (charge storage in the interior of a suspension due to the polarization of membranes of living cells, a.k.a "bulk capacitance") that we find to be more sensitive to changes in bacterial load, and using which proliferating bacteria can be detected at threshold concentrations ~ 10^3 to 10^4 CFU/ml (as opposed to 10^8 CFU/ml in other systems). We thus obtained TTDs of 2 hrs for E.coli with initial loads of 100 CFU/ml (without the

need to resort to any pre-concentration steps) (3).

While these approaches do reduce the long times-to-detection (TTDs) associated with automated culture-based systems, the TTDs remain unacceptably long for organisms whose metabolism is slow (doubling times are long). A clinically important example of such an organism is *Mycobacterium tuberculosis*, the organism that causes tuberculosis (TB) and which has a doubling time of ~24 hrs (272) (compared to ~20 min for E. coli (3)). Using systems currently on the market (such as MGIT ™), TTDs for clinical samples containing ~1000 CFU/ml can range from ~200 (8.3 days) to ~800 (33.33 days) hours (273). Even using our m-EIS method, we obtained only a modest (approximately 2X) reduction in TTD for *Mycobacterium bovis BCG* (a closely related biosafety level II organism with a doubling time of ~20 hrs (274)). [Our TTD was 60 hrs (2 ½ days) for initial loads of ~1000 CFU/ml, as opposed to 131 hrs (~ 5 ½ days) taken by MGIT ™ for a similar sample].

Thus the bottom line is that if one tries to detect living bacteria by asking "are they metabolically active?" or "do they grow?" one is limited by the growth/metabolic rate of the organisms (which may be unacceptably slow). On the other hand, cells can be killed at a much faster rate than growing them, and any technique that studies cell death in real time will be able to determine the presence of bacteria in a system much faster. Since only living cells can be killed, such a system will be able to determine the presence of viable bacteria in the system.

We monitor cell death in real-time using microchannel Electrical Impedance Spectroscopy (m-EIS), which is a novel, patented method (275) that is distinct from classical "impedance microbiology" approaches. The latter methods (207) detect changes

to the electrical properties (either solution conductivity (244) or capacitance of the electrode solution interface (243), or a combination of the two (246)) brought about by bacterial metabolism. Viable bacteria break down sugars to more conductive species such as lactate and carbonate. This makes the solution more conductive. Interfacial capacitance (C_i) is also affected since the ions in the double-layer are in electrochemical equilibrium with those in the bulk. It may be noted that these methods can only distinguish between growth and no-growth (the former being characterized by an increase in conductivity or interfacial capacitance) and not between no-growth and cell death (both of which result in there being no changes brought about to the solution properties).

In contrast, our method relies on the fact that in the presence of high frequency AC electric fields, charge accumulates at the membranes of cells across which there exist a potential difference (the membrane potential of living cells) (206). The charge storages (capacitances) at individual cells contribute to the overall "bulk capacitance" of the suspension (net charge stored in the interior). When the number of living cells present increases (due to proliferation), the bulk capacitance increases. More importantly for the current work, when cells die, the membrane potential falls significantly (206), and charge storage under an AC field no longer occurs at the membrane. This causes the bulk capacitance to drop. Thus, a set of measurements showing a decrease in bulk capacitance over time enables us to monitor cell death.

7.2 Methods

7.2.1 Rationale and Overview

Our objective is to demonstrate that the "detection by death" approach (which involves recording a loss of signal upon the death of microorganisms of interest) can

indicate the presence of viable microorganisms of interest much faster than using traditional approaches based on detection of growth/metabolism. We also believe that the most dramatic differences are likely to be observed in cases where the microorganism of interest is slow growing. One clinically important microorganism that takes a long time to be detected because of its long doubling time/slow metabolism is *Mycobacterium tuberculosis* (Mtb), which takes days (and sometimes weeks) to be detected using automated culture-based instruments like the BACTEC MGIT 960 (Becton Dickinson), MB/BacT ALERT system (BioMerieux), ESP Culture System II (Difco Labboratories) and Versa TREK Mycobacteria detection system (Versa TREK Diagnostics) (276).

One limitation which exists for samples obtained from tuberculosis-afflicted patients is that they contain both mycobacteria as well as non-mycobacteria species like *S. aureus*, *P. aeruginosa*, etc. (214). Therefore, to observe the growth dynamics/ action of the antibiotics on mycobacteria alone, one has to first eliminate all non-mycobacterial microorganisms present in the sample. There exist multiple standard protocols of digestion and decontamination for doing the same and companies like Becton Dickinson, Hardy Diagnostics etc. sell reagent kits designed to do so.

Since *Mycobacterium tuberculosis* is a Biosafety Level III (BSL-III) microorganism, we use *Mycobacterium smegmatis* and *Mycobacterium bovis BCG* as surrogate organisms to demonstrate proof-of-principle. *M. smegmatis* is a rapidly growing BSL-I organism with a doubling time of ~3 hours and has membrane characteristics very similar to *M. tuberculosis* (254, 277) while *M. bovis BCG* is a slow growing BSL-II organism, whose doubling time of ~20 hours (274) is comparable to that of *M. tuberculosis* ~24 hours (254, 277). We would ideally like to show that not only are we able to detect the

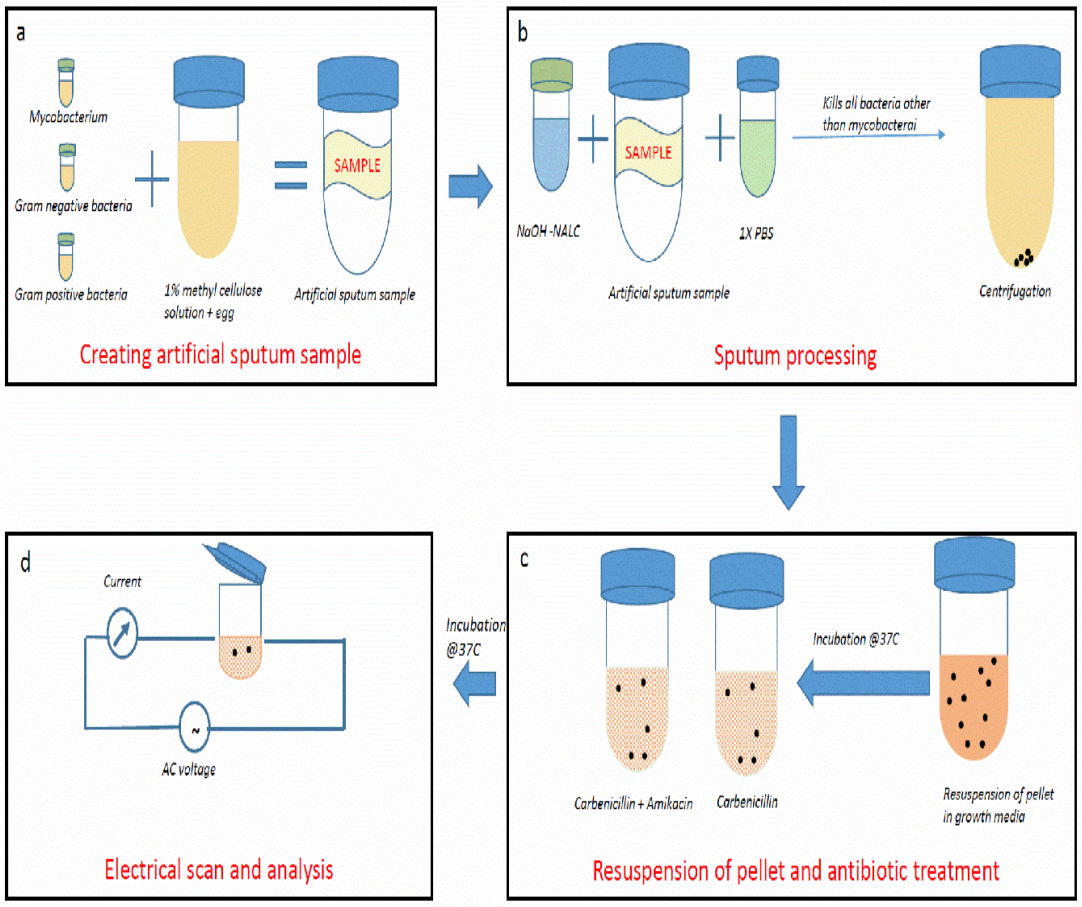

Figure 7-1 Experimental set-up to demonstrate the ability of the "detection by death" approach to detect the presence/absence of mycobacteria in a sputum sample (a) Artificial sputum sample, containing both pathogen of interest (mycobacteria) and commensal bacteria (gram positive and gram negative), is prepared (b) Standard protocol (treatment with NaOH-NALC) is used to liquefy the (artificial) sputum and decontaminate it (kill all non-mycobacterial microorganisms). The addition of PBS and centrifugation to obtain cells is also part of the protocol (c) Collected cells are resuspended in two broths: one containing Carbenicillin in 7H9 media, and the other containing both Carbenicillin and Ampicillin in 7H9 media, (d) at regular intervals of time (every hour), 50ul aliquots are extracted and scanned electrically.

using our method are independent of the doubling time of the organisms.

Our experimental protocol is summarized in Figure 7-1. As shown in the figure (panel (a)), we first create a sample of artificial sputum containing not only mycobacteria, but gram-positive and gram-negative bacteria as well.

Initial loads of ~ $1x10^5$ to $5x10^5$ CFU/ml of bacteria are used (maintaining a ratio of 1:1 between mycobacteria and other bacteria). A standard protocol for real-world samples of human sputum that involves the use of sodium hydroxide/ N-acetyl-L-cysteine (NaOH/NALC) (215, 216, 278) to digest and decontaminate the simulated sputum samples. This treatment kills all bacteria other than mycobacteria in the sample. Post-decontamination and centrifugation, the sample is re-suspended in fresh media and allowed to incubate at 37 ˚C for 2-3 hours. Antibiotic(s) are then added to the media, and thereafter, at regular intervals of time, small aliquots (~ 50 ul) are withdrawn, inserted into the thin channels of a microfluidic cassette and subjected to electric scans. Each scan involves applying a small AC voltage (500mV) at multiple frequencies ranging from 1 KHz to 100MHz across gold electrodes in contact with the suspension and recording the impedances at various frequencies. The data is processed to obtain an estimate of the bulk capacitance, a parameter that reflects the amount of charge stored by particles in the interior of the suspension and is thus correlated with the number of living microorganisms present. The manner in which the bulk capacitance changes over a few hours after the addition of the antibiotic(s) provides information on the presence of viable mycobacteria (microorganism of interest) in the original sample. Details of the individual steps (including data collection, analysis, and interpretation) are provided below.

7.2.2 Bacterial cell cultures

For the *in vitro* study, we used either *Mycobacterium smegmatis* (ATCC® 700084^{TM}), or *Mycobacterium bovis BCG* (ATCC® 35734^{TM}). *Staphylococcus aureus* (ATCC 29213) and *Pseudomonas aeruginosa* (ATCC 27853) are chosen as our model gram-positive and gram-negative organisms, respectively. *M. smegmatis* and *M. bovis BCG* are sub-cultured in Middlebrook 7H9 media supplemented with Middlebrook Albumin Dextrose Catalase (ADC) supplements at 37C. The optical density (OD) value for *M. smegmatis* is adjusted to OD_{600}=0.1 and for *M. bovis BCG* is adjusted to OD_{600}=0.05 using a spectrophotometer which corresponds to ~1X10^7 CFU/ml and (1-5)x10^6 CFU/ml respectively. (256, 279) All the other bacteria, other than mycobacteria are sub-cultured in Tryptic Soy Broth (TSB) at 37C to obtain log cultures. The OD value is adjusted to OD_{570}=1.5 and OD_{600}=0.1 which corresponds to 1x10^7 CFU/ml and 1x10^8 CFU/ml for *S. aureus* and *P. aeruginosa* respectively (280, 281).

7.2.3 Rationale for choice of antibiotics

Figure 7-2 shows, three different cases (rows) that are each tested under two conditions (columns). All tests are conducted in triplicate. The first case is a control (no bacteria present), the second (presence of gram positive, gram negative and mycobacteria) replicates the sputum of a patient with TB, and the third (absence of mycobacteria, but presence of other bacteria) replicates the sputum of a patient without TB. The samples of sputum are treated and exposed to two conditions. Under condition A, the samples are exposed to a cocktail of two antibiotics amikacin and carbenicillin while under condition B, the samples are exposed to carbenicillin only. Amikacin (32µg/ml) is obtained from Fisher Scientific and is known to have bactericidal effects towards *M. smegmatis* (282), *M. bovis BCG* (283) and *M. tuberculosis* (284). Carbenicillin disodium salt (25 µg/ml),

obtained from Research Products International Corporation, and is known to be ineffective against mycobacteria but bactericidal against most other non-mycobacterial species (285). The other possible case which is only mycobacteria and no non-mycobacterial species was not considered as relevant, since other commensal and pathogenic bacteria are invariably present in the sputum (214).

Case/ No.	Bacteria present	Condition A: Antibiotic used –Carbenicillin + Amikacin	Condition B: Antibiotic used –Carbenicillin
1	No bacteria	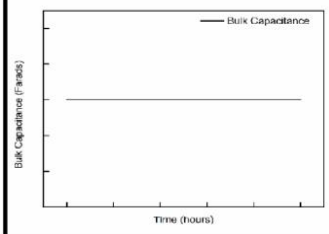	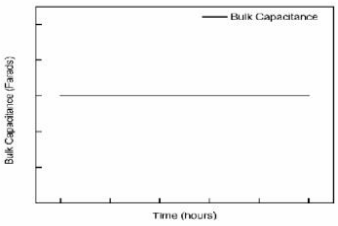
2	Mycobacteria + S. aureus + P. aeruginosa	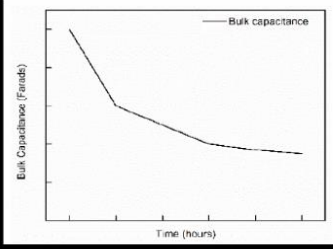	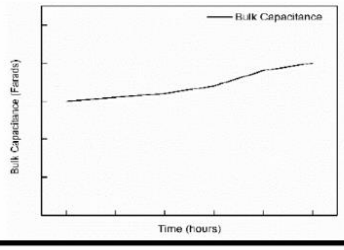
3	S. aureus + P. aeruginosa	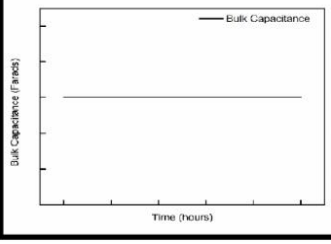	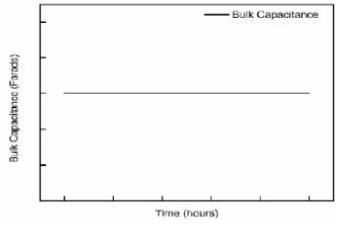

Figure 7-2 Expected plots of bulk capacitance versus time that we expect to obtain for the two conditions tested (with carbenicillin and amaikacin, and with carbenicillin alone) for the control (no-bacteria) and two possible cases likely to be encountered (mycobacteria present along with commensal bacteria and only commensal bacteria present).

All m-EIS readings are done post digestion and decontamination of the samples using NALC-NaOH (N-acetyl-L-cysteine- sodium hydroxide) technique. In the first case, the sample has no bacteria. Hence, no changes in charge storage (bulk capacitance) occur at any point in time, and we expect to see a flat line as there should be no change in the bulk capacitance over time. In case three, where the sample contains gram-positive and gram-negative bacteria, but no mycobacteria, all organisms are killed during decontamination (pre-treatment) itself, and the addition of the antibiotics is not expected to cause any changes to the measured value of bulk capacitance. However, if there are mycobacteria in the sample (as in case 2), they will survive the decontamination process and will continue to grow in the presence of Carbenicillin (case 2B). However, they will die in the presence of amikacin (case 2A). This combination (dip in the presence of amikacin, but not in the presence of Carbenicillin alone) will indicate the presence of mycobacteria. It may be noted that if the decontamination is done improperly, and some gram-positive and gram-negative bacteria survive, they will be killed under both conditions, and we can expect to see a dip in the bulk capacitance vs. time curve for both conditions.

7.2.4 Digestion and decontamination

We use artificial sputum, which is prepared according to protocols available in the literature (286-288). Briefly, 1L of 1% (w/v) aqueous methylcellulose solution is prepared. After autoclaving the same, 1 emulsified egg is added. This artificial sputum is then used for our experiments. The sputum processing technique adopted is based on standard techniques that use of N-acetyl-L-cysteine (NALC) to liquify and sodium hydroxide (NaOH) to decontaminate the sample (211, 261, 278). Briefly, for each 100ml of the

solution, 50 ml of 0.5N NaOH is combined with 50 ml of 0.1M trisodium citrate solution and 0.5gm of powdered NALC. 10 ml of the NALC-NaOH solution is added to 10ml of the sputum in a 50 ml tube and vortexed to mix. The solution is then allowed to stand at room temperature for 10 minutes. During this time, the sputum is digested and liquefied. After this, 1X PBS solution is added to make up the volume of the solution to 50 ml. The addition of PBS and the resulting dilution stops for all practical purposes the harmful action of the NaOH. Following this, the tubes are centrifuged at >3000g for 15 minutes, the supernatant is decanted, and the pellet is re-suspended in 20 ml of fresh media.

7.2.5 microchannel Electrical Impedance Spectroscopy (m-EIS)

The basic principles governing the use of m-EIS to detect microorganisms have been described in our prior work (205, 249). Briefly, we sense changes in bulk capacitance (C_b) by relying on geometric effects that enhance the effect of changes in C_b to the measured reactance (X) (the "imaginary" or "out-of-phase" component of the impedance). As shown in Figure 7-3(b), the use of long narrow microfluidic channel causes a larger fraction of the electrical flux lines to interact with the (few) microorganisms present. Another way to look at the effect is to study the equation embedded in Figure 7-3(a). Since for any given material, the resistance is inversely proportional to cross-sectional area and directly proportional to length, the long narrow geometry results in an increase in bulk resistance (R_b). It can be seen that for the reactance (X), the C_b is always multiplied by R_b. Thus, any changes to the value of X due to a change in C_b will be "magnified" by the higher R_b. Since the R_bC_b is also multiplied by the frequency (ω), this effect is further enhanced at high frequencies. In addition, our electrical sensitivity is further enhanced by using AC signal with higher frequencies (ω) as high as 100MHz. At these frequencies, the charge on

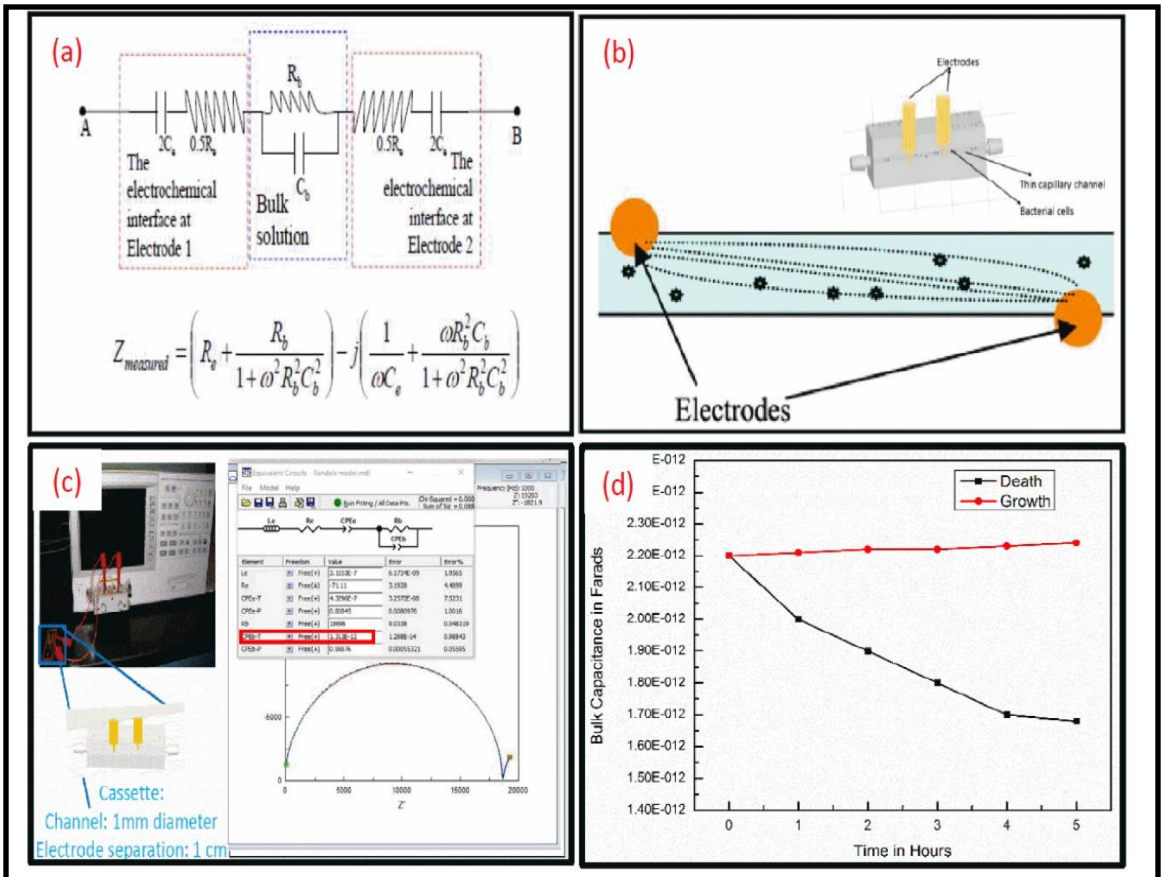

Figure 7-3 (a) Electrical equivalent circuit model that represents our microfluidic cassette which is used for measuring the impedance of the bacteria. (b) Microfluidic cassettes with two gold electrodes inserted at a distance of 1 cm (inset) and schematic of electric lines of forces present between the two electrodes when an AC voltage is applied to the system. [205] (c) Agilent Impedance Analyzer is used to do the electrical scans at multiple frequencies and commercially available Z view® software is used to analyze the data to obtain the values for the various electrical parameters, and (d) The bulk capacitance values obtained from data analysis is plotted against time. The decrease in the bulk capacitance values (black line) is due to cell death while the rise is due to bulk capacitance (red line) values is due to the cell growth.

the electrode reverses every ~10nsec. A consequence of this is that there is not enough time for ions of opposite charge to completely cover the electrode, and thus the electric field is able to penetrate into the bulk to a greater degree and cause a greater degree of charge accumulation at the cell membranes.

Our experimental protocol requires us to periodically (every hour) perform an electrical "scan" of sample aliquots in a microfluidic cassette, wherein we measure electrical impedance at multiple (200) frequencies ranging from 1 kHz to 100 MHz. As shown in figure 7-3b, the cassette contains a 1mm diameter microchannel with two gold electrodes, 1 cm apart in the channel. An AC voltage of 500 mV is applied across the two gold electrodes, using an Agilent 4294A Impedance Analyzer. At each frequency (ω), both the in-phase and out-of-phase components of the electrical impedance, Z, (resistance (R) and reactance (X)) are measured. In order to take the EIS measurements (scans), all aliquots from a given culture (across the different points in time) are introduced into the same individual cassette. As the cassettes used are handmade their readings vary from each other slightly and hence the data (values of bulk capacitance obtained) is scaled with respect to the value at the initial point in time (on the same cassette) to account for the cassette to cassette variation.

The Z vs. ω data is fitted to an equivalent electrical circuit shown in Figure 7-3c using a commercially available software package (Z-view^{TM}). The software provides an estimate for the various circuit parameters, including the "bulk capacitance", which happens to be our parameter of interest – that provides a measure of charges stored in the interior of the suspension (away from the electrodes). It may be noted that the bulk capacitance is represented as a constant-phase element (CPE) to account for the non-ideal

nature of the capacitance at cell membranes. The magnitude of the CPE, thus, reflects the amount of charge stored at the membranes of living microorganisms in suspension. Any decrease in the number of microorganisms in suspension should hence, in theory, lead to smaller amounts of charged stored in the interior of suspensions, and hence lead to a lower bulk capacitance (CPE_b-T) over time as shown in figure 7-3d.

When trying to observe cell death in a suspension suspected of harboring living microorganisms, our problem reduces to asking the question of "Is the current value of the bulk capacitance *significantly* lesser than its value at the initial point in time?" To enable us to answer this question with a greater degree of confidence, for each sample, capacitance of 4 replicates are measured at specified time interval and statistically compared to baseline using Mann-Whitney U test. The earliest time point, at which a significant decrease is found, is defined as the TTD for our "detection by death" method. Details of the statistical method is provided below.

7.2.6 Statistical analysis

Statistical analysis is performed in Microsoft Excel using Mann Whitney U-test. This non-parametric test compares if the population average between two groups is significantly different or not (260). We chose to adopt the Mann-Whitney U-test over the more popular tools like t-test since we have only a few (4) data points (bulk capacitance readings) per time point. More importantly, the normality assumption of the reading which is required for a t-test is not appropriate for our data. To check if the average of the bulk capacitance obtained at a time interval is significantly different from the bulk capacitance reading obtained in the first reading, the mean of the readings taken at the latter point in time is compared with the mean of the readings at the beginning of the culture (baseline

values) and the U values corresponding to a p -value of 0.05 (level of significance of 5%; two tailed test) are calculated. Our null hypothesis is that the two bulk capacitance values are equal and the alternate hypothesis is that there is a significant difference between the bulk capacitance values. The Mann-Whitney U value obtained for our readings is compared to the critical U value (260). If the Mann-Whitney U value obtained is equal to or less than the critical value (in this case, critical value =0), the null hypothesis is rejected, which means that there is a significant difference between the bulk capacitance values at the two time points. The earliest point in time where the U values obtained are equal to, or lower than, the critical U value is our time-to-detection (TTD) for a given sample.

7.3 Results

As outlined in Figure 7-2, three different cases are studied under two conditions. Figure 7-4 represents the results obtained when *M. smegmatis is used*. The initial loads of the bacteria used are (1 to 5) X 10^5 CFU/ml. In the case of controls (Case 1A and 1B), we observe that there is no change in the bulk capacitance values over time and we get flat lines parallel to the x-axis. Also, the U-values calculated show that there is no significant difference between the bulk capacitances obtained at various time intervals. In the case of 3A and 3B, the process of decontamination eliminates non-mycobacterial cells in the suspension and hence, in the absence of *M. smegmatis*, there is no significant change in the bulk capacitance values over time. For case 2, condition A, where a cocktail of *M. smegmatis*, *P aeruginosa,* and *S. aureus* is exposed to amikacin and carbenicillin after decontamination, we see that the impedance values show a decreasing trend over time, and the reading after 3 to 4 hours (depending on the experiment) is lower than the baseline value in a statistically significant manner. The decrease in the impedance values is due to

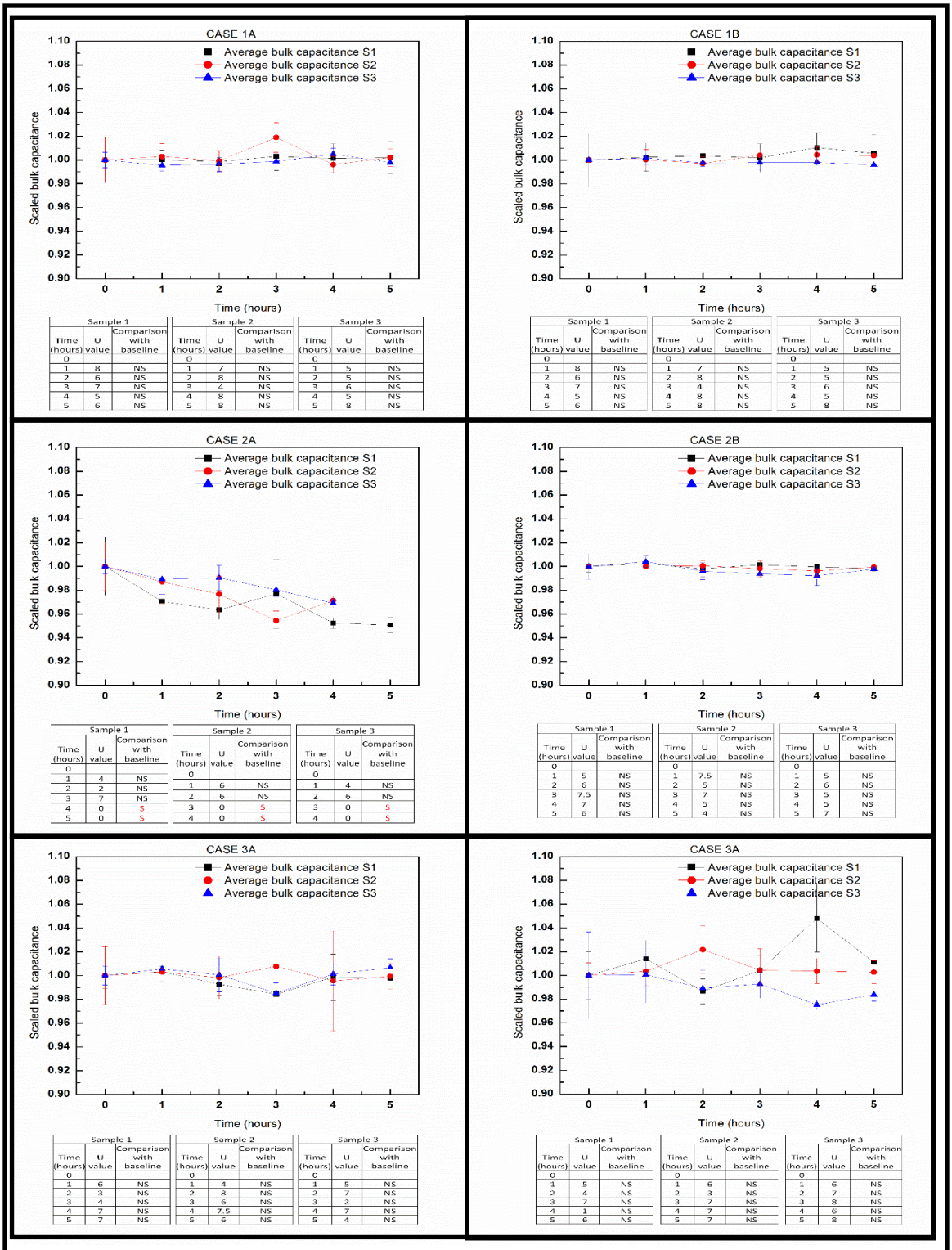

Figure 7-4 Average bulk capacitance versus time graph for the 6 cases using *M. smegmatis*. S = significant difference, NS= not significant difference

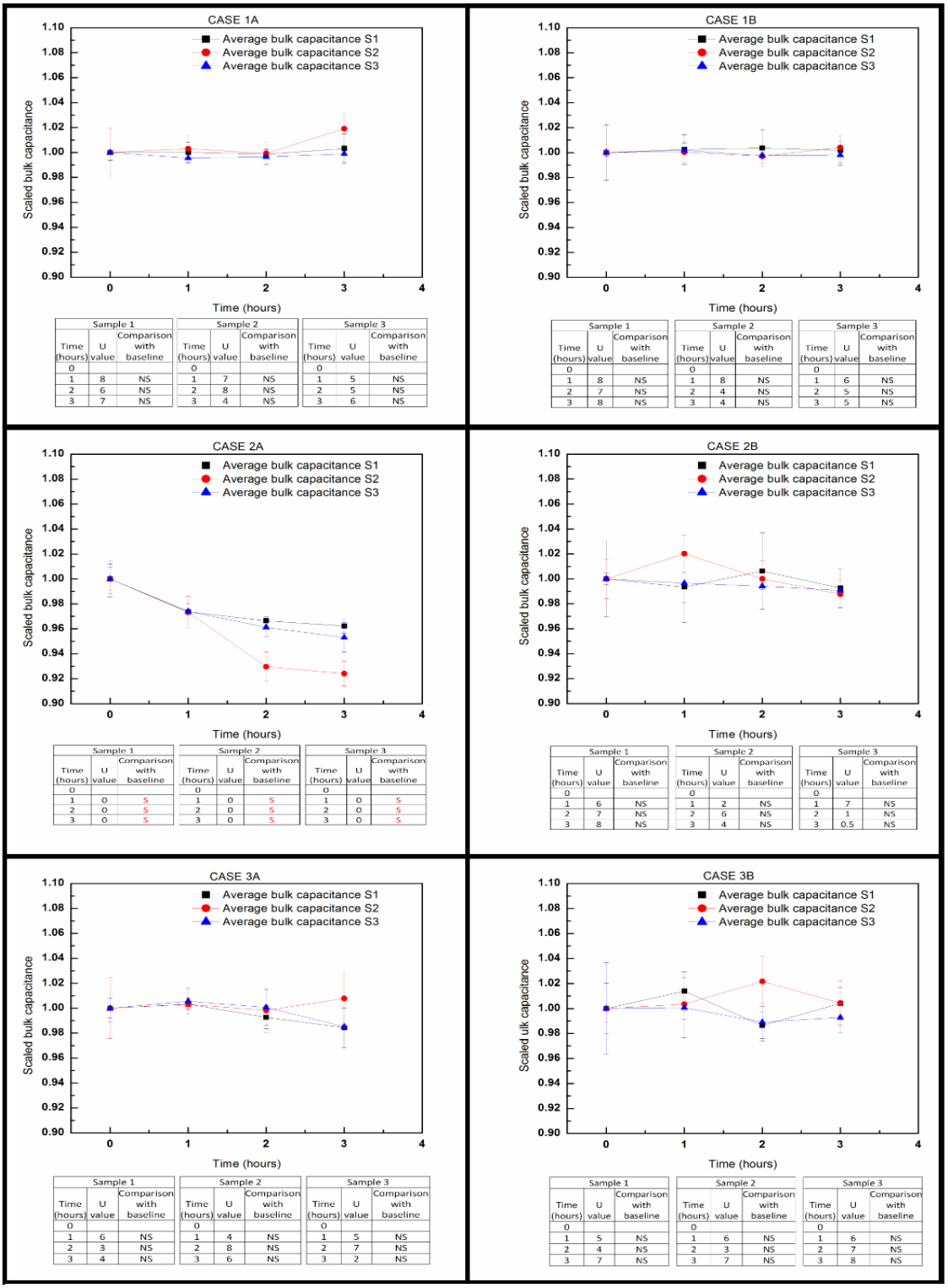

Figure 7-5 Average bulk capacitance versus time graph for the 6 cases using *M. bovis BCG*. S = significant difference, NS= not significant difference

the death of the remaining *M. smegmatis* in the presence of amikacin. Under condition B, a similarly decontaminated mixture of *M. smegmatis*, *P aeruginosa,* and *S. aureus* is not found to show any decrease over time. This is because in the absence of amikacin, the mycobacteria present are not killed. It is possible that the mycobacteria actually grow during this time, but the growth rate is too slow for us to discern any increase in bulk capacitance

Similar results are obtained in Figure 7-5, where the mycobacteria used is *M. bovis BCG*. Here in case 2A, decreasing bulk capacitance was observed after 1 hour itself but no growth was seen in in case 2B during the duration of observation (3 hours). It may be noted that while we expect cells to be proliferating in Case 2B, the rate of increase in bulk capacitance is observed to be negligible. This is not surprising since the doubling times

of the microorganisms is long (~20 hours for *M. bovis BCG* and ~ 3 hours for *M. smegmatis*), and in fact underlines the advantage in speed of our method vis-a-vis growth-based detection approaches.

As mentioned in Section 2.3 (rationale for choice of antibiotics), improper (incomplete) decontamination can lead to certain non-mycobacterial species surviving the decontamination step. This typically leads to false positives for culture (growth) based detection methods [5]. However, our approach provides a means to identify these false positives as well. If non-mycobacterial species are present in the sample after decontamination, death would be observed for both conditions A and B (unlike for condition A alone if decontamination is done correctly). To simulate a case of incomplete decontamination, samples of artificial sputum containing a cocktail of *S. aureus* and *P. aeruginosa* were exposed to NaOH-NALC for approximately 1 minute (as opposed to

the 10 minutes previously used to achieve complete decontamination). Also, the NaOH concentration used was 0.25N (as opposed to 0.5N used to achieve complete decontamination). The sample thus obtained was exposed to antibiotics: both carbenicillin alone (condition B) and carbenicillin in combination with amikacin (condition A). As shown in Figure 7-6, in such a situation, we observe decreases in bulk capacitance over time for *both* conditions, unlike when decontamination is complete and mycobacteria are the only surviving live species (case 2, condition A).

7.4 Discussion

In this piece of work, we have (a) introduced the idea that live organisms can be detected by observing them die, (b) shown our ability to observe the death of organisms using m-EIS, and (c) outlined and implemented a scheme involving monitoring death (or lack thereof) of microorganisms in a sample upon exposure to 2 sets of antibiotics using which one may detect the presence of live Mycobacteria in sputum samples. The times-to-detection (TTDs) we achieved using our method were 3 to 4 hours.

As we observed, our TTDs are not related to the doubling times / metabolic rate of organisms and compares extremely favorably with those of culture-based detection methods: both traditional ones, and other novel approaches under development. At the same time, our method retains the advantages of culture-based methods by being potentially inexpensive (not requiring expensive chemicals with strict storage requirements), automatable (not subject to observer judgement) and having high sensitivity. Moreover, it can rule out a major source of false positives seen in traditional culture-based methods (incomplete decontamination).

In terms of TTD, our method is comparable to that obtained by Xpert®

MTB/RIF. The XpertMTB/RIF instrument (with 4 modules that can run 16-20 tests per 8 hr shift) has a cost of ~$34,000 and each single use cartridge has a cost of ~$40. However, a consortium of charitable organizations that include the Foundation for Innovative New Diagnostics (FIND), the Gates Foundation, USAID and UN agencies, provide a 50% subsidy on the instrument and a 75% subsidy on the disposables to "approved" public health agencies in low-resource countries, making the Xpert^{TM} instrument available for $17,000 and disposables available for ~$10 a test (229). A fully automated version of our method would consist of a fixed instrument (that would house the electric circuits), and disposables (cassettes / tubes with growth media and antibiotics) and is likely to be much

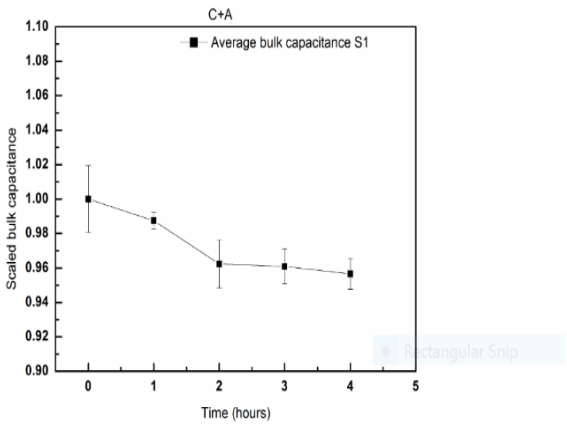

Sample 1		
Time (hours)	U value	Comparison with baseline
0		
1	4	NS
2	1	NS
3	0	S
4	0	S

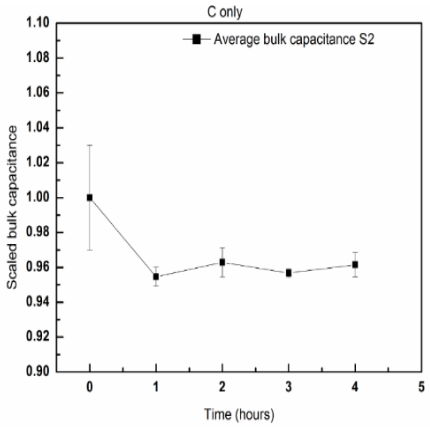

Sample 2		
Time (hours)	U value	Comparison with baseline
0		
1	0	S
2	0	S
3	0	S
4	0	S

Figure 7-6 Partial decontamination of simulated sputum samples containing non-mycobacterial cultures are exposed to two conditions namely, Condition A : cocktail of two antibiotics, Amikacin and Carbenicillin and Condition B: only Carbenicillin. Average bulk capacitance estimated from the m-EIS scans is plotted against time.

less expensive. An inexpensive device that is able to rapidly detect TB in human samples is a pressing global-health need.

Of course, we would have to build such an instrument, as well as demonstrate that our method works on *M. tuberculosis* present in actual human sputum (instead of *M. bovis BCG* in artificial sputum). We plan on doing both in the near future.

CHAPTER 8

8 CONCLUSION AND FUTURE WORK

Microorganisms are present everywhere. When the pathogenic microorganisms enter our body, they can cause various infections, illness and in extreme cases can result in death. Proper identification of microorganisms and consequent treatment is needed for patient welfare. Clearly, early identification will lead to more effective treatment.

Among the Healthcare-associated infections (HAIs), surgical site infections (SSIs) is critical and results in delayed patient recovery and huge financial burden to them. A foaming Betadine Spray is tested *in-vitro* against commercially available preoperative surgical site preparation techniques on two different substrates, namely, agar plates and porcine skin to ensure the increased effectiveness of preoperative surgical site preparation. It is observed that the foaming Betadine Spray has a strong antibacterial effect on the bacteria tested. The agar plates as a substrate having smooth surface can be thought to be an ideal case, where all the bacteria are killed when in contact with the foaming Betadine Spray. However, the porcine skin proves to be a more realistic model replicating the human skin; we observe a 2-log reduction in bacterial numbers. There is no statistically significant difference between our method and the commercially available technique. This is a preliminary study, and further studies need to be conducted on studies on animals/ humans to ascertain the efficacy of the foam.

In addition to looking at SSIs, the research project also involved development and optimization of a rapid, cost-effective microbiological platform for detection of viable, microorganisms having long generation times like mycobacteria, based on electrical

impedance spectroscopy. Several techniques are available in the market for identification and detection of mycobacteria that are responsible for various infectious diseases like tuberculosis. These methods may be culture-based, microscopy-dependent, serological-based, molecular-based or proteomics-based techniques. Each method has its pros and cons. It is worthwhile to note that time taking culture-based method is still considered the reference standard.

Our technique involves combining impedance spectroscopy to the culture-based technology to decrease the time-to-detection of microorganisms significantly. This technique involves measuring the bulk capacitance of the mycobacteria in a suspension over time. When an AC field is applied to a bacterial suspension, the bacterial cell membrane acts as an interface, and thus acts as a capacitor (stores charge). This phenomenon is only observed in the case of viable/ living bacteria. The cell membrane of non-viable/ dead cell is compromised, and it is not able to store charges under an applied AC field. Thus, using electrical impedance spectroscopy, we can distinguish between live/ viable and non-viable bacteria. When such a bacterial suspension is loaded into a thin, long channel of a microfluidic cassette, the bulk capacitance solely due to the bacteria can be ascertained. Any change in the number of bacteria (growth/ death) will result in a change in the bulk capacitance reading from the baseline value over time.

This technique is very different from the commercial, culture-based automated systems currently available in the market for detection of mycobacteria. These automated systems for detection of mycobacteria are based on detection of the metabolites produced by the bacteria or detection of changes in the media like pH, pressure due to bacterial metabolism. Though sensitive, these systems take a very long time to detect the presence

of mycobacteria. This is so because of the long doubling times, it takes a long time for the bacteria to grow and generate metabolic changes in the media that reach the detection threshold of the instrument and can be ascertained by it. Thus, using our technique (our threshold of detection is significantly lower than the commercially available culture-based instruments). We can get a reduction of ~50% in time-to-detection when compared with the commercially available culture-based automated system.

The currently available culture-based systems are based on detection of mycobacteria growth/ metabolic products in the media. However, we have successfully demonstrated that detection of mycobacteria based on their death as opposed to growth (as is used in most systems) is much faster. This is based on the insight that killing can be initiated much faster than cell growth for organisms having long generation times. This information is crucial for mycobacteria like *M. tuberculosis* which has a doubling time of ~24 hours. On exposure to antibiotics, bacterial cells are killed at a much faster rate in comparison to the growth rate of bacterial cells in the absence of antibiotics. The dead bacterial cells lose their ability to store charge when an AC field is applied. This results in the decrease in the bulk capacitance of the system. By observing the change in this parameter, we can ascertain the TTD in 3hours or less.

However, our platform is in its initial developmental phase. Small aliquots need to be withdrawn at regular intervals of time from the main suspension and loaded for spectroscopic reading. This manual intervention is labor intensive and can also lead to sample contamination. Further optimization with automation of the technique is needed to supplement the current technique and make it user-friendly. An automated system with the automatic withdrawal of aliquots at regular intervals of time can minimize human

intervention. Moreover, as the system will be enclosed, the chances of contamination can also be reduced. Such an automated system will be comparable to working with those systems which are currently being used but prove to be much faster.

REFERENCE

1. Gopinath SC, Tang TH, Chen Y, Citartan M, Lakshmipriya T. Bacterial detection: from microscope to smartphone. Biosensors & bioelectronics. 2014;60:332-42.
2. Ahmed A, Rushworth JV, Hirst NA, Millner PA. Biosensors for whole-cell bacterial detection. Clinical microbiology reviews. 2014;27(3):631-46.
3. Puttaswamy S, Sengupta S. Rapid detection of bacterial proliferation in food samples using microchannel impedance measurements at multiple frequencies. Sensing and Instrumentation for Food Quality and Safety. 2010;4(3-4):108-18.
4. Mead PS, Slutsker L, Dietz V, McCaig LF. Food-related illness and death in the United States. Journal of Environmental Health. 2000;62(7):9.
5. Emerson D, Agulto L, Liu H, Liu L. Identifying and characterizing bacteria in an era of genomics and proteomics. Bioscience. 2008;58(10):925-36.
6. Noble RT, Weisberg SB. A review of technologies for rapid detection of bacteria in recreational waters. J Water Health. 2005;3(4):381-92.
7. Ducel G, Fabry J, Nicolle L. Prevention of hospital acquired infections: a practical guide. Prevention of hospital acquired infections: a practical guide. 2002(Ed. 2).
8. Scott RD, Douglas R. The direct medical costs of healthcare-associated infections in US hospitals and the benefits of prevention. 2009.
9. Avery L, Bennett R, Brinsley-Rainisch K, Boyter M, Coffin N, Deshpande S, et al. National. 2015.
10. Zimlichman E, Henderson D, Tamir O, Franz C, Song P, Yamin CK, et al. Health care-associated infections: a meta-analysis of costs and financial impact on the US health care system. JAMA Intern Med. 2013;173(22):2039-46.

11. Darouiche RO. Treatment of infections associated with surgical implants. The New England journal of medicine. 2004;350(14):1422-9.
12. Klevens RM, Edwards JR, Richards CL, Jr., Horan TC, Gaynes RP, Pollock DA, et al. Estimating health care-associated infections and deaths in U.S. hospitals, 2002. Public health reports. 2007;122(2):160-6.
13. Hadiati DR, Hakimi M, Nurdiati DS. Skin preparation for preventing infection following caesarean section. Cochrane database of systematic reviews (Online). 2012;9:CD007462.
14. Grove GL, Eyberg CI. Comparison of two preoperative skin antiseptic preparations and resultant surgical incise drape adhesion to skin in healthy volunteers. J Bone Joint Surg Am. 2012;94(13):1187-92.
15. Mangram AJ, Horan TC, Pearson ML, Silver LC, Jarvis WR. Guideline for prevention of surgical site infection, 1999. American journal of infection control. 1999;27(2):97-134.
16. Lee I, Agarwal RK, Lee BY, Fishman NO, Umscheid CA. Systematic review and cost analysis comparing use of chlorhexidine with use of iodine for preoperative skin antisepsis to prevent surgical site infection. Infection Control and Hospital Epidemiology. 2010;31(12):1219-29.
17. Dumville JC, McFarlane E, Edwards P, Lipp A, Holmes A. Preoperative skin antiseptics for preventing surgical wound infections after clean surgery. Cochrane database of systematic reviews (Online). 2013;3:CD003949.
18. Organization WH. Removing obstacles to healthy development: report on infectious diseases. 1999.

19. Colwell RR. Global climate and infectious disease: the cholera paradigm. Science. 1996;274(5295):2025-31.
20. Stramer SL, Hollinger FB, Katz LM, Kleinman S, Metzel PS, Gregory KR, et al. Emerging infectious disease agents and their potential threat to transfusion safety. Transfusion. 2009;49(s2):1S-29S.
21. Morens DM, Fauci AS. Emerging infectious diseases: threats to human health and global stability. PLoS Pathog. 2013;9(7):e1003467.
22. Cohen ML. Changing patterns of infectious disease. Nature. 2000;406(6797):762-7.
23. Harris M, Reza J. Global report for research on infectious diseases of poverty: World Health Organization; 2012.
24. Nigam A, Gupta D, Sharma A. Treatment of infectious disease: beyond antibiotics. Microbiol Res. 2014;169(9-10):643-51.
25. Bhutta ZA, Sommerfeld J, Lassi ZS, Salam RA, Das JK. Global burden, distribution, and interventions for infectious diseases of poverty. Infect Dis Poverty. 2014;3(1):21.
26. Babady NE, Wengenack NL. Clinical Laboratory Diagnostics for Mycobacterium tuberculosis: INTECH Open Access Publisher; 2012.
27. Baron EJ, Miller JM, Weinstein MP, Richter SS, Gilligan PH, Thomson RB, et al. A guide to utilization of the microbiology laboratory for diagnosis of infectious diseases: 2013 recommendations by the Infectious Diseases Society of America (IDSA) and the American Society for Microbiology (ASM) a. Clin Infect Dis. 2013;57(4):e22-e121.
28. Mancini N, Carletti S, Ghidoli N, Cichero P, Burioni R, Clementi M. The era of molecular and other non-culture-based methods in diagnosis of sepsis. Clinical microbiology reviews. 2010;23(1):235-51.

29. Kokubo T, Kim HM, Kawashita M. Novel bioactive materials with different mechanical properties. Biomaterials. 2003;24(13):2161-75.
30. Darouiche RO. Device-associated infections: a macroproblem that starts with microadherence. Clinical infectious diseases : an official publication of the Infectious Diseases Society of America. 2001;33(9):1567-72.
31. Evans RP. Surgical site infection prevention and control: an emerging paradigm. J Bone Joint Surg Am. 2009;91 Suppl 6(Supplement_6):2-9.
32. Lentino JR. Prosthetic Joint Infections: Bane of Orthopedists, Challenge for Infectious Disease Specialists. Clin Infect Dis. 2003;36(9):1157-61.
33. Moran E, Byren I, Atkins BL. The diagnosis and management of prosthetic joint infections. The Journal of antimicrobial chemotherapy. 2010;65 Suppl 3:iii45-54.
34. Francolini I, Donelli G. Prevention and control of biofilm-based medical-device-related infections. FEMS Immunol Med Microbiol. 2010;59(3):227-38.
35. Graves EJ. Detailed diagnoses and procedures, national hospital discharge survey, 1990. Vital Health Stat 13. 1992(113):1-225.
36. IndustryExperts. Orthopedic Implants - A Global Market Overview - market research report. 2011.
37. Edwards JR, Peterson KD, Mu Y, Banerjee S, Allen-Bridson K, Morrell G, et al. National Healthcare Safety Network (NHSN) report: data summary for 2006 through 2008, issued December 2009. American journal of infection control. 2009;37(10):783-805.
38. Kurtz S, Mowat F, Ong K, Chan N, Lau E, Halpern M. Prevalence of primary and revision total hip and knee arthroplasty in the United States from 1990 through 2002.

J Bone Joint Surg Am. 2005;87(7):1487-97.

39. Van MP, Bekerom JS. The value of pre-operative aspiration in the diagnosis of an infected prosthetic knee: a retrospective study and review of literature. Acta orthopaedica belgica. 2006;72:441-7.
40. Fenollar F, Roux V, Stein A, Drancourt M, Raoult D. Analysis of 525 samples to determine the usefulness of PCR amplification and sequencing of the 16S rRNA gene for diagnosis of bone and joint infections. Journal of clinical microbiology. 2006;44(3):1018-28.
41. Rightmire E, Zurakowski D, Vrahas M. Acute infections after fracture repair: management with hardware in place. Clin Orthop Relat Res. 2008;466(2):466-72.
42. Arciola CR, Campoccia D, Speziale P, Montanaro L, Costerton JW. Biofilm formation in Staphylococcus implant infections. A review of molecular mechanisms and implications for biofilm-resistant materials. Biomaterials. 2012;33(26):5967-82.
43. Donlan RM, Costerton JW. Biofilms: survival mechanisms of clinically relevant microorganisms. Clinical microbiology reviews. 2002;15(2):167-93.
44. Davies D. Understanding biofilm resistance to antibacterial agents. Nature reviews Drug discovery. 2003;2(2):114-22.
45. Banerjee I, Pangule RC, Kane RS. Antifouling coatings: recent developments in the design of surfaces that prevent fouling by proteins, bacteria, and marine organisms. Adv Mater. 2011;23(6):690-718.
46. Costerton JW, Montanaro L, Arciola CR. Biofilm in implant infections: its production and regulation. The International journal of artificial organs. 2005;28(11):1062-8.
47. Flemming HC, Neu TR, Wozniak DJ. The EPS matrix: the "house of biofilm cells". J

Bacteriol. 2007;189(22):7945-7.

48. van de Belt H, Neut D, Schenk W, van Horn JR, van der Mei HC, Busscher HJ. Infection of orthopedic implants and the use of antibiotic-loaded bone cements. A review. Acta Orthop Scand. 2001;72(6):557-71.

49. Eiff Cv, Jansen B, Kohnen W, Becker K. Infections Associated with Medical Devices Pathogenesis, Management and Prophylaxis. Drugs. 2005;65(2):179-214.

50. Broussard A. CE EXAMINATION: Management and Prevention of Infection in-Orthopedic Surgical Procedures-Surgical-site infections cost US hospitals between $3.5-5.7 billion per year. This article examines the different means of contamination, as well as ways to combat the spread of infection within the OR. The Surgical technologist 2009;41(12):547-53.

51. Gillespie WJ. Prevention and management of infection after total joint replacement. Clinical infectious diseases : an official publication of the Infectious Diseases Society of America. 1997;25(6):1310-7.

52. Greene LR, Mills R, Moss R, Sposato K, Vignari M. Guide to the Elimination of Orthopedic Surgical Site Infections. 2010.

53. Vonberg RP, Gastmeier P. Prevention of surgical site infections in bone and joint procedures. Current infectious disease reports. 2012;14(5):576-84.

54. Rao N, Cannella BA, Crossett LS, Yates AJ, Jr., McGough RL, 3rd, Hamilton CW. Preoperative screening/decolonization for Staphylococcus aureus to prevent orthopedic surgical site infection: prospective cohort study with 2-year follow-up. J Arthroplasty. 2011;26(8):1501-7.

55. Langer R. New methods of drug delivery. Science. 1990;249(4976):1527-33.

56. Anagnostakos K, Schmid NV, Kelm J, Grun U, Jung J. Classification of hip joint infections. Int J Med Sci. 2009;6(5):227-33.
57. Trampuz A, Widmer AF. Infections associated with orthopedic implants. Current opinion in infectious diseases. 2006;19(4):349-56.
58. Widmer AF. New developments in diagnosis and treatment of infection in orthopedic implants. Clinical infectious diseases : an official publication of the Infectious Diseases Society of America. 2001;33 Suppl 2(s2):S94-106.
59. Mabrouk M, Mostafa AA, Oudadesse H, Mahmoud AA, El-Gohary MI. Effect of ciprofloxacin incorporation in PVA and PVA bioactive glass composite scaffolds. Ceramics International. 2014;40(3):4833-45.
60. Vergidis P, Patel R. Novel approaches to the diagnosis, prevention, and treatment of medical device-associated infections. Infect Dis Clin North Am. 2012;26(1):173-86.
61. Trebse R, Pisot V, Trampuz A. Treatment of infected retained implants. J Bone Joint Surg Br. 2005;87(2):249-56.
62. Marculescu CE, Berbari EF, Hanssen AD, Steckelberg JM, Harmsen SW, Mandrekar JN, et al. Outcome of prosthetic joint infections treated with debridement and retention of components. Clinical infectious diseases : an official publication of the Infectious Diseases Society of America. 2006;42(4):471-8.
63. Brandt CM, Sistrunk WW, Duffy MC, Hanssen AD, Steckelberg JM, Ilstrup DM, et al. Staphylococcus aureus prosthetic joint infection treated with debridement and prosthesis retention. Clinical infectious diseases : an official publication of the Infectious Diseases Society of America. 1997;24(5):914-9.
64. Jamsen E, Stogiannidis I, Malmivaara A, Pajamaki J, Puolakka T, Konttinen YT.

Outcome of prosthesis exchange for infected knee arthroplasty: the effect of treatment approach. Acta Orthop. 2009;80(1):67-77.

65. Dairaku K, Takagi M, Kawaji H, Sasaki K, Ishii M, Ogino T. Antibiotics-impregnated cement spacers in the first step of two-stage revision for infected totally replaced hip joints: report of ten trial cases. J Orthop Sci. 2009;14(6):704-10.
66. Hickok NJ, Shapiro IM. Immobilized antibiotics to prevent orthopaedic implant infections. Adv Drug Deliv Rev. 2012;64(12):1165-76.
67. Esposito M, Hirsch JM, Lekholm U, Thomsen P. Biological factors contributing to failures of osseointegrated oral implants. (I). Success criteria and epidemiology. European journal of oral sciences. 1998;106(1):527-51.
68. Puleo DA, Nanci A. Understanding and controlling the bone-implant interface. Biomaterials. 1999;20(23-24):2311-21.
69. Schultz D. INFUSE from Medtronic [Available from: http://www.accessdata.fda.gov/cdrh_docs/pdf/P000058a.pdf.
70. CarriGen from ETEX [Available from: https://secure.etexcorp.com/press_carrigen.html.
71. Cerasorb from Curasan [Available from: http://www.curasan.de/com/news/press_releases/2002/cerasorb-21-03-2002.php.
72. SpinePlex from Stryker [Available from: http://strykerivs.com/products/bone-cements.
73. Trajkovski B, Petersen A, Strube P, Mehta M, Duda GN. Intra-operatively customized implant coating strategies for local and controlled drug delivery to bone. Adv Drug Deliv Rev. 2012;64(12):1142-51.

74. Daghighi S, Sjollema J, van der Mei HC, Busscher HJ, Rochford ET. Infection resistance of degradable versus non-degradable biomaterials: an assessment of the potential mechanisms. Biomaterials. 2013;34(33):8013-7.
75. Gupta AP, Kumar V. New emerging trends in synthetic biodegradable polymers–Polylactide: A critique. European polymer journal. 2007;43(10):4053-74.
76. Middleton JC, Tipton AJ. Synthetic biodegradable polymers as orthopedic devices. Biomaterials. 2000;21(23):2335-46.
77. Bostman O, Pihlajamaki H. Clinical biocompatibility of biodegradable orthopaedic implants for internal fixation: a review. Biomaterials. 2000;21(24):2615-21.
78. Albertsson A-C, Varma IK. Recent developments in ring opening polymerization of lactones for biomedical applications. Biomacromolecules. 2003;4(6):1466-86.
79. Wang BL, Ren KF, Chang H, Wang JL, Ji J. Construction of degradable multilayer films for enhanced antibacterial properties. ACS Appl Mater Interfaces. 2013;5(10):4136-43.
80. Park KD, Kim YS, Han DK, Kim YH, Lee EHB, Suh H, et al. Bacterial adhesion on PEG modified polyurethane surfaces. Biomaterials. 1998;19:851–9.
81. Bridges AW, Garcia AJ. Anti-inflammatory polymeric coatings for implantable biomaterials and devices. J Diabetes Sci Technol. 2008;2(6):984-94.
82. Page K, Wilson M, Parkin IP. Antimicrobial surfaces and their potential in reducing the role of the inanimate environment in the incidence of hospital-acquired infections. J Mater Chem. 2009;19:3819-31.
83. Wang C, Yu B, Knudsen B, Harmon J, Moussy F, Moussy Y. Synthesis and performance of novel hydrogels coatings for implantable glucose sensors.

Biomacromolecules. 2008;9(2):561-7.

84. Yang Y, Zhang SF, Kingston MA, Jones G, Wright G, Spencer SA. Glucose sensor with improved haemocompatibilty. Biosensors & bioelectronics. 2000;15(5-6):221-7.
85. Azzaroni O. Polymer Brushes Here, There, and Everywhere: Recent Advances in Their Practical Applications and Emerging Opportunities in Multiple Research Fields. J Polym Sci A Polym Chem. 2012;50:3225–58.
86. Raynor JE, Capadona JR, Collard DM, Petrie TA, Garcia AJ. Polymer brushes and self-assembled monolayers: Versatile platforms to control cell adhesion to biomaterials (Review). Biointerphases. 2009;4(2):FA3-16.
87. Senaratne W, Andruzzi L, Ober CK. Self-assembled monolayers and polymer brushes in biotechnology: current applications and future perspectives. Biomacromolecules. 2005;6(5):2427-48.
88. Zhao B, Brittain WJ. Polymer brushes: surface-immobilized macromolecules. Prog Polym Sci. 2000;25:677–710
89. Ren X, Wu Y, Cheng Y, Ma H, Wei S. Fibronectin and bone morphogenetic protein-2-decorated poly(OEGMA-r-HEMA) brushes promote osseointegration of titanium surfaces. Langmuir : the ACS journal of surfaces and colloids. 2011;27(19):12069-73.
90. Anagnostoua F, Debet A, Pavon-Djavid G, Goudaby Z, Helary G, Migonney V. Osteoblast functions on functionalized PMMA-based polymers exhibiting Staphylococcus aureus adhesion inhibition. Biomaterials. 2006;27:3912–9
91. Guo Q, Cai X, Wang X, Yang J. “Paintable” 3D printed structures via a post-ATRP process with antimicrobial function for biomedical applications. J Mater Chem B. 2013;1:6644-9.

92. Hauert R. A review of modified DLC coatings for biological applications. Diamond and Related Materials. 2003;12:583–9.
93. Zhao Q, Liu Y, Wang C, Wang S. Evaluation of bacterial adhesion on Si-doped diamond-like carbon films. Applied Surface Science. 2007;253(17):7254–9.
94. Morrison ML, Buchanan RA, Liaw PK, Berry CJ, Brigmon RL, Riester L, et al. Electrochemical and antimicrobial properties of diamondlike carbon-metal composite films. Diamond & Related Materials. 2006;15:138– 46.
95. Matsunaga T, R. T, Nakajima T, Wake H. Photoelectrochemical Sterilization of Microbial-Cells by Semiconductor Powders. FEMS Microbiology Letters. 1985;29:211–4.
96. Hashimoto K, H. I, Fujishima A. TiO2 Photocatalysis: A Historical Overview and Future Prospects. AAPPS Bulletin. 2007;17(6):12-28.
97. Sunada K, Watanabe T, Hashimoto K. Bactericidal activity of copper-deposited TiO2 thin film under weak UV light illumination. Environ Sci Technol. 2003;37(20):4785-9.
98. Montanaro L, Speziale P, Campoccia D, Ravaioli S, Cangini I, Pietrocola G, et al. Scenery of Staphylococcus implant infections in orthopedics. Future Microbiol. 2011;6(11):1329-49.
99. De Giglio E, Cafagna D, Cometa S, Allegretta A, Pedico A, Giannossa LC, et al. An innovative, easily fabricated, silver nanoparticle-based titanium implant coating: development and analytical characterization. Analytical and bioanalytical chemistry. 2013;405(2-3):805-16.
100. Orlicki JA, Zander NE, Martin GR, Kosik WE, Derek Demaree J, Leadore JL, et al.

Self-segregating hyperbranched polymer/silver nanoparticle hybrids in thermoplastic polyurethane films. Journal of Applied Polymer Science. 2013;128(6):4181-8.

101. Colon G, Ward BC, Webster TJ. Increased osteoblast and decreased Staphylococcus epidermidis functions on nanophase ZnO and TiO2. J Biomed Mater Res A. 2006;78(3):595-604.
102. Hamm SC, Shankaran R, Korampally V, Bok S, Praharaj S, Baker GA, et al. Sputter-Deposition of Silver Nanoparticles into Ionic Liquid as a Sacrificial Reservoir in Antimicrobial Organosilicate Nanocomposite Coatings. ACS applied materials & interfaces. 2012;4(1):178-84.
103. Etienne O, Picart C, Taddei C, Haikel Y, Dimarcq JL, Schaaf P, et al. Multilayer polyelectrolyte films functionalized by insertion of defensin: a new approach to protection of implants from bacterial colonization. Antimicrobial agents and chemotherapy. 2004;48(10):3662-9.
104. Suna Y, Denga Y, Yeb Z, Liange S, Tang Z, Weia S. Peptide decorated nano-hydroxyapatite with enhanced bioactivity and osteogenic differentiation via polydopamine coating. Colloids and Surfaces B: Biointerfaces. 2013;111:107– 16.
105. Yeaman MR, Yount NY. Mechanisms of antimicrobial peptide action and resistance. Pharmacol Rev. 2003;55(1):27-55.
106. Kazemzadeh-Narbat M, Noordin S, Masri BA, Garbuz DS, Duncan CP, Hancock RE, et al. Drug release and bone growth studies of antimicrobial peptide-loaded calcium phosphate coating on titanium. Journal of biomedical materials research Part B, Applied biomaterials. 2012;100(5):1344-52.
107. Gottenbos B, van der Mei HC, Klatter F, Nieuwenhuis P, Busscher HJ. In vitro and in

vivo antimicrobial activity of covalently coupled quaternary ammonium silane coatings on silicone rubber. Biomaterials. 2002;23(6):1417-23.

108. Chen X, Cai K, Fang J, Lai M, Li J, Hou Y, et al. Dual action antibacterial TiO2 nanotubes incorporated with silver nanoparticles and coated with a quaternary ammonium salt (QAS). Surface & Coatings Technology. 2013;216:158–65.
109. Hetrick EM, Schoenfisch MH. Reducing implant-related infections: active release strategies. Chem Soc Rev. 2006;35: 780-9.
110. Holt J, Hertzberg B, Weinhold P, Storm W, Schoenfisch M, Dahners L. Decreasing bacterial colonization of external fixation pins via nitric oxide release coatings. J Orthop Trauma. 2011;25:432–7.
111. Hendriks JG, van Horn JR, van der Mei HC, Busscher HJ. Backgrounds of antibiotic-loaded bone cement and prosthesis-related infection. Biomaterials. 2004;25(3):545-56.
112. Kanellakopoulou K, Giamarellos-Bourboulis EJ. Carrier systems for the local delivery of antibiotics in bone infections. Drugs. 2000;59(6):1223-32.
113. Magnan B, Bondi M, Maluta T, Samaila E, Schirru L, Dall'Oca C. Acrylic bone cement: current concept review. Musculoskeletal surgery. 2013;97(2):93-100.
114. Tabutin J, D'Ollonne T, Cambas PM. Antibiotic addition to cement-is it beneficial. Hip international: the journal of clinical and experimental research on hip pathology and therapy. 2012;22(1):9.
115. Nair MB, Kretlow JD, Mikos AG, Kasper FK. Infection and tissue engineering in segmental bone defects--a mini review. Current opinion in biotechnology. 2011;22(5):721-5.

116. Cui Q, Mihalko WM, Shields JS, Ries M, Saleh KJ. Antibiotic-impregnated cement spacers for the treatment of infection associated with total hip or knee arthroplasty. J Bone Joint Surg Am. 2007;89(4):871-82.
117. Miola M, Bistolfi A, Valsania MC, Bianco C, Fucale G, Verné E. Antibiotic-loaded acrylic bone cements: An< i> in vitro</i> study on the release mechanism and its efficacy. Materials Science and Engineering: C. 2013.
118. Giers MB, McLaren AC, Schmidt KJ, Caplan MR, McLemore R. Distribution of molecules locally delivered from bone cement. Journal of biomedical materials research Part B, Applied biomaterials. 2014;102(4):806-14.
119. Webb JC, Gbejuade H, Lovering A, Spencer R. Characterisation of in vivo release of gentamicin from polymethyl methacrylate cement using a novel method. International orthopaedics. 2013:1-6.
120. Bohm E, Zhu N, Gu J, de Guia N, Linton C, Anderson T, et al. Does adding antibiotics to cement reduce the need for early revision in total knee arthroplasty? Clin Orthop Relat Res. 2014;472(1):162-8.
121. Gomes D, Pereira M, Bettencourt AF. Osteomyelitis: an overview of antimicrobial therapy. Brazilian Journal of Pharmaceutical Sciences. 2013;49:13-27.
122. Turesin F, Gursel I, Hasirci V. Biodegradable polyhydroxyalkanoate implants for osteomyelitis therapy: in vitro antibiotic release. Journal of biomaterials science Polymer edition. 2001;12(2):195-207.
123. Gürsel İ, Korkusuz F, Türesin F, Gürdal Alaeddinoğlu N, Hasırcı V. In vivo application of biodegradable controlled antibiotic release systems for the treatment of implant-related osteomyelitis. Biomaterials. 2000;22(1):73-80.

124. Shrivastav A, Kim HY, Kim YR. Advances in the applications of polyhydroxyalkanoate nanoparticles for novel drug delivery system. BioMed research international. 2013;2013:581684.
125. Xia W, Chang J. Well-ordered mesoporous bioactive glasses (MBG): a promising bioactive drug delivery system. Journal of controlled release : official journal of the Controlled Release Society. 2006;110(3):522-30.
126. Vallet-Regi M, Ruiz-Hernandez E. Bioceramics: from bone regeneration to cancer nanomedicine. Adv Mater. 2011;23(44):5177-218.
127. Wu T, Zhang Q, Ren W, Yi X, Zhou Z, Peng X, et al. Controlled release of gentamicin from gelatin/genipin reinforced beta-tricalcium phosphate scaffold for the treatment of osteomyelitis. Journal of Materials Chemistry B. 2013;1(26):3304.
128. De Giglio E, Cometa S, Ricci MA, Cafagna D, Savino AM, Sabbatini L, et al. Ciprofloxacin-modified electrosynthesized hydrogel coatings to prevent titanium-implant-associated infections. Acta biomaterialia. 2011;7(2):882-91.
129. Mariner PD, Wudel JM, Miller DE, Genova EE, Streubel SO, Anseth KS. Synthetic hydrogel scaffold is an effective vehicle for delivery of INFUSE (rhBMP2) to critical-sized calvaria bone defects in rats. Journal of orthopaedic research : official publication of the Orthopaedic Research Society. 2013;31(3):401-6.
130. Kulkarni RK, Pani KC, Neuman C, Leonard F. Polylactic acid for surgical implants. Archives of surgery. 1966;93(5):839-43.
131. Wuisman PI, Smit TH. Bioresorbable polymers: heading for a new generation of spinal cages. European spine journal : official publication of the European Spine Society, the European Spinal Deformity Society, and the European Section of the

Cervical Spine Research Society. 2006;15(2):133-48.

132. Pitarresi G, Palumbo FS, Calascibetta F, Fiorica C, Di Stefano M, Giammona G. Medicated hydrogels of hyaluronic acid derivatives for use in orthopedic field. International journal of pharmaceutics. 2013.

133. Price JS, Tencer AF, Arm DM, Bohach GA. Controlled release of antibiotics from coated orthopedic implants. Journal of biomedical materials research. 1996;30(3):281-6.

134. Gilchrist SE, Lange D, Letchford K, Bach H, Fazli L, Burt HM. Fusidic acid and rifampicin co-loaded PLGA nanofibers for the prevention of orthopedic implant associated infections. Journal of controlled release : official journal of the Controlled Release Society. 2013;170(1):64-73.

135. Simchi A, Tamjid E, Pishbin F, Boccaccini AR. Recent progress in inorganic and composite coatings with bactericidal capability for orthopaedic applications. Nanomedicine : nanotechnology, biology, and medicine. 2011;7(1):22-39.

136. Neut D, Kluin OS, Crielaard BJ, van der Mei HC, Busscher HJ, Grijpma DW. A biodegradable antibiotic delivery system based on poly-(trimethylene carbonate) for the treatment of osteomyelitis. Acta Orthop. 2009;80(5):514-9.

137. Gitelis S, Brebach GT. The treatment of chronic osteomyelitis with a biodegradable antibiotic-impregnated implant. Journal of orthopaedic surgery. 2002;10(1):53-60.

138. An YH, Woolf SK, Friedman RJ. Pre-clinical in vivo evaluation of orthopaedic bioabsorbable devices. Biomaterials. 2000;21(24):2635-52.

139. Ginebra MP, Traykova T, Planell JA. Calcium phosphate cements as bone drug delivery systems: a review. Journal of controlled release : official journal of the

Controlled Release Society. 2006;113(2):102-10.

140. Van Staden AD, Dicks LM. Calcium orthophosphate-based bone cements (CPCs): Applications, antibiotic release and alternatives to antibiotics. Journal of applied biomaterials & functional materials. 2012;10(1):2-11.

141. Verron E, Bouler JM, Guicheux J. Controlling the biological function of calcium phosphate bone substitutes with drugs. Acta biomaterialia. 2012;8(10):3541-51.

142. Geesink RG, de Groot K, Klein CP. Bonding of bone to apatite-coated implants. J Bone Joint Surg Br. 1988;70(1):17-22.

143. Goodman SB, Yao Z, Keeney M, Yang F. The future of biologic coatings for orthopaedic implants. Biomaterials. 2013;34(13):3174-83.

144. LeGeros RZ. Calcium phosphate-based osteoinductive materials. Chem Rev. 2008;108(11):4742-53.

145. Campbell AA, Song L, Li XS, Nelson BJ, Bottoni C, Brooks DE, et al. Development, characterization, and anti-microbial efficacy of hydroxyapatite-chlorhexidine coatings produced by surface-induced mineralization. Journal of biomedical materials research. 2000;53(4):400-7.

146. Huang J, Li X, Koller GP, Di Silvio L, Vargas-Reus MA, Allaker RP. Electrohydrodynamic deposition of nanotitanium doped hydroxyapatite coating for medical and dental applications. Journal of materials science Materials in medicine. 2011;22(3):491-6.

147. Liu X, Mou Y, Wu S, Man HC. Synthesis of silver-incorporated hydroxyapatite nanocomposites for antimicrobial implant coatings. Applied Surface Science. 2013.

148. Stigter M, Bezemer J, De Groot K, Layrolle P. Incorporation of different antibiotics

into carbonated hydroxyapatite coatings on titanium implants, release and antibiotic efficacy. Journal of controlled release. 2004;99(1):127-37.

149. Motoc MM, Axente E, Popescu C, Sima LE, Petrescu SM, Mihailescu IN, et al. Active protein and calcium hydroxyapatite bilayers grown by laser techniques for therapeutic applications. J Biomed Mater Res A. 2013;101(9):2706-11.

150. Zhang L, Chen Y, Rodriguez J, Fenniri H, Webster TJ. Biomimetic helical rosette nanotubes and nanocrystalline hydroxyapatite coatings on titanium for improving orthopedic implants. Int J Nanomedicine. 2008;3(3):323-33.

151. Huang D, Zuo Y, Zou Q, Zhang L, Li J, Cheng L, et al. Antibacterial chitosan coating on nano-hydroxyapatite/polyamide66 porous bone scaffold for drug delivery. Journal of biomaterials science Polymer edition. 2011;22(7):931-44.

152. Webster TJ, Ergun C, Doremus RH, Siegel RW, Bizios R. Enhanced osteoclast-like cell functions on nanophase ceramics. Biomaterials. 2001;22(11):1327-33.

153. Rauschmanna MA, Wichelhaus TA, Stirnal V, Dingeldein E, Zichner L, Schnettler R, et al. Nanocrystalline hydroxyapatite and calcium sulphate as biodegradable composite carrier material for local delivery of antibiotics in bone infections. Biomaterials. 2005;26:2677–84.

154. Smith JK, Bumgardner JD, Courtney HS, Smeltzer MS, Haggard WO. Antibiotic-loaded chitosan film for infection prevention: A preliminary in vitro characterization. Journal of biomedical materials research Part B, Applied biomaterials. 2010;94(1):203-11.

155. De Giglio E, Trapani A, Cafagna D, Ferretti C, Iatta R, Cometa S, et al. Ciprofloxacin-loaded Chitosan Nanoparticles as Titanium Coatings: A Valuable Strategy to Prevent

Implant-associated Infections. Nano Biomedicine and Engineering. 2012;4(4):163-9.

156. El-Husseiny M, Patel S, MacFarlane RJ, Haddad FS. Biodegradable antibiotic delivery systems. J Bone Joint Surg Br. 2011;93(2):151-7.

157. Tu J, Yu M, Lu Y, Cheng K, Weng W, Lin J, et al. Preparation and antibiotic drug release of mineralized collagen coatings on titanium. Journal of materials science Materials in medicine. 2012;23(10):2413-23.

158. Knaepler H. Local application of gentamicin-containing collagen implant in the prophylaxis and treatment of surgical site infection in orthopaedic surgery. International journal of surgery. 2012;10 Suppl 1(0):S15-20.

159. Guo YP, Long T, Song ZF, Zhu ZA. Hydrothermal fabrication of ZSM-5 zeolites: biocompatibility, drug delivery property, and bactericidal property. Journal of biomedical materials research Part B, Applied biomaterials. 2014;102(3):583-91.

160. Lewis CS, Supronowicz PR, Zhukauskas RM, Gill E, Cobb RR. Local antibiotic delivery with demineralized bone matrix. Cell and tissue banking. 2012;13(1):119-27.

161. Anagnostakos K, Schroder K. Antibiotic-impregnated bone grafts in orthopaedic and trauma surgery: a systematic review of the literature. International journal of biomaterials. 2012;2012:538061.

162. Holt DJ, Grainger DW. Demineralized bone matrix as a vehicle for delivering endogenous and exogenous therapeutics in bone repair. Adv Drug Deliv Rev. 2012;64(12):1123-8.

163. Hanker JS, Giammara BL. Biomaterials and biomedical devices. Science. 1988;242(4880):885-92.

164. Subbiahdoss G, Aleyt T, Kuijer R, Busscher HJ, van der Mei HC. Influence of

prophylactic antibiotics on tissue integration versus bacterial colonization on poly(methyl methacrylate). Int J Artif Organs. 2012;35(10):840-6.

165. Auclair-Daigle C, Bureau MN, Legoux JG, Yahia L. Bioactive hydroxyapatite coatings on polymer composites for orthopedic implants. J Biomed Mater Res A. 2005;73(4):398-408.

166. Barrere F, Layrolle P, Van Blitterswijk CA, De Groot K. Biomimetic coatings on titanium: a crystal growth study of octacalcium phosphate. Journal of materials science Materials in medicine. 2001;12(6):529-34.

167. Liu Y, de Groot K, Hunziker EB. BMP-2 liberated from biomimetic implant coatings induces and sustains direct ossification in an ectopic rat model. Bone. 2005;36(5):745-57.

168. Blom EJ, Klein-Nulend J, Wolke JGC, Van Waas MAJ, Driessens FCM, Burger EH. Transforming growth factor-β1 incorporation in a calcium phosphate bone cement: Material properties and release characteristics. Journal of biomedical materials research. 2002;59(2):265-72.

169. Liu Y, Li J, Hunziker E, De Groot K. Incorporation of growth factors into medical devices via biomimetic coatings. Philosophical Transactions of the Royal Society A: Mathematical, Physical and Engineering Sciences. 2006;364(1838):233-48.

170. Sumner DR, Turner TM, Urban RM, Turek T, Seeherman H, Wozney JM. Locally delivered rhBMP-2 enhances bone ingrowth and gap healing in a canine model. Journal of orthopaedic research : official publication of the Orthopaedic Research Society. 2004;22(1):58-65.

171. Reyes CD, Petrie TA, Burns KL, Schwartz Z, Garcia AJ. Biomolecular surface coating

to enhance orthopaedic tissue healing and integration. Biomaterials. 2007;28(21):3228-35.

172. Naghib SM, Ansari M, Pedram A, Moztarzadeh F, Feizpour A, Mozafari M. Bioactivation of 304 stainless steel surface through 45S5 bioglass coating for biomedical applications. International Journal of Electrochemical Science. 2012;7:2890-903.

173. Tomsia AP, Saiz E, Song J, Bertozzi CR. Biomimetic bonelike composites and novel bioactive glass coatings. Advanced Engineering Materials. 2005;7(11):999-1004.

174. Arcos D, Vallet-Regi M. Sol-gel silica-based biomaterials and bone tissue regeneration. Acta biomaterialia. 2010;6(8):2874-88.

175. Gonzalez P, Serra J, Liste S, Chiussi S, Leon B, Perez-Amor M, et al. New biomorphic SiC ceramics coated with bioactive glass for biomedical applications. Biomaterials. 2003;24(26):4827-32.

176. Dey A, van den Hoogen CJ, Rosso M, Lousberg N, Hendrix MMRM, Friedrich H, et al. Biomimetic Mineralization of Calcium Phosphate on a Functionalized Porous Silicon Carbide Biomaterial. ChemPlusChem. 2012;77(8):694-9.

177. Rammelt S, Illert T, Bierbaum S, Scharnweber D, Zwipp H, Schneiders W. Coating of titanium implants with collagen, RGD peptide and chondroitin sulfate. Biomaterials. 2006;27(32):5561-71.

178. Bernhardt R, van den Dolder J, Bierbaum S, Beutner R, Scharnweber D, Jansen J, et al. Osteoconductive modifications of Ti-implants in a goat defect model: characterization of bone growth with SR muCT and histology. Biomaterials. 2005;26(16):3009-19.

179. Lee DW, Yun YP, Park K, Kim SE. Gentamicin and bone morphogenic protein-2 (BMP-2)-delivering heparinized-titanium implant with enhanced antibacterial activity and osteointegration. Bone. 2012;50(4):974-82.
180. Tan H, Peng Z, Li Q, Xu X, Guo S, Tang T. The use of quaternised chitosan-loaded PMMA to inhibit biofilm formation and downregulate the virulence-associated gene expression of antibiotic-resistant staphylococcus. Biomaterials. 2012;33(2):365-77.
181. Macdonald ML, Samuel RE, Shah NJ, Padera RF, Beben YM, Hammond PT. Tissue integration of growth factor-eluting layer-by-layer polyelectrolyte multilayer coated implants. Biomaterials. 2011;32(5):1446-53.
182. Cheng H, Li Y, Huo K, Gao B, Xiong W. Long-lasting in vivo and in vitro antibacterial ability of nanostructured titania coating incorporated with silver nanoparticles. J Biomed Mater Res A. 2014;102(10):3488-99.
183. Svensson S, Suska F, Emanuelsson L, Palmquist A, Norlindh B, Trobos M, et al. Osseointegration of titanium with an antimicrobial nanostructured noble metal coating. Nanomedicine : nanotechnology, biology, and medicine. 2013;9(7):1048-56.
184. Wang J, Wang Z, Guo S, Zhang J, Song Y, Dong X, et al. Antibacterial and anti-adhesive zeolite coatings on titanium alloy surface. Microporous and Mesoporous Materials. 2011;146:216–22.
185. Jensen JB, Torjalkar A. Composition for wound dressings safely using metallic compounds to produce anti-microbial properties. US Patent 6,592,888. 2003.
186. Magill SS, Hellinger W, Cohen J, Kay R, Bailey C, Boland B, et al. Prevalence of healthcare-associated infections in acute care hospitals in Jacksonville, Florida. Prevalence. 2012;33(3):283-91.

187. Awad SS. Adherence to surgical care improvement project measures and post-operative surgical site infections. Surgical infections. 2012;13(4):234-7.
188. Jeng DK, Severin JE. Povidone iodine gel alcohol: a 30-second, onetime application preoperative skin preparation. American journal of infection control. 1998;26(5):488-94.
189. Hemani ML, Lepor H. Skin preparation for the prevention of surgical site infection: which agent is best? Reviews in urology. 2009;11(4):190.
190. Darouiche RO, Wall MJ, Jr., Itani KM, Otterson MF, Webb AL, Carrick MM, et al. Chlorhexidine-Alcohol versus Povidone-Iodine for Surgical-Site Antisepsis. The New England journal of medicine. 2010;362(1):18-26.
191. Ellenhorn JDI, Smith DD, Schwarz RE, Kawachi MH, Wilson TG, McGonigle KF, et al. Paint-only is equivalent to scrub-and-paint in preoperative preparation of abdominal surgery sites. Journal of the American College of Surgeons. 2005;201(5):737-41.
192. Moen MD, Noone MB, Kirson I. Povidone-iodine spray technique versus traditional scrub-paint technique for preoperative abdominal wall preparation. American journal of obstetrics and gynecology. 2002;187(6):1434-6; discussion 6-7.
193. Swenson BR, Hedrick TL, Metzger R, Bonatti H, Pruett TL, Sawyer RG. Effects of preoperative skin preparation on postoperative wound infection rates: a prospective study of 3 skin preparation protocols. Infection control and hospital epidemiology : the official journal of the Society of Hospital Epidemiologists of America. 2009;30(10):964-71.
194. McGrath DR, McCrory D. An audit of pre-operative skin preparative methods. Annals

of the Royal College of Surgeons of England. 2005;87(5):366-8.

195. Macario A. What does one minute of operating room time cost? Journal of clinical anesthesia. 2010;22(4):233-6.

196. Reichman DE, Greenberg JA. Reducing surgical site infections: a review. Reviews in obstetrics & gynecology. 2009;2(4):212-21.

197. Parks PJ. Patient Pre-operative Skin Preparations to Reduce Surgical Site Infections. Touch Briefings. 2007:53-5.

198. Carson J, Lui B, Rosmus L, Rennick H, Fuller J. Interpretation of MRSASelect screening agar at 24 hours of incubation. Journal of clinical microbiology. 2009;47(3):566-8.

199. Wiegand I, Hilpert K, Hancock RE. Agar and broth dilution methods to determine the minimal inhibitory concentration (MIC) of antimicrobial substances. Nat Protoc. 2008;3(2):163-75.

200. Meurens F, Summerfield A, Nauwynck H, Saif L, Gerdts V. The pig: a model for human infectious diseases. Trends in microbiology. 2012;20(1):50-7.

201. Zalko D, Jacques C, Duplan H, Bruel S, Perdu E. Viable skin efficiently absorbs and metabolizes bisphenol A. Chemosphere. 2011;82(3):424-30.

202. Deeken CR, Esebua M, Bachman SL, Ramshaw BJ, Grant SA. Assessment of the biocompatibility of two novel, bionanocomposite scaffolds in a rodent model. Journal of biomedical materials research Part B, Applied biomaterials. 2011;96(2):351-9.

203. Cozad MJ, Bachman SL, Grant SA. Assessment of decellularized porcine diaphragm conjugated with gold nanomaterials as a tissue scaffold for wound healing. Journal of Biomedical Materials Research Part A. 2011;99(3):426-34.

204. Lvovich VF. Fundamentals of Electrochemical Impedance Spectroscopy. Impedance Spectroscopy: John Wiley & Sons, Inc.; 2012. p. 1-21.
205. Sengupta S, Battigelli DA, Chang HC. A micro-scale multi-frequency reactance measurement technique to detect bacterial growth at low bio-particle concentrations. Lab on a chip. 2006;6(5):682-92.
206. Markx GH, Davey CL. The dielectric properties of biological cells at radiofrequencies: applications in biotechnology. Enzyme and Microbial Technology. 1999;25(3):161-71.
207. Yang L, Bashir R. Electrical/electrochemical impedance for rapid detection of foodborne pathogenic bacteria. Biotechnol Adv. 2008;26(2):135-50.
208. Hruska K, Kaevska M. Mycobacteria in water, soil, plants and air: a review. Vet Med. 2012;57(12):623-79.
209. Brennan PJ, Nikaido H. The envelope of mycobacteria. Annual review of biochemistry. 1995;64(1):29-63.
210. Cole ST, Brosch R, Parkhill J, Garnier T, Churcher C, Harris D, et al. Deciphering the biology of Mycobacterium tuberculosis from the complete genome sequence. Nature. 1998;393(6685):537-44.
211. Carroll KC, Jorgensen JH, Pfaller MA. Manual of Clinical Microbiology2015.
212. Boehme CC, Nabeta P, Hillemann D, Nicol MP, Shenai S, Krapp F, et al. Rapid molecular detection of tuberculosis and rifampin resistance. The New England journal of medicine. 2010;363(11):1005-15.
213. Society AT. Diagnostic standards and classification of tuberculosis in adults and children. Am J Respir Crit Care Med. 2000;161:1376-95.

214. McClean M, Stanley T, Stanley S, Maeda Y, Goldsmith CE, Shepherd R, et al. Identification and characterization of breakthrough contaminants associated with the conventional isolation of Mycobacterium tuberculosis. J Med Microbiol. 2011;60(Pt 9):1292-8.

215. Burdz TVN, Wolfe J, Kabani A. Evaluation of sputum decontamination methods for Mycobacterium tuberculosis using viable colony counts and flow cytometry. Diagnostic microbiology and infectious disease. 2003;47(3):503-9.

216. Sharma M, Misra RN, Gandham NR, Jadhav SV, Angadi K, Wilson V. Comparison of modified Petroff's and N-acetyl-l-cysteine-sodium hydroxide methods for sputum decontamination in tertiary care hospital in India. Medical Journal of Dr DY Patil University. 2012;5(2):97.

217. Organization WH. Global Tuberculosis Report 2014. 2014 [Available from: http://www.who.int/tb/publications/global_report/en/.

218. Chan WC, Li LK, Yung PT, editors. Wearable patch for the electrical, durometry and optical skin measurements in tuberculin skin test. Biomedical and Health Informatics (BHI), 2012 IEEE-EMBS International Conference on; 2012: IEEE.

219. Parsons LM, Somoskovi A, Gutierrez C, Lee E, Paramasivan CN, Abimiku A, et al. Laboratory diagnosis of tuberculosis in resource-poor countries: challenges and opportunities. Clinical microbiology reviews. 2011;24(2):314-50.

220. He F, Zhao J, Zhang L, Su X. A rapid method for determining Mycobacterium tuberculosis based on a bulk acoustic wave impedance biosensor. Talanta. 2003;59(5):935-41.

221. Cui H, Li S, Yuan Q, Wadhwa A, Eda S, Chambers M, et al. An AC electrokinetic

impedance immunosensor for rapid detection of tuberculosis. The Analyst. 2013;138(23):7188-96.

222. Noordhoek GT, Kolk A, Bjune G, Catty D, Dale JW, Fine P, et al. Sensitivity and specificity of PCR for detection of Mycobacterium tuberculosis: a blind comparison study among seven laboratories. Journal of clinical microbiology. 1994;32(2):277-84.

223. De Beenhouwer H, Lhiang Z, Jannes G, Mijs W, Machtelinckx L, Rossau R, et al. Rapid detection of rifampicin resistance in sputum and biopsy specimens from tuberculosis patients by PCR and line probe assay. Tuber Lung Dis. 1995;76(5):425-30.

224. Dalovisio JR, Montenegro-James S, Kemmerly SA, Genre CF, Chambers R, Greer D, et al. Comparison of the amplified Mycobacterium tuberculosis (MTB) direct test, Amplicor MTB PCR, and IS6110-PCR for detection of MTB in respiratory specimens. Clinical infectious diseases : an official publication of the Infectious Diseases Society of America. 1996;23(5):1099-106; discussion 107-8.

225. Helb D, Jones M, Story E, Boehme C, Wallace E, Ho K, et al. Rapid detection of Mycobacterium tuberculosis and rifampin resistance by use of on-demand, near-patient technology. Journal of clinical microbiology. 2010;48(1):229-37.

226. Pozzato N, Gwozdz J, Gastaldelli M, Capello K, Dal Ben C, Stefani E. Evaluation of a rapid and inexpensive liquid culture system for the detection of Mycobacterium avium subsp. paratuberculosis in bovine faeces. J Microbiol Methods. 2011;84(3):413-7.

227. van Zyl-Smit RN, Binder A, Meldau R, Mishra H, Semple PL, Theron G, et al. Comparison of quantitative techniques including Xpert MTB/RIF to evaluate

mycobacterial burden. PLoS One. 2011;6(12):e28815.

228. Harausz E, Lusiba JK, Nsereko M, Johnson JL, Toossi Z, Ogwang S, et al. Comparison of MGIT and Myco/F lytic liquid-based blood culture systems for recovery of Mycobacterium tuberculosis from pleural fluid. Journal of clinical microbiology. 2015;53(4):1391-4.

229. Organization WH. Frequently asked questions on xpert mtb/rif assay. World Health Organization, Geneva, Switzerland http://www who int/tb/laboratory/xpert_faqs pdf. 2015.

230. Laboratories AoPH. NATIONAL TB SERVICES SURVEY REPORT. 2012.

231. Wilson ML. Recent advances in the laboratory detection of Mycobacterium tuberculosis complex and drug resistance. Clinical infectious diseases : an official publication of the Infectious Diseases Society of America. 2011;52(11):1350-5.

232. Pai M, Kalantri S, Dheda K. New tools and emerging technologies for the diagnosis of tuberculosis: part II. Active tuberculosis and drug resistance. Expert Rev Mol Diagn. 2006;6(3):423-32.

233. Pfyffer GE, Welscher HM, Kissling P, Cieslak C, Casal MJ, Gutierrez J, et al. Comparison of the Mycobacteria Growth Indicator Tube (MGIT) with radiometric and solid culture for recovery of acid-fast bacilli. Journal of clinical microbiology. 1997;35(2):364-8.

234. Tortoli E, Cichero P, Piersimoni C, Simonetti MT, Gesu G, Nista D. Use of BACTEC MGIT 960 for recovery of mycobacteria from clinical specimens: Multicenter study. Journal of clinical microbiology. 1999;37(11):3578-82.

235. Romano L, Sanguinetti M, Posteraro B, Ardito F, Gesu G, Schito AM, et al. Early

detection of negative BACTEC MGIT 960 cultures by PCR-reverse cross-blot hybridization assay. Journal of clinical microbiology. 2002;40(9):3499-501.

236. Aggarwal P, Singal A, Bhattacharya SN, Mishra K. Comparison of the radiometric BACTEC 460 TB culture system and Löwenstein–Jensen medium for the isolation of mycobacteria in cutaneous tuberculosis and their drug susceptibility pattern. International journal of dermatology. 2008;47(7):681-7.
237. Yuksel P, Saribas S, Bagdatli Y. Comparison of the VersaTrek and BACTEC MGIT 960 systems for the contamination rate, time of detection and recovery of mycobacteria from clinical specimens. African Journal of Microbiology Research. 2011;5(9):985-9.
238. Sharma B, Pal N, Malhotra B, Vyas L. Evaluation of a rapid differentiation test for Mycobacterium tuberculosis from other mycobacteria by selective inhibition with p-nitrobenzoic acid using MGIT 960. Journal of laboratory physicians. 2010;2(2):89.
239. Angeby KA, Werngren J, Toro JC, Hedstrom G, Petrini B, Hoffner SE. Evaluation of the BacT/ALERT 3D system for recovery and drug susceptibility testing of Mycobacterium tuberculosis. Clin Microbiol Infect. 2003;9(11):1148-52.
240. Stewart GN. The Charges Produced by the Growth of Bacteria in the Molecular Concentration and Electrical Conductivity of Culture Media. J Exp Med. 1899;4(2):235-43.
241. Cole KS. Electric Impedance of Suspensions of Spheres. J Gen Physiol. 1928;12(1):29-36.
242. Rosen D. 6 - DIELECTRIC MEASUREMENTS OF PROTEINS. A Laboratory Manual of Analytical Methods of Protein Chemistry: Pergamon; 1966. p. 191-222.

243. Richards JC, Jason AC, Hobbs G, Gibson DM, Christie RH. Electronic measurement of bacterial growth. J Phys E. 1978;11(6):560-8.

244. Ur A, Brown DF. Impedance monitoring of bacterial activity. J Med Microbiol. 1975;8(1):19-28.

245. Cady P. Rapid automated bacterial identification by impedance measurement. Wiley: New York, NY, USA; 1975. p. 73-99.

246. Felice CJ, Valentinuzzi ME. Medium and interface components in impedance microbiology. IEEE Trans Biomed Eng. 1999;46(12):1483-7.

247. Muñoz-Berbel X, Godino N, Laczka O, Baldrich E, Muñoz FX, Del Campo FJ. Impedance-based biosensors for pathogen detection. Principles of Bacterial Detection: Biosensors, Recognition Receptors and Microsystems: Springer; 2008. p. 341-76.

248. Basuray S, Chang HC. Induced dipoles and dielectrophoresis of nanocolloids in electrolytes. Physical review E, Statistical, nonlinear, and soft matter physics. 2007;75(6 Pt 1):060501.

249. Puttaswamy S, Lee BD, Sengupta S. Novel electrical method for early detection of viable bacteria in blood cultures. Journal of clinical microbiology. 2011;49(6):2286-9.

250. Banada PP, Koshy R, Alland D. Detection of Mycobacterium tuberculosis in blood by use of the Xpert MTB/RIF assay. Journal of clinical microbiology. 2013;51(7):2317-22.

251. Nakedi KC, Nel AJM, Garnett S, Blackburn JM, Soares NC. Comparative Ser/Thr/Tyr phosphoproteomics between two mycobacterial species: the fast growing

Mycobacterium smegmatis and the slow growing Mycobacterium bovis BCG. Frontiers in Microbiology. 2015;6.

252. Gill WP, Harik NS, Whiddon MR, Liao RP, Mittler JE, Sherman DR. A replication clock for Mycobacterium tuberculosis. Nat Med. 2009;15(2):211-4.

253. Gordon RE, Smith MM. RAPIDLY GROWING, ACID FAST BACTERIA I.: Species' Descriptions of Mycobacterium phlei Lehmann and Neumann and Mycobacterium smegmatis (Trevisan) Lehmann and Neumann1. J Bacteriol. 1953;66(1):41.

254. Smith I. Mycobacterium tuberculosis pathogenesis and molecular determinants of virulence. Clinical microbiology reviews. 2003;16(3):463-96.

255. Manual of Clinical Microbiology. Washington, DC, USA: ASM Press; 2015.

256. Murugasu-Oei B, Dick T. Bactericidal activity of nitrofurans against growing and dormant Mycobacterium bovis BCG. The Journal of antimicrobial chemotherapy. 2000;46(6):917-9.

257. Bettencourt P, Pires D, Carmo N, Anes E. Application of confocal microscopy for quantification of intracellular mycobacteria in macrophages. FORMATEX Research Center, Badajoz. 2010.

258. Chan CE, Zhao BZ, Cazenave-Gassiot A, Pang SW, Bendt AK, Wenk MR, et al. Novel phage display-derived mycolic acid-specific antibodies with potential for tuberculosis diagnosis. J Lipid Res. 2013;54(10):2924-32.

259. Puttaswamy S, Lee BD, Amighi B, Chakraborty S, Sengupta S. Novel Electrical Method for the Rapid Determination of Minimum Inhibitory Concentration (MIC) and Assay of Bactericidal/Bacteriostatic Activity. J Biosens Bioelectron S. 2012;2:003.

260. Hinton PR. Statistics explained: Routledge; 2014.
261. Kubica G, Dye W, Cohn M, Middlebrook G. Sputum Digestion and Decontamination with N-Acetyl-L-Cysteine—Sodium Hydroxide for Culture of Mycobacteria. American review of respiratory disease. 1963;87(5):775-9.
262. Chatterjee M, Bhattacharya S, Karak K, Dastidar SG. Effects of different methods of decontamination for successful cultivation of Mycobacterium tuberculosis. Indian J Med Res. 2013;138(4):541-8.
263. Steingart KR, Ng V, Henry M, Hopewell PC, Ramsay A, Cunningham J, et al. Sputum processing methods to improve the sensitivity of smear microscopy for tuberculosis: a systematic review. The Lancet infectious diseases. 2006;6(10):664-74.
264. Piersimoni C, Scarparo C. Relevance of commercial amplification methods for direct detection of Mycobacterium tuberculosis complex in clinical samples. Journal of clinical microbiology. 2003;41(12):5355-65.
265. Ronco C, Levin N. Advances in Chronic Kidney Disease 2007: 9th International Conference on Dialysis, Austin, Tex., January 2007: Special Issue: Blood Purification 2007, Vol. 25: Karger Medical and Scientific Publishers; 2006.
266. Rowther FB, Rodrigues CS, Deshmukh MS, Kapadia FN, Hegde A, Mehta AP, et al. Prospective comparison of eubacterial PCR and measurement of procalcitonin levels with blood culture for diagnosing septicemia in intensive care unit patients. J Clin Microbiol. 2009;47(9):2964-9.
267. Drake MA, Harrison SL, Asplund M, Barbosa-Canovas G, Swanson BG. High pressure treatment of milk and effects on microbiological and sensory quality of Cheddar cheese. Journal of Food Science. 1997;62(4):843-60.

268. Leiner S, Mays M. Diagnosing latent and active pulmonary tuberculosis: a review for clinicians. Nurse Pract. 1996;21(2):86, 8, 91-2 passim.

269. Kirn TJ, Weinstein MP. Update on blood cultures: how to obtain, process, report, and interpret. Clinical Microbiology and Infection. 2013;19(6):513-20.

270. Smith JM, Serebrennikova YM, Huffman DE, Leparc GF, García-Rubio LH. A new method for the detection of microorganisms in blood cultures: Part I. Theoretical analysis and simulation of blood culture processes. The Canadian journal of chemical engineering. 2008;86(5):947-59.

271. Gomez-Sjoberg R, Morisette DT, Bashir R. Impedance microbiology-on-a-chip: Microfluidic bioprocessor for rapid detection of bacterial metabolism. Journal of Microelectromechanical Systems. 2005;14(4):829-38.

272. Shi L, Jung YJ, Tyagi S, Gennaro ML, North RJ. Expression of Th1-mediated immunity in mouse lungs induces a Mycobacterium tuberculosis transcription pattern characteristic of nonreplicating persistence. Proc Natl Acad Sci U S A. 2003;100(1):241-6.

273. Diacon AH, van der Merwe L, Demers AM, von Groote-Bidlingmaier F, Venter A, Donald PR. Time to positivity in liquid culture predicts colony forming unit counts of Mycobacterium tuberculosis in sputum specimens. Tuberculosis (Edinb). 2014;94(2):148-51.

274. Moriwaki Y, Begum NA, Kobayashi M, Matsumoto M, Toyoshima K, Seya T. Mycobacterium bovis bacillus Calmette-Guerin and its cell wall complex induce a novel lysosomal membrane protein, SIMPLE, that bridges the missing link between lipopolysaccharide and p53-inducible gene, LITAF(PIG7), and estrogen-inducible

gene, EET-1. Journal of Biological Chemistry. 2001;276(25):23065-76.

275. Sengupta S, Puttaswamy S, Chang HC. Rapid detection of viable bacteria system and method. Google Patents; 2014.

276. Bemer P, Palicova F, Rusch-Gerdes S, Drugeon HB, Pfyffer GE. Multicenter evaluation of fully automated BACTEC Mycobacteria Growth Indicator Tube 960 system for susceptibility testing of Mycobacterium tuberculosis. Journal of clinical microbiology. 2002;40(1):150-4.

277. Nakedi KC, Nel AJ, Garnett S, Blackburn JM, Soares NC. Comparative Ser/Thr/Tyr phosphoproteomics between two mycobacterial species: the fast growing Mycobacterium smegmatis and the slow growing Mycobacterium bovis BCG. Front Microbiol. 2015;6:237.

278. Ratnam S, Stead FA, Howes M. Simplified acetylcysteine-alkali digestion-decontamination procedure for isolation of mycobacteria from clinical specimens. Journal of clinical microbiology. 1987;25(8):1428-32.

279. Bettencourt P, Pires D, Carmo N, Anes E. Application of confocal microscopy for quantification of intracellular mycobacteria in macrophages. Microscopy: Science, Technology, Applications and Education. 2010;614.

280. Griffeth GC, Callori N, Rankin SC, Boston RC, Morris DO. Optimization of a Staphylococcus aureus adhesion assay for equine corneocytes. Vet Dermatol. 2012;23(1):57-60, e13.

281. Culotti A, Packman AI. Pseudomonas aeruginosa promotes Escherichia coli biofilm formation in nutrient-limited medium. PLoS One. 2014;9(9):e107186.

282. Maurer FP, Bruderer VL, Ritter C, Castelberg C, Bloemberg GV, Böttger EC. Lack

of antimicrobial bactericidal activity in Mycobacterium abscessus. Antimicrobial agents and chemotherapy. 2014;58(7):3828-36.

283. Arain TM, Resconi AE, Hickey MJ, Stover CK. Bioluminescence screening in vitro (Bio-Siv) assays for high-volume antimycobacterial drug discovery. Antimicrob Agents Chemother. 1996;40(6):1536-41.

284. Heifets L, Lindholm-Levy P. Comparison of bactericidal activities of streptomycin, amikacin, kanamycin, and capreomycin against Mycobacterium avium and M. tuberculosis. Antimicrob Agents Chemother. 1989;33(8):1298-301.

285. McClatchy JK, Waggoner RF, Kanes W, Cernich MS, Bolton TL. Isolation of mycobacteria from clinical specimens by use of selective 7H11 medium. American journal of clinical pathology. 1976;65(3):412-5.

286. Demers A, Boulle A, Warren R, Verver S, Van Helden P, Behr M, et al. Use of simulated sputum specimens to estimate the specificity of laboratory-diagnosed tuberculosis. The International Journal of Tuberculosis and Lung Disease. 2010;14(8):1016-23.

287. Rogers JV, Choi YW. Preliminary Evaluation of Mycobacterium tuberculosis Detection in Culture and Artificial Sputum Using a BioNanoPore Membrane and Realtime PCR. Journal of Microbial & Biochemical Technology. 2013;2012.

288. Organization WH. Laboratory services in tuberculosis control. Organization and managment Part 1. Geneva, Switzerland: WHO. 1998.

VITA

Roli Kargupta was born in Ranchi, India to Mr. Sujit Kargupta and Mrs. Sucheta Kargupta. She is their second child and the youngest member of the family. She completed her schooling in Ranchi and then moved to Kolkata, India to complete her undergraduate studies. She did a Bachelor of Science in Chemistry from St. Xavier's College in Kolkata, India. Following which, she did Bachelor of Technology in Food Technology and Biochemical Engineering from Jadavpur University, which is a renowned university in Eastern India. After completing her undergraduate studies, she worked in Britannia Industries Limited which is a leading food company in India for about 3.5 years. Britannia specialized in bakery products like biscuits, cookies, rusks, cakes, bread. It also makes milk products like butter, cheese. As a Quality Assurance Officer, she was responsible for various facets of quality as the overall quality of the plant.

In 2012, Roli decided to improve her skillset and gain some international exposure. So she joined the University of Missouri, to pursue her PhD in Bioengineering. Her primary project involves development and optimization of a rapid, cost-effective microbiological platform based on electrical impedance spectroscopy and microfluidics.

She is married to Dr. Sagnik Basuray, who is an Assistant Professor at New Jersey Institute of Technology. She is very friendly and dependable and in her spare time likes to read, travel, dabble in arts and crafts and loves dancing.